Comparative internal anatomy of Staurozoa (Cnidaria), with functional and evolutionary inferences

Lucília S Miranda [Corresp., 1] , Allen G Collins [2] , Yayoi M Hirano [3] , Claudia E Mills [4] , Antonio C Marques [1, 5]

[1] Department of Zoology, Instituto de Biociências, Universidade de São Paulo, São Paulo, São Paulo, Brazil

[2] National Systematics Laboratory, National Marine Fisheries Service (NMFS), National Museum of Natural History, Smithsonian Institution, Washington, DC, United States of America

[3] Coastal Branch of Natural History Museum and Institute, Chiba, Katsuura, Chiba, Japan

[4] Friday Harbor Laboratories and the Department of Biology, University of Washington, Friday Harbor, Washington, United States of America

[5] Centro de Biologia Marinha, Universidade de São Paulo, São Sebastião, São Paulo, Brazil

Corresponding Author: Lucília S Miranda
Email address: mirandals@ib.usp.br

Comparative efforts to understand the body plan evolution of stalked jellyfishes are scarce. Most characters, and particularly internal anatomy, have neither been explored for the class Staurozoa, nor broadly applied in its taxonomy and classification. Recently, a molecular phylogenetic hypothesis was derived for Staurozoa, allowing for the first broad histological comparative study of staurozoan taxa. This study uses comparative histology to describe the body plans of nine staurozoan species, inferring functional and evolutionary aspects of internal morphology based on the current phylogeny of Staurozoa. We document rarely-studied structures, such as ostia between radial pockets, intertentacular lobules, gametoducts, pad-like adhesive structures, and white spots of nematocysts (the last four newly proposed putative synapomorphies for Staurozoa). Two different regions of nematogenesis are documented. This work falsifies the view that the peduncle region of stauromedusae only retains polypoid characters, discussing that metamorphosis from stauropolyp to stauromedusa occurs both at the apical region (calyx) and basal region (peduncle). Intertentacular lobules, observed previously in only a small number of species, are shown to be widespread. Similarly, gametoducts were documented in all analyzed genera, both in males and females, thereby elucidating gamete release. Finally, ostia connecting adjacent gastric radial pockets appear to be universal for Staurozoa. Detailed histological studies of medusozoan polyps and medusae are necessary to further understand the relationships between staurozoan features and those of other medusozoan cnidarians.

1   Comparative internal anatomy of Staurozoa (Cnidaria), with functional and evolutionary

2   inferences

4   Miranda, L.S.[1]; Collins, A.G.[2]; Hirano, Y.M.[3]; Mills, C.E.[4]; Marques, A.C.[1,5]

6   [1]Departamento de Zoologia, Instituto de Biociências, Universidade de São Paulo, São Paulo, São

7   Paulo, Brazil.

8   [2]National Systematics Laboratory, National Marine Fisheries Service (NMFS), National

9   Museum of Natural History, Smithsonian Institution, Washington DC, United States of America.

10   [3]Coastal Branch of Natural History Museum and Institute, Chiba, Katsuura, Chiba, Japan.

11   [4]Friday Harbor Laboratories and the Department of Biology, University of Washington, Friday

12   Harbor, Washington, United States of America.

13   [5]Centro de Biologia Marinha, Universidade de São Paulo, São Sebastião, São Paulo, Brazil.

15   **ABSTRACT**

16   Comparative efforts to understand the body plan evolution of stalked jellyfishes are

17   scarce. Most characters, and particularly internal anatomy, have neither been explored for the

18   class Staurozoa, nor broadly applied in its taxonomy and classification. Recently, a molecular

19   phylogenetic hypothesis was derived for Staurozoa, allowing for the first broad histological

20   comparative study of staurozoan taxa. This study uses comparative histology to describe the

21   body plans of nine staurozoan species, inferring functional and evolutionary aspects of internal

22   morphology based on the current phylogeny of Staurozoa. We document rarely-studied

23   structures, such as ostia between radial pockets, intertentacular lobules, gametoducts, pad-like

24   adhesive structures, and white spots of nematocysts (the last four newly proposed putative

25   synapomorphies for Staurozoa). Two different regions of nematogenesis are documented. This

26   work falsifies the view that the peduncle region of stauromedusae only retains polypoid

27   characters, discussing that metamorphosis from stauropolyp to stauromedusa occurs both at the

28   apical region (calyx) and basal region (peduncle). Intertentacular lobules, observed previously in

29   only a small number of species, are shown to be widespread. Similarly, gametoducts were

30   documented in all analyzed genera, both in males and females, thereby elucidating gamete

31   release. Finally, ostia connecting adjacent gastric radial pockets appear to be universal for

32   Staurozoa. Detailed histological studies of medusozoan polyps and medusae are necessary to

33   further understand the relationships between staurozoan features and those of other medusozoan

34   cnidarians.

36   **INTRODUCTION**

37   The class Staurozoa of the phylum Cnidaria (Marques & Collins, 2004; Collins et al.,

38   2006) includes representatives with a peculiar life cycle: creeping larvae settle and develop into

39   juvenile stauropolyps that later metamorphose into non-free-swimming, adult stauromedusae

40   while still being attached to a substrate by a peduncle (Wietrzykowski, 1912; Kikinger &

41   Salvini-Plawen, 1995; Miranda, Collins & Marques, 2010). In general, the apical half of the

42   metamorphosed stauromedusa (calyx) has characters similar to those of adult scyphomedusae

43   and cubomedusae, such as hollow structures of tentacular origin (rhopalioids/rhopalia), circular

44   coronal muscle, gastric filaments, and gonads (Collins, 2002; Collins et al., 2006). The basal

45   region (peduncle), on the other hand, retains polypoid characters such as gastric septa associated

46   with four interradial longitudinal muscles (Collins, 2002; Stangl, Salvini-Plawen & Holstein,

47   2002). Consequently, understanding the body plan of a stauromedusa is more complex than for

48   other medusozoans because of its dual nature (Collins et al., 2006; Miranda, Collins & Marques,

49   2013).

50   Internal anatomy is an important source of characters used in staurozoan taxonomy

51   (Miranda, Collins & Marques, 2013), mainly because stauromedusae have relatively few

52   macromorphological characters useful to differentiate species (Hirano, 1997). There are several

53   detailed histological studies (Clark, 1878; Gross, 1900; Wietrzykowski, 1912; Uchida, 1929;

54   Uchida & Hanaoka, 1933, 1934; Ling, 1939; Miranda, Collins & Marques, 2013), but

55   comparative efforts to understand the evolution of the body plan of staurozoans are scarce and

56   based only on a small number of species (Berrill, 1963; Thiel, 1966). Comprehensive

57   histological studies are important to establish detailed similarities and differences in character

58   states within Staurozoa and other clades of Cnidaria, providing basis to infer character evolution

59   in these clades (Miranda, Collins & Marques, 2013).

60   Recently, histological characters used in the taxonomy of Staurozoa were reviewed based

61   on the study of the internal anatomy of *Haliclystus antarcticus* (Miranda, Collins & Marques,

62   2013). Among other features, poorly known structures such as intertentacular lobules, ostia

63   between adjacent gastric radial pockets, and male and female gonadal vesicles were described,

64   and two possible regions of cnida formation were hypothesized (Miranda, Collins & Marques,

65   2013). However, most of these characters have neither been explored for the class, nor broadly

66   applied to its taxonomy and classification.

67   A microanatomical comparison benefits greatly from the historical context provided by

68   the molecular phylogenetic analysis of Staurozoa (Fig. 1), which has led to an extensive

69   reassessment of the traditional classification of the group (Miranda et al., 2016). This analysis

70   corroborated the non-monophyly of the suborders Cleistocarpida and Eleutherocarpida, formerly

71   recognized based on the presence and absence of claustrum, respectively (Clark, 1863).

72   Apparently, the claustrum, an internal tissue that divides the gastrovascular cavity (Clark, 1863;

73   Gross, 1900), is either homoplastic in different groups or was lost several times (Collins & Daly,

74   2005; Miranda et al., 2016). In contrast, the interradial longitudinal muscles in the peduncle have

75   a strong phylogenetic signal, supporting the proposal of the new suborders Myostaurida and

76   Amyostaurida, with and without such muscles in peduncle, respectively (Miranda et al., 2016).

77   Many traits employed in the taxonomy of Staurozoa come from incomplete and/or

78   misinterpreted histological studies, leading to their inaccuracy and inefficiency as taxonomic

79   characters (Miranda, Collins & Marques, 2013). Hence, a broad histological comparative study

80   of staurozoan taxa is necessary both to allow inferences about the evolution of their body plan as

81   well to add more morphological perspective on the new staurozoan classification (Miranda et al.,

82   2016). Therefore, the aim of this study is to use comparative histology to describe the body plan

83   of a broad range of staurozoan species, inferring functional and evolutionary aspects of internal

84   morphology, and reviewing their taxonomic use in the context of the new understanding of the

85   phylogeny of Staurozoa (Miranda et al., 2016).

87   **MATERIAL & METHODS**

88   We studied nine species of Staurozoa (stauromedusa stage) representing five genera and

89   four families (Table 1), previously fixed directly in 4% formaldehyde solution with seawater,

90   either sampled by us or from museum collections (Table 1). The histological procedures were

91   carried out according to the methods developed for Staurozoa (Miranda, Collins & Marques,

92   2013; modified from Humason, 1962; Mahoney, 1966). Specimens were cleaned in distilled

93   water; dehydrated in a graded ethanol series (70-100%); cleared in xylene (three steps);

94   infiltrated and embedded in paraffin; serially sectioned transversely (7.0-10.0 μm thick) with a

95   microtome Leica RM2025; cleared in xylene (twice); rehydrated in a graded ethanol series (100-

96   70%); cleaned in distilled water; and stained, using acid fuchsin (15') (Mallory; Humason, 1962:

97   147) and acetic aniline blue (3') (Mallory; modified from Humason, 1962: 231), intercalated

98   with distilled water to improve the contrast between structures. Prepared slides were observed

99   and photographed under a Zeiss microscope AXIO Imager M2. The slides are deposited in the

100   collection of the Laboratory of Marine Evolution of the Institute of Bioscience, University of São

101   Paulo (Table 1, LEM 09-17) and are available for loan. The abbreviations of the morphological

102   structures indicated in Figures 2-58 are listed in Table 2.

103   Based on the species examined and on the literature information (Gosse, 1860; Clark,

104   1863; Mayer, 1910; Uchida, 1929; Uchida & Hanaoka, 1933, 1934; Carlgren, 1935; Ling, 1937;

105   Kramp, 1961; Larson, 1980, 1988; Hirano, 1986, 1997; Larson & Fautin, 1989; Kikinger &

106   Salvini-Plawen, 1995; Marques & Collins, 2004; Collins & Daly, 2005; Collins et al., 2006; Van

107   Iten et al., 2006; Pisani et al., 2007; and Miranda et al., 2016), we present a matrix of characters

108   for staurozoan genera (Table 3). Some characters have not been investigated in detail for some

109   taxa, especially *Depastrum*, *Halimocyathus*, *Kyopoda*, *Lipkea*, and *Stylocoronella*.

110   Morphological characters were optimized at the generic level by using ACCTRAN (accelerated

111   transformation) in TNT 1.1 (Goloboff et al., 2008), based on the recent staurozoan phylogeny

112   (Figs 1, 59) (Miranda et al., 2016).

114   **RESULTS**

115   **General Body Anatomy**

116   The internal anatomy of nine species of stalked jellyfishes is described below (Figs 2-58;

117   Table 2). For each species we included detailed information on general body plan, peduncle and

118   septa, gonads and gametoducts, intertentacular lobules, and claustrum (when applicable). The

119   muscular system, manubrium and gastric radial pockets, gastric filaments, perradial and

120   interradial anchors/primary tentacles, ostia, arms delimitation, white spots of nematocysts,

121   batteries of nematocysts, internal subumbrellar layer of nematocysts, secondary tentacles, and

122   pad-like adhesive structures were comparatively analyzed. Therefore, the figures used to

123   illustrate these structures (Figs 5-7, 9-13, 15-17, 24, 32) will be mentioned in the descriptions

124   independently of the species.

126   **Suborder Myostaurida** Miranda, Hirano, Mills, Falconer, Fenwick, Marques & Collins, 2016

127   1. Family Haliclystidae Haeckel, 1879

128   1.1. Genus *Haliclystus* Clark, 1863

129   1.1.1. *Haliclystus tenuis* Kishinouye, 1910 (Figs 2E, F; 3; 4; 5M, Q, V; 6; 8; 9A-I; 10A-F; 11A-

130   H; 12A-C; 13C; 14; 15I-Q; 17N-Q; 21A; 57; 58A, C, D)

131   Basal region formed by pedal disk of peduncle (stalk) with increased surface area due to

132   invaginations (Fig. 3A, B). Peduncle with four perradial chambers (delimited by gastrodermis),

133   alternating with four interradial longitudinal muscle bands (epitheliomuscular cells) embedded in

134   mesoglea (Fig. 4); chambers and muscles developed throughout peduncle (Fig. 4A-C) except at

135   pedal disk. Perradial chambers fusing at junction of peduncle and calyx (Fig. 4D-G).

136   Gastrodermis envelops interradial longitudinal muscles at basal region of calyx (Fig. 4H),

137   defining four interradial gastric septa: one thin layer of mesoglea surrounded by two layers of

138   gastrodermis (Fig. 4I, J). Four infundibula (peristomal pits) funnel-shaped with blind end,

139 delimited by epidermis, deeply developed down to base of calyx, widening apically, with broad

140 apertures on subumbrella (Figs 2F, 4J). Gastrovascular cavity without claustrum. At base of

141 infundibula, interradial longitudinal muscle becomes compressed and flattened, being V-shaped

142 in cross section apically (as in other species examined, e.g., Fig. 5C, D, G, H, K, L),

143 progressively dividing into two adradial bands toward the arms (Fig. 11A, B). Adjacent septal

144 gastrodermis merge defining four perradial regions and dividing gastrovascular cavity (Fig. 6B-

145 D). Fusion of septal gastrodermis forms basal region of manubrium and gastric radial pockets

146 (perradial pockets), i.e., central part of gastrodermis of each septum joins forming four-sided

147 manubrial gastrodermis while lateral parts of adjacent septa join forming gastric radial pockets

148 (Fig. 6). Similarly, each infundibular epidermis also progressively merges apically: central part

149 of each infundibular epidermis becomes manubrial epidermis, and epidermis of adjacent

150 infundibula forms epidermis of gastric radial pockets (Fig. 6E-N). Therefore, each gastric radial

151 pocket is formed by fusion of gastrodermis and epidermis of adjacent septa, and manubrium is

152 formed by fusion of all four septa (Fig. 6). Four gastric radial pockets laterally separated from

153 each other by interradial septa (Fig. 6L, N); gastric radial pockets directly connected only by

154 means of small interradial ostia at margin of calyx (Fig. 10A-F); each gastric radial pocket

155 connected to main gastrovascular cavity. Manubrium (Fig. 3H) internally defined by

156 gastrodermis, externally by epidermis (Fig. 6O, P). Gastric filaments composed of one layer of

157 mesoglea surrounded by gastrodermis, formed by lateral evaginations of gastrodermal layer of

158 septa at base of manubrium, concentrated at perradii (as in other species examined; Fig. 7).

159 Gonads (Fig. 3F-H) with approximately six rows of vesicles (follicles), which are serial

160 gastrodermal evaginations at lateral regions of interradial septa, gastric radial pockets and arms

161 (Fig. 8); vesicles of same gastric radial pocket formed by gastrodermis of two different

162   interradial septa (two adjacent septa) (Fig. 8B). Vesicles composed of an internal layer of

163   gastrodermis, mesoglea, an external (subumbrellar) layer of epidermis, and inner gonadal content

164   (gastrodermal origin) (Fig. 8A, D, E). Female specimen analyzed (Fig. 8) with ovarian vesicles;

165   gonadal content composed of two main layers: peripheral layer with immature oocytes in

166   different developmental stages (Fig. 8C, D), internal layer with mature oocytes with scattered

167   yolk granules (Fig. 8C, D). Mature oocytes surrounded by cells of gastrodermal origin (probably

168   follicle cells), leading to gastric radial pockets through fusion of these cells with gastrodermis of

169   the ovarian vesicles (Fig. 8D-M), forming gametoducts (Fig. 8N, O). Cilia often associated with

170   gametoducts. Anchors (rhopalioids) (Fig. 3D, E) hollow, with hollow stem as evaginations of

171   body surface. Eight large anchors, each located between adjacent arms at calyx margin (Fig. 3D,

172   E), four perradial (Fig. 9A-I) and four interradial (Fig. 10A-F). Gastrodermis of perradial

173   anchors directly connected to gastrodermis of gastric radial pockets through stem (Fig. 9A-I). At

174   interradial regions, septa prevent direct connection of gastrodermis of interradial anchors with

175   gastrodermis of calyx (Fig. 10A), but at margin of calyx, small ostia connect adjacent gastric

176   radial pockets along margin of calyx, allowing gastrodermis of anchors to be contiguous with

177   gastrodermis of calyx (gastric radial pocket) (Fig. 10B-F). Anchors without nematocysts. Each

178   gastric radial pocket extending throughout calyx margin, apically continuing into two adradial

179   arms and respective tentacular clusters (Fig. 11A-H). Subumbrellar epidermis (continuous with

180   epidermis of infundibula) marginally merges with exumbrellar epidermis, dividing gastric radial

181   pockets at origin of arms (Fig. 11A-H). Eight bands of longitudinal muscles running between

182   calyx base and arms, each band toward each one of eight arms (Fig. 11B-H), then becoming

183   thinner diffuse muscle bundles toward secondary tentacles (as in other species examined; Fig.

184   5Q-V). Eight sections of coronal muscle (Fig. 3E) at calyx margin, each between adjacent arms

185 (as in most of species examined; Figs 5, 11). Each arm with two bands (perradial and interradial)

186 of coronal muscle (Figs 5Q; 11G, H). Perradial and interradial white spots of nematocysts on

187 subumbrella (Fig. 3G), between a layer of epidermis and gastrodermis, internally composed of

188 peripheral layer of nematoblasts, and central mature nematocysts (Fig. 12A-C). Epidermal

189 thickening at central region of white spots of nematocysts (Fig. 12C). Batteries of nematocysts

190 sparsely distributed in exumbrellar epidermis (Fig. 13C). Distal exumbrellar end of arms with

191 "U-shaped" space, a platform connecting arm with secondary tentacles, defined by gastrodermis

192 and a thick layer of mesoglea (Fig. 14). Continuous layer of internal unorganized nematocysts

193 visible in subumbrellar epidermis, from base of infundibula, passing through gastric radial

194 pockets, arms, to tips of secondary tentacles (as in most of species examined; Figs 15, 16).

195 Internal layer of nematocysts continuous with groups of nematocysts at tentacular base, in

196 epidermis, with different sizes and types, also unorganized (as in other species examined; Fig.

197 16). Secondary hollow tentacles (Fig. 3I) composed of two parts, knob and stem (Fig. 17N).

198 Secondary tentacles without pad-like adhesive structures. Each stem with inner layer of

199 gastrodermis, and external layer of epidermis; epidermis with longitudinal muscles extending

200 throughout tentacular stem (Fig. 17O). Nematocysts found at different regions of epidermis of

201 stem of secondary tentacles (as in other species examined; Fig. 16Q). Tentacular knob with a

202 thin layer of gastrodermis and a thick layer of epidermis with an external row of organized

203 nematocysts (Fig. 17P, Q). Nematocysts also found at internal region of knob, among supporting

204 cells of epidermis.

205

206 1.2. Genus *Manania* Clark, 1863

207 1.2.1. *Manania uchidai* (Naumov, 1961) (Figs 2I, J; 5A, B, N; 7I; 12D, E; 13A, B; 17K-M; 18;

208 19; 20; 21B; 22; 23; 24L-N; 57; 58B, E)

209   Basal region formed by pedal disk of peduncle with increased surface area due to

210 invaginations (Fig. 18 F, G). Peduncle with one chamber (delimited by gastrodermis) and four

211 interradial longitudinal muscle bands (epitheliomuscular cells) embedded in mesoglea, near the

212 base (Fig. 19A-F). Single chamber progressively divided into four chambers, at median region of

213 peduncle, alternating with four interradial longitudinal muscle bands (Fig. 19G-R). Perradial

214 chambers do not merge at junction of peduncle and calyx, unlike other stauromedusae (Figs 19S,

215 T; 20A, B). Instead, claustra are defined below complete connection of perradial chambers (Fig.

216 20C-G). Union of lateral projections of adjacent interradial septa forming claustra (Fig. 20D-F),

217 tissues composed of central layer of mesoglea surrounded by gastrodermis, dividing

218 gastrovascular cavity (Fig. 20G, H). Four accessory radial pockets delimited (separated from

219 main gastrovascular cavity) by claustra (Fig. 20F-M). Four infundibula funnel-shaped with blind

220 end, delimited by epidermis, deeply developed down to base of calyx, widening apically, with

221 broad apertures on subumbrella (Figs 19T; 20C, G, H). At base of infundibula, interradial

222 longitudinal muscles remain intramesogleal (Fig. 21B), being progressively (toward manubrium)

223 compressed, flattened, and divided into two thin bands (Fig. 20I, L, M). Adjacent septal

224 gastrodermis merge again, dividing gastrovascular cavity once more, forming four principal

225 radial pockets and manubrium (Fig. 20H-M), similarly (and homologous) to formation of gastric

226 radial pockets in all staurozoan species without claustrum such as *H. tenuis* (Fig. 6). Central part

227 of gastrodermis of each septum joins forming four-sided manubrial gastrodermis, while lateral

228 parts of adjacent septa join forming principal radial pockets (as in the formation of gastric radial

229 pockets of *H. tenuis*, Fig. 6B-D). Similarly, each infundibular epidermis progressively merges

230 apically: central part of each infundibular epidermis becomes manubrial epidermis, and

231 epidermis of adjacent infundibula forms epidermis of principal radial pockets (as in *H. tenuis*

232 Figs 6E-G; 20I, J). Principal radial pockets (Fig. 20J-M) are true gastric radial pockets,

233 composed of same structures as gastric radial pockets in stauromedusae without claustrum (Fig.

234 6) and associated with gonads (and gametoduct) (Fig. 20M). Therefore, *M. uchidai* has eight

235 radial pockets: four accessory radial pockets, directly associated with chambers in peduncle,

236 anchors and arms; and four principal radial pockets, associated with manubrium and gonads (Fig.

237 20J, L). Four accessory and principal radial pockets separated by claustra (Fig. 20L, M). Four

238 accessory radial pockets laterally separated from each other by interradial septa (Fig. 20L);

239 accessory radial pockets directly connected only by means of small interradial ostia at margin of

240 calyx (as in the gastric pocked of *H. tenuis*, Fig. 10A-F). Manubrium internally defined by

241 gastrodermis, externally by epidermis. Gastric filaments similar to those described for *H. tenuis*

242 (as in other species examined; Fig. 7), and associated with principal radial pockets. Gonads (Fig.

243 18H-J) in principal radial pockets, not organized in vesicles (Fig. 22). Gonadal content restricted

244 to one layer between gastrodermis and epidermis of septa (Fig. 22B, D, G). Gonadal layers of

245 same principal radial pocket formed by lateral tissue of two different interradial septa (two

246 adjacent septa) (Fig. 20H-K). Male specimen analyzed (Fig. 22), with spermatocytes adjacent to

247 gastrodermis of principal radial pockets (internal), and spermatozoa adjacent to epidermis of

248 principal radial pockets (external) (Figs 20M, 22G). Spermatozoa divided into different sacs,

249 delimited by cells of gastrodermal origin, which are connected to gastrodermis of principal radial

250 pocket, forming gametoduct (Fig. 22E, I-N). Cilia often associated with gametoduct. Anchors

251 (Fig. 18C-E) hollow, with hollow stem, as evaginations of body surface (Fig. 5N). Eight small

252 anchors, each anchor located between adjacent arms at calyx margin, four perradial and four

253   interradial, (Fig. 18C-E). Internal organization similar to *H. tenuis*, with interradial ostia (Figs

254   9A-I, 10A-F). Anchors connected to accessory radial pocket. Nematocysts present in knobbed

255   remnant of primary tentacles at tip of anchors (Figs 5N, 18E). Coronal muscle entire at calyx

256   margin, and external (exumbrellar) in relation to anchor (Fig. 18C, D). Each accessory radial

257   pocket extending throughout calyx margin, apically continuing into two adradial arms and

258   respective tentacular clusters. Internal organization of arms similar to *H. tenuis* (Fig. 11A-H).

259   Perradial white spots of nematocysts on subumbrella, associated with gonads (Figs 18H-J, 20K-

260   M), between epidermis and gastrodermis of principal radial pockets, with internal organization

261   (Fig. 12D, E) similar to *H. tenuis*. Batteries of nematocysts sparsely distributed in exumbrellar

262   epidermis (Fig. 13A, B). Distal end of arms with intertentacular lobules, a structure between

263   adjacent secondary tentacles delimited by gastrodermis and one central layer of mesoglea (Figs

264   17M, 23). Outermost secondary tentacles with pad-like adhesive structures (epidermal

265   thickening) (Fig. 24L-N). Continuous layer of internal unorganized nematocysts in subumbrellar

266   epidermis not clearly recognizable. Secondary hollow tentacles composed of two parts, knob and

267   stem, with organization (Fig. 17K, L) similar to *H. tenuis*. At stem base, secondary tentacles

268   tightly joined, separated only by thin layer of mesoglea, with beehive appearance in cross section

269   (Fig. 17K).

270

271   2. Family Lucernariidae Johnston, 1847

272   2.1. Genus *Lucernaria* Müller, 1776

273   2.2.1. *Lucernaria quadricornis* Müller, 1776 (Figs 7G; 16D-H; 17D-F; 25; 26; 27; 28; 57)

274   Basal region formed by pedal disk of peduncle with increased surface area due to

275   invaginations (Fig. 25C). Peduncle with one chamber (delimited by gastrodermis), and four

276 interradial gastric septa: each septum consisting of mesoglea surrounded by gastrodermis and an

277 internal longitudinal muscle band (epitheliomuscular cells) embedded in mesoglea (Fig. 26E, F).

278 Organization of infundibula (Fig. 26H) similar to *H. tenuis*. Gastrovascular cavity without

279 claustrum. At base of infundibula, muscle becomes compressed and flattened, progressively

280 divided into two thin bands apically (as *Lucernaria sainthilairei*; Fig. 5C, D). Organization of

281 manubrium and gastric radial pockets similar to *H. tenuis* (Fig. 6). Four gastric radial pockets

282 laterally separated from each other by interradial septa; gastric radial pockets directly connected

283 only by means of small interradial ostia at margin of calyx (as in other species examined; Fig.

284 10M-U); each gastric radial pocket connected to main gastrovascular cavity. Organization of

285 gastric filaments (Fig. 7G) similar to those of *H. tenuis*. Vesicles of gonads not clearly defined

286 (Fig. 25H), with irregular shape: gametes located between a layer of gastrodermis and epidermis

287 of septa, and this layer can be more or less wavy (Fig. 27A-C). Vesicles of same gastric radial

288 pocket formed by gastrodermis of two different interradial septa (two adjacent septa). Female

289 specimen analyzed, with no evident regionalization of mature and immature oocytes (Fig. 27),

290 although gametoduct is recognizable (Fig. 27D-I). Oocytes surrounded by cells of gastrodermal

291 origin (probably follicle cells), leading to gastric radial pockets through fusion of these cells with

292 gastrodermis of the ovarian vesicles (Fig. 27D-I), forming a gametoduct (Fig. 27I). Cilia often

293 associated with gametoduct (Fig. 27G-I). Anchors absent (Fig. 25). Arms paired at interradii

294 (Fig. 25A, D, E), with internal organization similar to *H. tenuis* (Fig. 11). Eight sections of

295 coronal muscle at calyx margin, each between adjacent arms. Organization of longitudinal and

296 coronal muscles in arms similar to *H. tenuis* (as in other species examined; Figs 5, 11). Perradial

297 and interradial white spots of nematocysts on subumbrella, with internal organization similar to

298 *H. tenuis* (Fig. 12A-C). Distal end of arms with intertentacular lobules, a structure between

299 adjacent secondary tentacles delimited by gastrodermis and a central layer of mesoglea (Figs

300 17D, E; 28). Secondary tentacles of arms without pad-like adhesive structures (Fig. 25D, F, G).

301 Continuous layer of internal unorganized nematocysts visible in subumbrellar epidermis, from

302 base of infundibula, passing through gastric radial pockets, arms, to tips of secondary tentacles

303 (as in most of species examined; Figs 15, 16). Internal layer of nematocysts continuous with

304 groups of nematocysts at tentacular base, in epidermis, with different sizes and types, also

305 unorganized (Fig. 16D-H). Secondary hollow tentacles composed of two parts, knob and stem,

306 with organization similar to *H. tenuis* (as in other species examined; Fig. 17). At stem base,

307 secondary tentacles tightly joined, separated only by thin layer of mesoglea, with beehive

308 appearance in cross section (Fig. 17F).

309

310 *2.2.2. Lucernaria bathyphila* Haeckel, 1879 (Figs 17G, H; 29; 30; 31; 32N-W; 33; 57)

311   Internal anatomy similar to *Lucernaria quadricornis*. Peduncle with one chamber

312 (delimited by gastrodermis), and four interradial gastric septa: each septum consisting of

313 mesoglea surrounded by gastrodermis and an interradial longitudinal muscle band

314 (epitheliomuscular cells) embedded in mesoglea (Fig. 30). Gastrovascular cavity without

315 claustrum. Four gastric radial pockets laterally separated from each other by interradial septa;

316 gastric radial pockets directly connected only by means of small interradial ostia at margin of

317 calyx (as in other species examined; Fig. 10M-U); each gastric radial pocket connected to main

318 gastrovascular cavity. Organization of gastric filaments similar to those of *H. tenuis* (as in other

319 species examined, Fig. 7). Vesicles of gonads not clearly defined (Figs 29G, H; 31A-C), with

320 irregular shape: gametes located between a layer of gastrodermis and epidermis of septa, and this

321 layer can be more or less wavy (Fig. 31A-C). Vesicles of same gastric radial pocket formed by

322   gastrodermis of two different interradial septa (two adjacent septa). Specimen analyzed probably

323   an immature male and spermatozoa could not be distinguished (Fig. 31). Gametoduct clearly

324   recognizable: cells of gastrodermal origin connected to spermatocytes, leading to gastric radial

325   pockets through fusion of these cells with gastrodermis of vesicles (Fig. 31F-Q). Cilia often

326   associated with gametoduct (Fig. 31Q). Anchors absent (Fig. 29E). Eight sections of coronal

327   muscle at calyx margin, each between adjacent arms. Organization of longitudinal and coronal

328   muscles in arms similar to *H. tenuis* (as in other species examined; Figs 5, 11). Perradial and

329   interradial white spots of nematocysts on subumbrella (Fig. 29H), with internal organization

330   similar to *H. tenuis* (Fig. 12A-C). Aperture of white spots at subumbrellar epidermis clearly

331   recognizable in its central thicker region (Fig. 32N-W): a pore divides subumbrellar epidermis

332   and adjacent layer of mesoglea into two regions in a longitudinal section, allowing an outflow to

333   central mature nematocysts (Fig. 32Q-W). Batteries of nematocysts sparsely distributed in

334   exumbrellar epidermis (Fig. 29C), similar in internal organization to other species examined

335   (Fig. 13). Distal end of arms with intertentacular lobules (Fig. 33). Secondary tentacles of arms

336   (Fig. 29E, F, H) without pad-like adhesive structures. Continuous layer of internal unorganized

337   nematocysts in subumbrellar epidermis, from base of infundibula, passing through gastric radial

338   pockets, arms, to tips of secondary tentacles (as in most of species examined; Figs 15, 16).

339   Internal layer of nematocysts continuous with groups of nematocysts at tentacular base, in

340   epidermis, with different sizes and types, also unorganized. Organization of secondary tentacles

341   (Fig. 17G, H) similar to *H. tenuis*. At stem base, secondary tentacles tightly joined, separated

342   only by thin layer of mesoglea, with beehive appearance in cross section (as in *L. quadricornis*;

343   Fig. 17F).

344

345 2.2.3. *Lucernaria sainthilairei* (Redikorzev, 1925) (Figs 5C, D; 12I; 16J-L; 17I, J; 34; 35; 36; 37;

346 57)

347   Internal anatomy similar to *Lucernaria quadricornis*. Peduncle with one chamber

348 (delimited by gastrodermis), and four interradial gastric septa: each septum consisting of

349 mesoglea surrounded by gastrodermis and an internal longitudinal muscle band

350 (epitheliomuscular cells) embedded in mesoglea (Fig. 35). Gastrovascular cavity without

351 claustrum. Four gastric radial pockets laterally separated from each other by interradial septa;

352 gastric radial pockets directly connected only by means of small interradial ostia at margin of

353 calyx (as in other species examined; Fig. 10M-U); each gastric radial pocket connected to main

354 gastrovascular cavity. Organization of gastric filaments similar to those of *H. tenuis* (as in other

355 species examined, Fig. 7). Vesicles of gonads not clearly defined, with irregular shape (Fig. 36):

356 gametes located between a layer of gastrodermis and epidermis of septa, and this layer can be

357 more or less wavy (Fig. 36A-D). Vesicles of same gastric radial pocket formed by gastrodermis

358 of two different interradial septa (two adjacent septa). Specimen analyzed probably an immature

359 male; spermatozoa and gametoduct could not be recognized (Fig. 36). Anchors absent (Fig. 34A,

360 B, F). Eight sections of coronal muscle at calyx margin, each between adjacent arms.

361 Organization of longitudinal and coronal muscles in arms similar to *H. tenuis* (as in other species

362 examined; Figs 5, 11). Perradial and interradial white spots of nematocysts on subumbrella (Fig.

363 34B, F), with internal organization similar to *H. tenuis* (Fig. 12I). Batteries of nematocysts

364 sparsely distributed in exumbrellar epidermis (Fig. 34D), similar in internal organization to other

365 species examined (Fig. 13). Distal end of arms with intertentacular lobules (Fig. 37). Secondary

366 tentacles of arms without pad-like adhesive structures (Fig. 34). Continuous layer of internal

367 unorganized nematocysts in subumbrellar epidermis, from base of infundibula, passing through

368 gastric radial pockets, arms, to tips of secondary tentacles (as in most of species examined; Figs

369 15, 16). Internal layer of nematocysts continuous with groups of nematocysts at tentacular base,

370 in epidermis, with different sizes and types, also unorganized (Fig. 16J-L). Organization of

371 secondary tentacles (Fig. 17I, J) similar to *H. tenuis*. At stem base, secondary tentacles tightly

372 joined, separated only by thin layer of mesoglea, with beehive appearance in cross section (as in

373 *L. quadricornis*; Fig. 17F).

374

375 **Suborder Amyostaurida** Miranda, Hirano, Mills, Falconer, Fenwick, Marques & Collins, 2016

376 1. Family Kishinouyeidae Uchida, 1929

377 1.1. Genus *Calvadosia* Clark, 1863

378 1.1.1. *Calvadosia corbini* (Larson, 1980) (Figs 5I-L, O, P, T, U; 7A-F; 10P-U; 12J-M; 13H-M;

379 15R, S; 16I; 17A-C; 24A-K; 38; 39; 40; 41; 57)

380   Peduncle with a broad basal pedal disk (Fig. 38A-C). Base of peduncle with four

381 perradial chambers (delimited by gastrodermis), with numerous evaginations (Fig. 39C-H).

382 Gradual connection of four perradial chambers, defining one central gastric chamber, and

383 delimiting four interradial gastric septa toward apical region (Fig. 39E, F, I). Peduncle without

384 interradial longitudinal muscles (Fig. 39I-M). Size of septa decreases at peduncle/calyx

385 connection (Fig. 39N-Q), where interradial longitudinal muscles (epitheliomuscular cells) inside

386 septa become visible (Fig. 39R, S). Internal organization of infundibula (Fig. 39X, Y) similar to

387 *H. tenuis*. Gastrovascular cavity without claustrum. At base of infundibulum, interradial

388 longitudinal muscle is compressed, and then becomes divided into two bands (Fig. 5I-L). Internal

389 organization of gastric radial pockets and manubrium similar to *H. tenuis* (Fig. 6). Four gastric

390 radial pockets laterally separated from each other by interradial septa; gastric radial pockets

391   directly connected only by means of small interradial ostia at margin of calyx (Fig. 10P-U); each

392   gastric radial pocket connected to main gastrovascular cavity. Manubrium internally defined by

393   gastrodermis, externally by epidermis. Gastric filaments (Fig. 7A-F) similar to those of *H. tenuis*.

394   Gonads with numerous vesicles, irregularly arranged in asymmetrical erected nodules, formed by

395   an external fold of subumbrellar tissue (Figs 38E-I, 40A-E). Male specimen analyzed, with

396   spermatocytes adjacent to gastrodermis, in peripheral position; spermatozoa adjacent to

397   epidermis, in central position (Fig. 40H). Spermatozoa divided into different sacs, delimited by

398   cells of gastrodermal origin, connected to gastrodermis of gastric radial pocket, forming

399   gametoduct (Fig. 40J, L-P). Large batteries of nematocysts in subumbrellar epidermis, associated

400   with gonads, between internal vesicles (Figs 13L, M; 40H, I). Anchors absent (Fig. 38A, B, J).

401   Arms sharply paired at interradii (perradial notches deeper than interradial notches) (Fig. 38A, B,

402   I, J), with internal organization similar to *H. tenuis* (Fig. 11). Eight sections of coronal muscle at

403   calyx margin (Fig. 38D), each between adjacent arms. Organization of longitudinal and coronal

404   muscles in arms similar to *H. tenuis* (as in other species examined; Figs 5, 11). Perradial and

405   interradial white spots of nematocysts on subumbrella (Fig. 38G), with internal organization

406   similar to *H. tenuis* (Fig. 12J-M). Batteries of nematocysts sparsely distributed in exumbrellar

407   epidermis (Fig. 13H-K). Distal end of arms with intertentacular lobules, a structure between

408   adjacent secondary tentacles delimited by gastrodermis and a central layer of mesoglea (Fig. 41).

409   Tip of each arm with large pad-like adhesive structures (Fig. 38K, L), with thick epidermis,

410   mesoglea, and hollow canals delimited by thin layer of gastrodermis; hollow gastrodermal canals

411   gradually connected to gastrovascular cavity at tip of arms (Fig. 24A-K). Continuous layer of

412   internal unorganized nematocysts in subumbrellar epidermis (as in most of species examined;

413   Figs 15, 16). Secondary hollow tentacles composed of two parts, knob and stem, with

414   organization (Fig. 17A-C) similar to *H. tenuis*. At stem base, secondary tentacles tightly joined,

415   separated only by thin layer of mesoglea, with beehive appearance in cross section as in most of

416   species examined (Fig. 17F).

417

418   1.1.2. *Calvadosia cruciformis* (Okubo, 1917) (Figs 2G, H; 9J-S; 10G-L; 12G, H; 13D; 42; 43;

419   44; 45; 57)

420   Basal pedal disk of peduncle (Fig. 42A) with epidermal axial canal, a pronounced and

421   delimited invagination with blind end (Figs 42I, 43A-D). Base of peduncle with four gastric

422   perradial chambers (delimited by gastrodermis) (Fig. 43A-G). Gradual connection of four

423   perradial chambers, defining one central gastric chamber, and delimiting four interradial gastric

424   septa toward apical region (Fig. 43H-L). Peduncle without interradial longitudinal muscles (Fig.

425   43A-M). Size of septa decreases at peduncle/calyx connection, and interradial longitudinal

426   muscles (epitheliomuscular cells) inside septa become visible (Fig. 43N-P). Internal organization

427   of infundibula (Fig. 43N-P) similar to *H. tenuis*. Gastrovascular cavity without claustrum. At

428   base of infundibulum, interradial longitudinal muscle is compressed, and then becomes divided

429   into two bands as in *C. corbini* (Fig. 5I-L). Internal organization of gastric radial pockets and

430   manubrium similar to *H. tenuis* (Fig. 6). Four gastric radial pockets laterally separated from each

431   other by interradial septa; gastric radial pockets directly connected only by means of small

432   interradial ostia at margin of calyx (Fig. 10G-L); each gastric radial pocket connected to main

433   gastrovascular cavity. Manubrium internally defined by gastrodermis, externally by epidermis.

434   Gastric filaments similar to those of other species examined (Fig. 7). Gonads with vesicles,

435   which are serial gastrodermal evaginations at lateral regions of interradial septa, gastric radial

436   pockets, and arms (Fig. 44A-C); vesicles of same gastric radial pocket formed by gastrodermis of

437 two different interradial septa (two adjacent septa). Female specimen analyzed (Fig. 44), with

438 ovarian vesicles with two main layers: peripheral layer with immature oocytes in different

439 developmental stages, internal layer with mature oocytes with scattered yolk granules (Fig. 44B,

440 F-L). Mature oocytes surrounded by cells of gastrodermal origin (probably follicle cells), which

441 are connected to gastrodermis of gastric radial pocket, forming gametoduct (Fig. 44D-L).

442 Perradial and interradial primary tentacles present, presenting curved knob with nematocysts,

443 and a small white disk at stem (Figs 9J-S; 10G-L; 42D, E). Interradial ostia connecting

444 interradial primary tentacles with gastrovascular cavity (Fig. 10G-L). Arms sharply paired at

445 interradii (Fig. 42A, B), with internal organization similar to *H. tenuis* (Fig. 11). Eight sections

446 of coronal muscle at calyx margin, each between adjacent arms. Organization of longitudinal and

447 coronal muscles in arms similar to *H. tenuis* (as in other species examined; Figs 5, 11). Perradial

448 and interradial white spots of nematocysts on subumbrella (Figs 12G, H; 42B, C), with internal

449 organization similar to *H. tenuis*. Batteries of nematocysts sparsely distributed in exumbrellar

450 epidermis (Fig. 13D). Distal end of arms with intertentacular lobules, a structure between

451 adjacent secondary tentacles delimited by gastrodermis and a central layer of mesoglea (Fig. 45).

452 Outermost secondary tentacles with pad-like adhesive structures (epidermal thickening) (as in *M.*

453 *uchidai*; Figs 24L-N, 42H). Clearly recognizable continuous layer of internal unorganized

454 nematocysts in subumbrellar epidermis, from base of infundibula to tips of secondary tentacles,

455 as in most of species examined (Figs 15, 16). Secondary hollow tentacles composed of two parts,

456 knob and stem, with organization similar to *H. tenuis* (as in other species examined; Figs 17, 45).

457

458 1.1.3. *Calvadosia vanhoeffeni* (Browne, 1910) (Figs 5E-H, R, S; 7H; 10M-O; 11I-L; 12F; 13E-

459 G; 15A-H; 16A-C; 46; 47; 48; 49; 50; 57)

460   Basal pedal disk of peduncle with increased surface area due to invaginations (Fig. 46E,

461   F). Base of peduncle with four gastric radial chambers (delimited by gastrodermis) (Fig. 47D, E).

462   Gradual connection of four perradial chambers, defining one central gastric chamber, and

463   delimiting four interradial gastric septa toward apical region (Fig. 47F-K). Peduncle without

464   interradial longitudinal muscles, which are visible inside septa only at peduncle/calyx connection

465   (Fig. 47L, M). Internal organization of infundibula (Fig. 47O, P) similar to *H. tenuis*.

466   Gastrovascular cavity without claustrum. At base of infundibulum, interradial longitudinal

467   muscle is compressed, and then becomes divided into two bands (Fig. 5E-H). Internal

468   organization of gastric radial pockets and manubrium similar to *H. tenuis* (Fig. 6). Four gastric

469   radial pockets laterally separated from each other by interradial septa; gastric radial pockets

470   directly connected only by means of small interradial ostia at margin of calyx (Fig. 10M-O);

471   each gastric radial pocket connected to main gastrovascular cavity. Manubrium internally

472   defined by gastrodermis, externally by epidermis. Gastric filaments (Fig. 7H) similar to those of

473   *H. tenuis*. Vesicles of gonads with irregular shape, but clearly defined, with prominent

474   gastrodermis (Figs 48, 49). Two sets of vesicles in each gastric radial pocket; each vesicle

475   formed by gastrodermis of two different interradial septa (two adjacent septa). Male specimen

476   analyzed (Figs 48, 49), with spermatocytes adjacent to gastrodermis, in peripheral position;

477   spermatozoa adjacent to epidermis, in central position (Figs 48B, 49L). Spermatozoa divided

478   into different sacs, delimited by cells of gastrodermal origin, connected to gastrodermis of gastric

479   radial pockets, forming gametoduct (Figs 48F-X, 49). Anchors absent (Fig. 46A, B). Arms with

480   internal organization similar to *H. tenuis* (Fig. 11I-L). Eight sections of coronal muscle at calyx

481   margin, each between adjacent arms. Organization of longitudinal and coronal muscles in arms

482   (Figs 5R, S; 11L) similar to *H. tenuis*. Perradial and interradial white spots of nematocysts on

483   subumbrella (Fig. 46H), with internal organization (Fig. 12F) similar to *H. tenuis*. Batteries of

484   nematocysts sparsely distributed in exumbrellar epidermis (Fig. 13E-G). Distal end of arms with

485   intertentacular lobules (Fig. 50), a structure between adjacent secondary tentacles delimited by

486   gastrodermis and a central layer of mesoglea. Outermost secondary tentacles with pad-like

487   adhesive structures (epidermal thickening) as in *M. uchidai* (Figs 24L-N, 46J-L). Clearly

488   recognizable continuous layer of internal unorganized nematocysts in subumbrellar epidermis,

489   from base of infundibula to tips of secondary tentacles (as in most of species examined; Figs

490   15A-H, 16A-C). Secondary hollow tentacles (Fig. 46B, J, L) composed of two parts, knob and

491   stem, with organization similar to *H. tenuis* (Figs 17N-Q, 50). At stem base, secondary tentacles

492   tightly joined, separated only by thin layer of mesoglea, with beehive appearance in cross section

493   as in most of species examined (Fig. 17).

494

495   2. Family Craterolophidae Uchida, 1929

496   2.1. Genus *Craterolophus* Clark, 1863

497   2.1.1. *Craterolophus convolvulus* (Johnston, 1835) (Figs 7J; 17R-U; 32A-M; 51; 52; 53; 54; 55;

498   56; 57)

499   Basal pedal disk of peduncle with increased surface area due to invaginations and a

500   central pit (Fig. 51B-C). Peduncle with four perradial chambers (delimited by gastrodermis), and

501   without interradial longitudinal muscles (Fig. 52A-K). Size of four chambers gradually increases

502   to merge as a single chamber at peduncle/calyx connection (Fig. 52 M, N, P), delimiting four

503   interradial septa (Fig. 52O, P). At peduncle/calyx connection, lateral projections of adjacent

504   interradial septa, composed of a central layer of mesoglea surrounded by gastrodermis,

505   progressively merges, defining the claustra, tissues that divide gastrovascular cavity (Figs 52Q-S,

506 53A-F). Four accessory radial pockets delimited (separated from main gastrovascular cavity) by

507 claustra (Fig. 53B-D, F). Four infundibula funnel-shaped with blind end, delimited by epidermis,

508 deeply developed down to base of calyx, widening apically, with broad apertures on subumbrella

509 (Fig. 53C, F). Interradial longitudinal muscle (epitheliomuscular cells) divided into two bands,

510 visible only after complete formation of claustra (Fig. 53G, H). Septa with complex lateral folds,

511 delimiting auxiliary radial pockets (Figs 53G, H, J; 54). Below manubrium delimitation, lateral

512 folds of septa produce auxiliary radial pockets inside infundibula (Fig. 53G, H), composed of

513 external epidermis, a layer of gonadal content, and internal gastrodermis (Fig. 54B). As adjacent

514 septal gastrodermis and epidermis merge, dividing once more the gastrovascular cavity and

515 delimiting four principal radial pockets and manubrium (similarly to *M. uchidai*, Fig. 20), these

516 auxiliary radial pockets are externalized, still connected to subumbrella (Figs 53J; 54A, B).

517 Above manubrium and principal radial pocket delimitation, new auxiliary radial pockets formed

518 inside principal radial pocket (Fig. 54C), also as a result of irregular folds of lateral tissue of

519 principal radial pocket, always containing gonads (Fig. 54E-H). Auxiliary radial pocket inside

520 principal radial pocket composed of external gastrodermis, a layer of gonadal content, and

521 internal epidermis (Fig. 54D). Gastrodermis and epidermis of auxiliary radial pockets

522 progressively merge with lateral gastrodermis and epidermis of principal radial pocket,

523 externalizing auxiliary radial pockets (Fig. 54I-L). Therefore, gastrovascular system in *C.*

524 *convolvulus* divided into numerous radial pockets (Figs 53J; 54A, L): four accessory radial

525 pockets, directly associated with perradial chambers in peduncle, arms and secondary tentacles;

526 four principal radial pockets, associated with manubrium and gonads; and numerous auxiliary

527 radial pockets (external and internal), associated with gonads (Figs 53, 54). Accessory and

528 principal radial pockets separated by claustra (Figs 53J; 54A, L). Accessory radial pockets

529   laterally separated from each other by interradial septa (Fig. 53F); directly connected only by

530   means of small interradial ostia at margin of calyx as in *M. uchidai*, and in gastric radial pockets

531   of species without claustrum, such as *C. vanhoeffeni* and *C. corbini* (Fig 10M-U). Manubrium

532   (Figs 51I, 54C) internally defined by gastrodermis, externally by epidermis. Gastric filaments

533   similar to those of *H. tenuis* in internal organization, associated with principal radial pocket (Fig.

534   7J). Gonadal content restricted to one layer between gastrodermis and epidermis of septa,

535   principal radial pockets, and auxiliary radial pockets, not organized in vesicles (Figs 53-55).

536   Gonadal layers of same principal radial pocket formed by two different adjacent interradial septa.

537   Female specimen analyzed (Figs 53-55), with immature oocytes adjacent to gastrodermis and

538   peripheral; mature oocytes adjacent to epidermis and central (Fig. 55A-C). Mature oocytes

539   surrounded by a layer of cells with gastrodermal origin (probably follicle cells), which merges

540   with gastrodermis of gastrovascular cavity (including gastrodermis of principal radial pocket and

541   gastrodermis of auxiliary radial pocket), forming gametoduct (Fig. 55D-Q). Cilia often

542   associated with gametoduct (Fig. 55D). Anchors absent (Fig. 51A). Each accessory radial pocket

543   extending throughout calyx, apically continuing into two adradial arms and respective tentacular

544   clusters. Internal organization of arms similar to *H. tenuis* (Fig. 11). Eight sections of coronal

545   muscle at calyx margin, each between adjacent arms (Fig. 51A). Organization of longitudinal

546   and coronal muscles in arms similar to *H. tenuis* (as in other species examined; Figs 5, 11).

547   Perradial and interradial white spots of nematocysts on subumbrella, with internal organization

548   (Fig. 32A-M) similar to *H. tenuis*. Aperture of white spots at subumbrellar epidermis clearly

549   recognizable in its central thicker region (Fig. 32G-M): a pore divides subumbrellar epidermis

550   and adjacent layer of mesoglea into two regions in a longitudinal section, allowing an outflow to

551   central mature nematocysts (Fig. 32M). Batteries of nematocysts sparsely distributed in

552 exumbrellar epidermis (as in other species examined; Fig. 13). Distal end of arms with

553 intertentacular lobules, a structure between adjacent secondary tentacles delimited by

554 gastrodermis and a central layer of mesoglea (Fig. 56). Outermost secondary tentacles with pad-

555 like adhesive structures (epidermal thickening) as in *M. uchidai* (Figs 24L-N, 51E-G).

556 Continuous layer of internal unorganized nematocysts in subumbrellar epidermis as in most of

557 other species examined (Figs 15, 16). Secondary hollow tentacles composed of two parts, knob

558 and stem (Figs 17R-U, 56), with organization similar to *H. tenuis*. At stem base, secondary

559 tentacles tightly joined, separated only by thin layer of mesoglea, with beehive appearance in

560 cross section as in most of species examined (Fig. 17).

561

562 **DISCUSSION**

563   Taxonomic characters of Staurozoa, such as the number of secondary tentacles,

564 presence/absence of anchors/primary tentacles, the shape of anchors, presence/absence of

565 claustrum, the number of chambers in the peduncle, and the presence/absence of four interradial

566 longitudinal muscles in the peduncle have traditionally been employed in the taxonomy of the

567 group (Clark, 1863; Uchida, 1929; Kramp, 1961). However, some of these characters vary

568 ontogenetically, and must be cautiously employed to differentiate species (Uchida, 1929; Hirano,

569 1986; Miranda, Morandini & Marques, 2009). Additionally, the recent molecular phylogenetic

570 hypothesis indicates the need to reassess and reinterpret many of the internal characters, such as

571 the claustrum and the longitudinal muscles (see Miranda et al., 2016). We will focus our

572 discussion of the internal anatomy of staurozoans from functional and evolutionary perspectives,

573 in the historical context provided by the phylogenetic hypothesis and classification proposed for

574 the group (Figs 1, 57, 59; Miranda et al., 2016).

575

1. Longitudinal and coronal muscles

576

577   The musculature of stalked jellyfishes is organized into two muscular arrangements:

578 circular (coronal) and longitudinal (radial) muscles (Uchida, 1929; Berrill, 1963; Miranda,

579 Collins & Marques, 2013). The main muscular arrangement in stauromedusae is longitudinal,

580 and not circular as generally observed in active and planktonic scyphomedusae and cubomedusae

581 (Gwilliam, 1960; Arai, 1997; Satterlie, Thomas & Gray, 2005), consistent with the benthic and

582 sessile habit of staurozoans (Gwilliam, 1960; Miranda, Collins & Marques, 2015).

583   The recently proposed phylogenetic hypothesis for Staurozoa (Fig. 1) suggests that

584 interradial longitudinal muscles in the peduncle played a fundamental role in the evolution of the

585 class (Miranda et al., 2016). The new phylogeny-based classification scheme separates the group

586 into two suborders, Myostaurida and Amyostaurida, animals with and without interradial

587 longitudinal muscle in the peduncle at the stauromedusa stage, respectively (Figs 1, 5, 57, 59;

588 Table 3; Miranda et al., 2016). Because the last common ancestor of Staurozoa is inferred to

589 have had peduncular muscles (Table 3), a loss of these muscles can be inferred to have happened

590 in the lineage leading to Amyostaurida (Fig. 59). As expected, our new observations of internal

591 anatomy corroborate the absence of interradial longitudinal muscles in the peduncle in

592 representatives of Amyostaurida, *Craterolophus* and *Calvadosia*, differing from the condition in

593 Myostaurida, as represented by species of *Haliclystus*, *Lucernaria*, and *Manania* (Fig. 57).

594   In *Lucernaria* species, the interradial longitudinal muscles are associated with the

595 interradial septa (occupying an internal position in the septa) from the base of the peduncle (Figs

596 26, 30, 35, 57; Collins & Daly, 2005), whereas in *H.* tenuis and *M. uchidai* the interradial

597 longitudinal muscles in the peduncle are intramesogleal because the septa are only present in the

598   region where the calyx connects to the peduncle (Figs 4, 19, 57; Uchida, 1929; Ling, 1939;

599   Miranda, Collins & Marques, 2013). In species of *Haliclystus*, the gastrodermis of the central

600   chamber envelops the interradial longitudinal muscles in the region of the peduncle/calyx

601   connection (Fig. 4H; Uchida, 1929; Uchida & Hanaoka, 1934; Ling, 1939; Miranda, Collins &

602   Marques, 2013), delimiting the four interradial septa with internal interradial longitudinal

603   muscles, similar to *Lucernaria* (Fig. 57). On the other hand, *M. uchidai* has a slightly different

604   organization (Figs 19, 20): the interradial septa are gradually formed as the size of the four

605   perradial chambers increases in the region of the peduncle/calyx connection. The interradial

606   longitudinal muscles do not occupy an internal position in the septa, remaining external in

607   relation to the septal constriction (Fig. 21), a condition that changes only at the base of the

608   manubrium (Fig. 20I). *Manania uchidai* has a central tissue (mesoglea and gastrodermis) (Fig.

609   20A, B) connecting the four interradial septa that disappears only after the formation of claustra

610   (Fig. 20D-G). However, our observations contrast with those of Uchida & Hanaoka (1933), who

611   reported that the septa are completely separated below the formation of the claustra in *M. uchidai*

612   (identified therein as *Manania distincta*). Either the central connection of septa varies

613   intraspecifically or one result is an artefact.

614   Species of Amyostaurida do not have interradial longitudinal muscle in the peduncle

615   (Figs 5, 57, 59; Table 3). The examined species of *Calvadosia* have four perradial chambers at

616   the base of the peduncle, which progressively merge, producing four interradial septa and one

617   central gastric chamber (Figs 39, 43, 47, 57). The interradial longitudinal muscles only appear at

618   the peduncle/calyx connection, internal to the septa (Figs 39, 43, 47, 57). *Craterolophus*

619   *convolvulus* has four perradial chambers separated by mesoglea throughout the peduncle (Fig.

620   52). At the peduncle/calyx connection, the perradial chambers of *C. convolvulus* increase in size

621 and merge centripetally, delimiting the interradial septa (Fig. 52J-N). A central mesoglea

622 delimited by gastrodermis is still visible (Fig. 52N-P), but progressively disappears apically (Fig.

623 52R, S). Interradial muscles associated with septa are clearly visible only after claustra formation

624 (Fig. 53G), differing from other species of Amyostaurida, in which the interradial longitudinal

625 muscles become visible at the base of the infundibula (Figs 39, 43, 47).

626   Interradial longitudinal muscles are divided into two bands in the calyx of all species

627 (Fig. 5D, H, L). These bands gradually assume an adradial position toward the calyx margin

628 (Figs 5M, 11B). In the amyostaurid *C. convolvulus*, when the interradial longitudinal muscles are

629 visible in the cross sections of the calyx, they are already divided into two bands (Fig. 53G, H)

630 that progressively assume a more adradial position. Each longitudinal muscle band is associated

631 apically with one arm and the correspondent stems of secondary tentacles (Figs 5Q-V, 11).

632 Accordingly, there is a continuum of the longitudinal muscles found in the peduncle (in

633 Myostaurida) or at the base of the calyx (Amyostaurida), with the muscles in the stem of

634 secondary tentacles. In addition, other regions of the body, such as the manubrium, are provided

635 with thin muscle fibers (Gwilliam, 1960; Miranda, Collins & Marques, 2015).

636   The coronal muscle can be entire, as in *M. uchidai* (Fig. 18C, D), running as an external

637 (exumbrellar) and non-interrupted band in the arms; or discontinuous, divided into perradial and

638 interradial sections by the arms, as in *H. tenuis* (Fig. 59; Table 3; Clark, 1863; Carlgren, 1935;

639 Gwilliam, 1956; Kramp, 1961). Cross sections in the arms clearly show two lateral bands of

640 coronal muscle, one from interradii and the other from perradii (Figs 5Q, R; 11H, L). The

641 presence of coronal muscle (vestigial in *Stylocoronella*; Kikinger & Salvini-Plawen, 1995) and

642 its relative position with respect to the anchors/primary tentacles have also been used to

643 differentiate genera (Clark, 1863; Mayer, 1910; Uchida, 1929; Carlgren, 1935; Gwilliam, 1956;

644 Kramp, 1961; Miranda et al., 2016).

645 The contraction of the coronal musculature, along with contraction of the longitudinal

646 muscles, considerably reduces the total volume of the animal, probably making its adherence to

647 substratum more efficient in wave-exposed habitats (Hyman, 1940; Miranda, Collins & Marques,

648 2013; see also Kier, 2012, for discussion about the arrangement of muscular fibers and their role

649 in support and movement in hydrostatic skeletons). In addition, longitudinal muscles in arms and

650 secondary tentacles are likely related to feeding behaviors (Hyman, 1940; Larson, 1980;

651 Miranda, Collins & Marques, 2013). Spontaneous neuromuscular activity in *Haliclystus* is

652 arrhythmic, and stauromedusae lack the ability to perform pulsating swimming motions, unlike

653 free-swimming jellyfishes (Gwilliam, 1960).

654

655 **2. Chambers in the peduncle**

656 Most of the staurozoan genera have four chambers in the peduncle and this state was

657 suggested as a potential synapomorphy of Staurozoa (Fig. 59; Table 3; Collins & Daly, 2005;

658 Miranda et al., 2016). However, the number of chambers in the peduncle has been considered to

659 be a useful character to distinguish staurozoan genera (Clark, 1863; Mayer, 1910; Uchida, 1929;

660 Kramp, 1961; Larson & Fautin, 1989). The stalked jellyfishes can have either (a) one chamber in

661 the peduncle (e.g., *Lucernaria*, *Lipkea*; Kramp, 1961); (b) four perradial chambers (e.g.,

662 *Haliclystus*, *Craterolophus*; Kramp, 1961); (c) four perradial chambers at the base, merging into

663 one chamber medially (e.g., *Calvadosia*; Mayer, 1910; Miranda et al., 2016); (d) one chamber at

664 the base splitting into four chambers medially (e.g., some *Manania*, Larson & Fautin, 1989).

665   In addition, the numbers of chambers in the peduncle were also proposed as the "most

666   useful" character for differentiating species of *Manania* (Larson & Fautin, 1989: 1547). The

667   genus *Manania* includes species with one chamber throughout the peduncle, four chambers

668   throughout the peduncle, or one chamber basally with four chambers at the median region

669   (Larson & Fautin, 1989). However, the number of chambers varies during staurozoan

670   development (Mayer, 1910; Uchida, 1929; Hirano, 1986), as reported in *Haliclystus* and

671   *Manania* (Wietrzykowski, 1911, 1912; Uchida, 1929; Hirano, 1986), and this character must be

672   cautiously employed in taxonomic studies (Miranda et al., 2016).

673   According to the classification proposed by Miranda et al. (2016; Fig. 1) based mainly on

674   molecular phylogenetic analyses, *Lucernariopsis*, *Sasakiella*, and *Kishinouyea* are synonyms of

675   *Calvadosia*. At least in principle, species of former *Lucernariopsis* would have one chamber

676   throughout the peduncle, whereas former *Kishinouyea* and *Sasakiella* would have four chambers

677   at the base of the peduncle (sometimes separated by an axial canal resulting from an invagination

678   of epidermis), which gradually merge apically to form a single chamber (Kramp, 1961).

679   However, the presence of four chambers only at the base of the peduncle is not easy to observe,

680   demanding serial transversal sections of a well-preserved and straight peduncle (the bodies of

681   stauromedusae frequently contract during preservation). Indeed, cross sections at the bases of

682   peduncles are rare in the descriptions of species, and most of them include only information

683   about the median region of the peduncle (Edmondson, 1930; Carlgren, 1938; Miranda et al.,

684   2012). Consequently, it is difficult to be sure that this distinction was correctly applied in former

685   determinations. We have sectioned and analyzed the base of the peduncle of *Calvadosia*

686   *vanhoeffeni*, formerly *Lucernariopsis vanhoeffeni* (Fig. 47), and although the species has been

687   described with a one-chambered peduncle (Browne, 1910), it has four chambers at the peduncle

688   base (Fig. 47D-E). Therefore, the peduncle should be re-examined in detail for other species of

689   the genus *Calvadosia*, in order to verify the universality and/or variability of number of

690   chambers in the group.

691   A possible function for the chambers in the peduncle of stauromedusae has never been

692   discussed, but they probably work as a hydrostatic skeleton (fluid filled cavities; see review in

693   Kier, 2012), in addition to being an important part of the gastrovascular system, increasing

694   surface area (Hand, 1966). In hydrostatic skeletons the force of muscle contraction is transmitted

695   by internal pressure (Kier, 2012). The association of antagonist muscles (longitudinal and

696   circular) with the hydrostatic skeleton can change the shape, size, and orientation of the body

697   (Kier, 2012), as well as possibly improving temporary attachment – all actions particularly

698   important to these animals.

699   The four chambers are formed during the metamorphosis of the stauropolyp to the

700   stauromedusa, and their organization is complete only late in development (Wietrzykowski,

701   1912), so they should not be considered typical "polypoid" structures. For instance, the peduncle

702   of developing *Haliclystus octoradiatus* has one chamber until the 32-tentacle stage, and then,

703   progressively, four independent chambers are formed upwards (Wietrzykowski, 1911, 1912).

704   Similar observations were also described for other species of *Haliclystus*, whose juveniles have a

705   single-chambered peduncle, later divided into four chambers that extend from the base to the top

706   of the peduncle (Hirano, 1986). Accordingly, the general understanding that the peduncle region

707   retains polypoid characters (Stangl, Salvini-Plawen & Holstein, 2002) is not completely correct

708   for stauromedusae.

709   Therefore, the internal anatomy of the peduncle of many stauromedusae is different and

710   more complex than the condition found in stauropolyps (Wietrzykowski, 1912) and in other

711 medusozoan polyps, indicating that metamorphosis in Staurozoa (stauropolyp to stauromedusa)

712 occurs both at the apical region (calyx) and basal region (peduncle) (Uchida, 1929; Hirano,

713 1986). A simple comparison between states of the stauromedusa peduncle and those of polyps of

714 medusozoans is an oversimplification. Consequently, a detailed investigation of the

715 metamorphosis of stauropolyps into stauromedusae would help evaluate hypotheses concerning

716 the evolution of morphological characters in Staurozoa and in cnidarians in general.

717

718 **3. Claustrum**

719   The gastrovascular system of some stauromedusae has an additional level of complexity

720 because of the presence of the claustrum (Fig. 2D; Clark, 1863; Gross, 1900; Berrill, 1963;

721 Collins & Daly, 2005). The claustra are structures formed by the fusion of lateral evaginations of

722 adjacent interradial septa, and each claustrum is composed of a central layer of mesoglea

723 surrounded by gastrodermis (Figs 2D, 20, 53). We documented the claustra in *M. uchidai* (Fig.

724 20) and *C. convolvulus* (Fig. 53). Besides *Manania* and *Craterolophus*, claustra have also been

725 recorded in *Depastrum*, *Depastromorpha*, and *Halimocyathus* (Table 3; Clark, 1863; Kramp,

726 1961; Miranda et al., 2016).

727   In *M. uchidai* and in *C. convolvulus*, the claustra delimit the accessory radial pockets

728 (Figs 20, 53), and the principal radial pockets are formed in association with the manubrium

729 (Fig. 20I, J). The accessory and principal radial pockets are separated by claustra (Figs 2D; 20L,

730 M; 53J; 54A). Consequently, there are eight gastric pockets in the calyx instead of four in the

731 animals without the claustrum (Fig. 6; Gross, 1900; Berrill, 1963). The four external pockets,

732 known as accessory pockets (or exogon; Thiel, 1966), extend into the anchors, arms, and

733 secondary tentacles, continuing into the peduncle as perradial chambers (Fig. 57; Berrill, 1963).

734   Although the accessory radial pockets occupy the same position as gastric radial pockets (of the

735   animals without the claustrum), the four internal pockets, also known as principal (main) radial

736   pockets (or mesogon, Thiel, 1966), are apparently the true gastric radial pockets of these

737   stauromedusae because they contain the gonads and the gastric filaments (Figs 20, 53, 54, 57;

738   Clark, 1863; Gross, 1900; Berrill, 1963).

739   Because of the internal organization, the principal radial pockets of the animals with

740   claustra occupy a perradial position. Consequently, their associated gonads are also perradial

741   (Figs 57, 58). The accessory radial pockets, which do not contain gonads, are associated with the

742   arms that, likewise, do not contain gonads (Figs 57, 58). On the contrary, animals without the

743   claustrum have gonads associated with the gastric radial pockets, therefore in an adradial

744   position extending into the arms (Fig. 58). Animals with interradial paired arms (such as *C.*

745   *cruciformis*, *C. corbini*, *L. quadricornis*) have the gonads still associated with the gastric radial

746   pockets in the arms, but then positioned at the interradii/adradii.

747   Therefore, as a consequence of the internal architecture, the position of gonads is a useful

748   external character for distinguishing animals with and without the claustrum (Fig. 58). Although

749   the claustrum is a valuable character for distinguishing genera in Staurozoa, making histological

750   sections to ascertain the presence or absence of this structure is not always possible. Externally,

751   animals with claustra have exclusively perradial gonads located from the base of the manubrium

752   to the perradial margin of calyx; whereas animals without the claustrum have perradial gonads

753   only at the base of the manubrium, assuming an adradial position at calyx margin and arms, or

754   they are associated with the interradial paired arms (Fig. 58). This can be observed in species of

755   *Manania*, *Craterolophus*, and *Depastromorpha*, but needs to be checked for species of

756   *Depastrum* and *Halimocyathus* (the other staurozoan genera with claustra).

757   According to Berrill (1963: 749), species with and without claustrum indicate "two

758 biological engineering solutions to nutritional problems but does not imply a superiority of one

759 type over the other". The claustra compartmentalize the body of stalked jellyfishes, and this

760 could be a response to biotic or abiotic pressures, but does not seem to be directly related to other

761 internal structures, such as the number of gastric chambers or the presence of interradial

762 longitudinal muscles in peduncle. However, the claustra create an exclusive compartment for the

763 gonads, separating them from the gastric chambers, anchors, arms, and secondary tentacles

764 (differently from the animals without the claustrum), although basal communication exists before

765 claustra delimitation is complete (Fig. 53A-C). The gonads in *C. convolvulus* and *M. uchidai*,

766 species with claustra, are similar, organized as a simple layer, between the gastrodermis and

767 epidermis, and not as numerous vesicles (Figs 22, 54). In addition, they are constrained to the

768 interior of the calyx, never associated with arms, and therefore they would be more protected

769 from predators that graze part of a stauromedusa (Prell, 1910; Uchida & Hanaoka, 1933;

770 Davenport, 1998; Mills & Hirano, 2007).

771   Clark (1863) was apparently the first author to describe the claustrum, and used the

772 feature to divide the stalked jellyfishes into two main groups: Cleistocarpida (claustrum present)

773 and Eleutherocarpida (claustrum absent). Since then, the claustrum has played a central role in

774 the taxonomy of Stauromedusae (Collins & Daly, 2005), and most of the main proposals of

775 classification have been based on that feature (see review in Miranda et al., 2016). Molecular

776 phylogenies make it clear that neither Cleistocarpida nor Eleutherocarpida are monophyletic,

777 dismissing the importance of the claustrum for diagnosing the primary subgroups of Staurozoa

778 (Collins & Daly, 2005; Miranda et al., 2016). A question derived from the homoplastic

779 appearance of the claustrum is whether it is comprised of the same structures among the different

780   and non-closely related staurozoan genera. We analyzed the distantly related *C. convolvulus* and

781   *M. uchidai*, and the structures of claustra in these species are morphologically similar, i.e., lateral

782   projections of the septa composed only of mesoglea and gastrodermis (Figs 20, 53). In *C.*

783   *convolvulus*, besides the accessory and principal radial pockets, there are also numerous auxiliary

784   radial pockets containing gonads, as a result of folds of septa and principal radial pockets (Figs

785   53, 54). Collins & Daly (2005) questioned whether a claustrum might be an ancestral character

786   for Staurozoa (Fig. 59; Table 3). If so, the claustrum was lost several times in staurozoan

787   evolution (Fig. 59; Table 3; Miranda et al., 2016). Indeed, the claustrum has also been described

788   in the medusa stage of Cubozoa, but the gonads are associated with the exogon in box-jellyfishes

789   (Thiel, 1966), and the existence of a typical staurozoan-type claustrum in Cubozoa needs to be

790   assessed (Fig. 59; Table 3; Miranda et al., 2016).

791

792   **4. Internal layer of nematocysts, white spots of nematocysts, and**

793   **exumbrellar/subumbrellar batteries of nematocysts**

794   A continuous internal layer of nematocysts at different stages of development has been

795   recently described for *H. antarcticus* in the subumbrellar epidermis of arms, radial pockets, and

796   infundibula (Miranda, Collins & Marques, 2013). It has been hypothesized that these

797   nematocysts are produced in the epidermis of the infundibula and migrate through the

798   subumbrellar epidermis to the tips of the secondary tentacles in the knob, where mature

799   nematocysts are organized in one external row and can perform their function of defense from

800   predators, capture of prey, and adherence to substrate (Figs 15-17; Miranda, Collins & Marques,

801   2013; see also Gross, 1900; Kassianow, 1901; Wietrzykowski, 1912; Weill, 1925, 1935;

802   Leuschel, 1932; Uchida & Hanaoka, 1933, 1934). Wietrzykowski (1912) observed this layer in

803 the epidermis of the infundibula, adjacent to the septa, beginning with the 4-tentacle stage of the

804 stauropolyps of *H. octoradiatus*. According to him, most of the cells in these regions become

805 nematoblasts and, as development proceeds, the epidermis contains nematocysts at different

806 stages of development without direct contact with the external environment (Wietrzykowski,

807 1912).

808   We observed this internal layer of nematocysts from the epidermis at the bases of the

809 infundibula to the knobs of the secondary tentacles (Figs 15-17) in all species (with the possible

810 exception of *M. uchidai*, in which this layer was not clearly discernible, but has been previously

811 described by Uchida & Hanaoka, 1933: 145, identified as *M. distincta*), indicating its likely

812 universality in Staurozoa. Additionally, this layer seems to be associated with the accumulation

813 of unorganized nematocysts at the base of the secondary tentacles (Fig. 16L), internal to the

814 epidermis and just opposite to the intertentacular lobules (Miranda, Collins & Marques, 2013).

815 This region of accumulation was observed in all species analyzed in this study (Fig. 16), and

816 could be important for providing the animal with a constant and dynamic supply of nematocysts.

817   Although Weill (1925) has suggested a similar scenario for the migration of nematocysts,

818 he associated the internal layer of nematocysts with another set of structures, the white spots of

819 nematocysts (Figs 12, 32). The white spots are located on the subumbrella at the perradii and/or

820 interradii (depending on the species), frequently associated with the calyx margin, gonads, and

821 arms. In a cross section, they look like "bubbles" in the mesoglea, between layers of

822 subumbrellar gastrodermis and epidermis, containing abundant nematocysts (Fig. 12). The

823 process responsible for the formation of these structures has been proposed as invagination

824 (Weill, 1925) or delamination (Leuschel, 1932) of the subumbrellar epidermis (Uchida &

825 Hanaoka, 1933). The presence of white spots of nematocysts is widespread in Staurozoa,

826   occurring in all genera, but they were never reported as taxonomically important until Corbin

827   (1978) and, more broadly, Hirano (1997) and Kahn et al. (2010) used their presence and position

828   (perradial *versus* perradial and interradial) to diagnose and differentiate staurozoan species. As

829   far as we know, white nematocyst spots are only known for Staurozoa, and their presence is a

830   probable synapomorphy for the class (Fig. 59; Table 3).

831   Three hypothetical functions of the white spots can be raised. First, they could be

832   structures for defense and attack, with the nematocysts able to escape outside the sacs by

833   pressure through a narrow slit between ectodermal cells (Kling, 1879; Kassianow, 1901; Uchida

834   & Hanaoka, 1933). Alternatively, the sacs could simply be a place for the production of

835   nematocysts (Uchida & Hanaoka, 1933), an idea offered due to the inferred lack of an aperture in

836   the white spots (Leuschel, 1932). The third hypothesis is that the white spots could be selective

837   reservoirs of nematocysts produced at the base of the infundibula (Weill, 1925, 1935) and that

838   after a period of maturation, they would migrate out to the secondary tentacles (Weill, 1925,

839   1935).

840   The white spots of the species studied herein all have the same morphology, in

841   accordance with that described by Uchida & Hanaoka (1933: 146) for *M. uchidai* (as *M.*

842   *distincta*), with a basal peripheral layer of nematoblasts adjacent to the gastrodermis, and a

843   central group of loosely aggregated mature nematocysts (Fig. 12). The nematoblasts have opaque

844   and darker capsules, whereas in the mature nematocysts, internal structures such as the shaft and

845   tubule are visible. An epidermal thickening at the central region of white spots (Figs 12, 32) was

846   also consistently observed.

847   Importantly, serial longitudinal sections of the white spots of nematocysts of *C.*

848   *convolvulus* and *L. bathyphila* revealed a small opening in these sacs (Fig. 32), located in the

849 region with the thickest epidermis, in which a well-delimited pore passing through the epidermis

850 and adjacent mesoglea connects mature nematocysts with the outside (Fig. 32). This strengthens

851 the hypothesis that the white spots are structures for defense and attack because there is indeed

852 an opening through which the nematocysts could be released. Furthermore, the basal and

853 peripheral layer of nematoblasts suggests that the nematocysts from the white spots are produced

854 locally, contrary to the hypothesis that they would be related to maturation of nematocysts

855 produced at the subumbrellar epidermis (Weill, 1925, 1935). Besides, there are species without

856 white spots, such as *H. antarcticus* (cf. Miranda, Morandini & Marques, 2009), suggesting that

857 the nematocysts produced in the internal subumbrellar epidermis would not need a "selective

858 reservoir" (Weill, 1925, 1935) in order to become mature and migrate to the secondary tentacles.

859 Although the function of the white spots is still not known with certainty, it has also been

860 hypothesized that they protect the stauromedusan gonads from predators (Kling, 1879;

861 Kassianow, 1901; Weill, 1925). Indeed, we observed that they are often associated with the

862 gonads (Fig. 20M). In addition, white spots appear concomitantly with the gonads during the

863 development of *Haliclystus octoradiatus* (32-tentacle stage; Wietrzykowski, 1912, figure XXI).

864 The striking color pattern provided by the presence of these white spots could also be a visual

865 signal to either attract prey or deter visual predators, as their bright reflecting white color

866 diverges from the usually camouflaged body of stauromedusae (Mills & Hirano, 2007).

867 There is no information about whether the white spots are permanent or transitory

868 structures, i.e., whether or not these structures are retained after (and if) nematocysts are

869 released. However, apparently their perradial/interradial position is constant, making them useful

870 in species differentiation (Corbin, 1978; Hirano, 1997; Kahn et al., 2010). During development

871 of different species of Staurozoa, the perradial white spots generally appear first (e.g.,

872   *Haliclystus borealis*, *H. tenuis*), but in some species (e.g., *Haliclystus stejnegeri*, *H.*

873   *octoradiatus*) eight adradial white spots appear at the same time (Wietrzykowski, 1912; Uchida,

874   1929; Hirano, 1986). This pattern of appearance of the white spots was used to support a close

875   relationship between *H. tenuis* and *H. borealis* (Hirano, 1986), corroborated in the recent

876   molecular phylogeny (Miranda et al., 2016).

877   In summary, based on our results and on information in the literature, there are at least

878   two regions of nematocyst formation in stauromedusae: 1) in the epidermis of the infundibula,

879   supplying nematocysts to the secondary tentacles (Figs 15, 16); and 2) at the peripheral region of

880   white spots, supplying nematocysts exclusively to the white spots (Figs 12, 32). However, there

881   is not enough information to suggest whether the nematocysts of the secondary tentacles are

882   being formed exclusively in the basal epidermis of the infundibula or throughout the whole

883   subumbrellar epidermis, i.e., throughout the internal layer of nematocysts.

884   Many species of Staurozoa also have exumbrellar batteries (warts) of nematocysts (Fig.

885   13), comparable to those of other cnidarians. These batteries are simple epidermal clusters of

886   nematocysts that probably play a role in the defense of stalked jellyfishes. These batteries of

887   nematocysts are also common on the subumbrella of *C. corbini*, and are associated with the

888   nodular gonads, between the areas internally corresponding to two adjacent vesicles (Figs 13L,

889   M; 40H, I). These subumbrellar batteries could provide additional protection to the gonads,

890   which are probably more susceptible in these animals because they are projected to the exterior

891   (Fig. 38). The origin of the nematocysts in these batteries, as well as the origin of the

892   nematocysts found elsewhere, such as the gastric filaments (Miranda, Collins & Marques, 2013),

893   is uncertain.

894

5. Intertentacular lobules and "U-shaped" space

895

896   The base of the tentacular cluster at the internal tip of the arms can have either several

897   intertentacular lobules, or a deep "U-shaped" space (Table 3; Hirano, 1997). The intertentacular

898   lobules are internal projections between adjacent secondary tentacles composed of a central layer

899   of mesoglea surrounded by a layer of gastrodermis (the gastrodermis belonging to adjacent

900   secondary tentacles; see examples in Figs 33C, 50C). In a cross section, it is possible to see a

901   circular gastrodermis surrounded by mesoglea (Fig. 17E, M). However, some species, such as *H.*

902   *tenuis*, do not have intertentacular lobules, but have a "U-shaped" space at the base of the

903   tentacular cluster (Figs 14; 59; Table 3). In this region, there is a platform composed of mesoglea

904   and gastrodermis, similar to a large lobule in a longitudinal section (Fig. 14K), which connects

905   the exumbrellar side of the arms to the base of secondary tentacles.

906   These structures were rarely mentioned hitherto. Apparently, Clark (1878) was the first

907   author to describe the intertentacular lobules, in the stauromedusa *Haliclystus auricula*. More

908   than a century later, the internal anatomy of the base of secondary tentacles was used to

909   differentiate species of *Haliclystus* (Hirano, 1997): *Haliclystus californiensis*, *H. tenuis*, and *H.*

910   *borealis* do not have intertentacular lobules but have a "U-shaped" space, whereas *Haliclystus*

911   *"sanjuanensis"* (*nomen nudum*), *H. auricula*, *H. octoradiatus*, and *H. stejnegeri* have

912   intertentacular lobules (also present in *H. antarcticus*, Miranda, Morandini & Marques, 2009).

913   The possible function of these structures and consequences of the different shapes of the internal

914   base of the tentacular clusters have never been discussed, but they increase the gastrovascular

915   area (see Hand, 1966) and also likely function as a point of anchorage and communication

916   between secondary tentacles, possibly related to their movement/contraction (Hand, 1966; Kier,

917   2012).

918   Although these structures are relatively well known for *Haliclystus*, their general

919   occurrence in Staurozoa has never been studied before. We observed intertentacular lobules of

920   different sizes in *Craterolophus* (*C. convolvulus*), *Calvadosia* (*C. corbini*, *C. vanhoeffeni*, and *C.*

921   *cruciformis*), *Lucernaria* (*L. bathyphila*, *L. quadricornis*, and *L. sainthilairei*), and *Manania* (*M.*

922   *uchidai*). Therefore, intertentacular lobules seem to be widespread in Staurozoa and their

923   presence is a probable synapomorphy for the class (Fig. 59; Table 3), whereas the "U-shaped"

924   space may be restricted to some *Haliclystus* species (Table 3).

925

926   **6. Gonads and gametoduct**

927   The gonads of Staurozoa have been considered an important character to understand the

928   evolution of the group, and the complex ovaries with follicle cells (Eckelbarger & Larson, 1993)

929   have been suggested as a potential synapomorphy for the class (Marques & Collins, 2004;

930   Collins & Daly, 2005; Collins et al., 2006; Van Iten et al., 2006), although this was recently

931   questioned (Tiemann & Jarms, 2010).

932   The gonads are organized inside the gastric radial pockets in species lacking claustra,

933   from the base of the calyx to the tips of the arms (Fig. 57). In *C. corbini*, evaginations of the

934   gastric radial pockets produce nodular gonads as external projections on the wide-open

935   subumbrella (Figs 38E-I, 40). In animals with claustra (e.g., *M. uchidai*, *C. convolvulus*), the

936   gonads are associated with the principal radial pockets (mesogon), at perradii, and do not extend

937   into the arms. *Craterolophus convolvulus* is unique in our observations in possessing auxiliary

938   radial pockets, which also contain gonadal tissue (Figs 53G-J, 54).

939   Gonads are generally organized in vesicles as evaginations of gastrodermis, more (i.e., *H.*

940   *tenuis*; Fig. 8) or less (i.e., species of *Lucernaria*; Figs 27, 31, 36) delimited. Gonadal content

941 can also be restricted to a simple layer between gastrodermis and epidermis (i.e., *M. uchidai*; Fig.

942 22), without the organization of vesicles.

943   Male and female gonads can only be recognized with histological sections, and their

944 internal structures have been described in a few different studies (Uchida, 1929; Berrill, 1963;

945 Eckelbarger & Larson, 1993; Eckelbarger, 1994; Miranda, Collins & Marques, 2013). The

946 gonadal content in males is organized in one peripheral layer of spermatocytes adjacent to

947 gastrodermis and a central and internal layer of spermatozoa generally adjacent to epidermis. In

948 females, a peripheral immature layer of oocytes is adjacent to gastrodermis and the mature

949 oocytes occupy a central position, generally adjacent to epidermis. Each gonadal male and

950 female structure contains numerous developing and mature spermatozoa and many immature and

951 mature oocytes, respectively. Additionally, follicle-like accessory cells surround individual

952 oocytes in *Haliclystus "sanjuanensis"* (Eckelbarger & Larson, 1993).

953   In this study, clear regionalization was recognized in all species other than species of

954 *Lucernaria*. In *L. quadricornis*, the oocytes, surrounded by follicle cells, are randomly arranged

955 in the mesoglea between gastrodermis and epidermis (Fig. 27). Oocyte organization in this genus

956 is somewhat similar to the pattern of Scyphozoa and Cubozoa (Eckelbarger, 1994). The

957 specimens of *L. bathyphila* and *L. sainthilairei* examined are apparently males, as they have

958 structures similar to spermatocytes, but probably immature because spermatozoa could not be

959 recognized (Figs 31, 36).

960   Gametoducts are a direct connection between the gonadal content and the gastrodermis of

961 the vesicles (or correspondent gonadal structures), which likely carry spermatozoa or mature

962 oocytes to the gastrovascular cavity. In females, they are associated with cells, probably the

963 follicle-like cells of Eckelbarger & Larson (1993), that surround and isolate mature oocytes at

964   the central region of vesicles (or correspondent gonadal structures). The organization is similar in

965   males; gametoducts are associated with cells surrounding the spermatozoa, sometimes producing

966   different sacs, and directly connected with spermatocytes (Figs 48, 49) most likely of

967   gastrodermal origin. Moreover, cilia (Fig. 27G-I) were observed in the connection of

968   gametoducts with the gastrodermis of vesicles (or correspondent gonadal structures), probably

969   contributing to a more efficient transport of gametes. It is noteworthy that gametoducts were

970   observed in all but one analyzed species. The only exception was *L. sainthilairei*, for which no

971   gametes were observed in the specimen, raising questions about whether the permanence or

972   transitory presence of gametoducts is related to gonadal maturity.

973   The presence of gametoducts in stalked jellyfishes has been described for *H. auricula* as

974   "mouth of genital sac", "entrance of the sac", "aperture of genital sac" (Clark, 1878: 67, figures

975   54, 62, 74, 75, 77), for *L. bathyphila* as "oviduct" or "oviductulus" (Haeckel, 1882: 61, plate

976   XVII, figures 17, 19), and for *H. octoradiatus* as "*étroit canal*" (Wietrzykowski, 1912: 77, figure

977   30), but has been completely ignored for over 100 years. This is the first study to indicate the

978   universality of gametoducts in Staurozoa, present in all analyzed genera, both in males and

979   females, and even in species without delimited vesicles (viz., *M. uchidai, C. convolvulus*), and

980   their presence is reconstructed as a putative synapomorphy for the class (Fig. 59; Table 3).

981   Nevertheless, more detailed studies in other cnidarian classes are necessary to better understand

982   the evolution of these structures within Cnidaria (see also discussion below about gonopores in

983   *Periphylla periphylla*, Tiemann & Jarms, 2010).

984   Berrill (1963: 742, 745) proposed that the "expulsion of gametes" in *Haliclystus salpinx*

985   and in *L. quadricornis* "results from the rupture of the endodermis enclosing the gonads". Our

986   histological studies, however, suggest that gametes are released through specialized structures,

987 indicating a complex functional mechanism. Gametoducts allow the selective release of mature

988 gametes, preventing damage or destruction of the gonads, and not wasting immature oocytes

989 (peripheral) in female vesicles and spermatocytes in male vesicles (or correspondent gonadal

990 structures).

991 A similar structure, the gamete-releasing pore, was described for the coronate

992 scyphomedusa *Periphylla periphylla* (Tiemann & Jarms, 2010). These special pores would work

993 as gonopores, therefore the structure of the gonad would not be destroyed, allowing a continuous

994 gamete release (Tiemann & Jarms, 2010). Spermatozoa were seen associated with these pores, as

995 well as oocytes, which were expelled through this narrow pore, becoming deformed, but then

996 regaining their spherical shape (Tiemann & Jarms, 2010). In addition, there is a strong maturity

997 gradient in gonads of both sexes, simultaneously presenting all developmental stages of gametes

998 (Tiemann & Jarms, 2010), a regionalization also observed in Staurozoa. Tiemann & Jarms

999 (2010) concluded that complex and specialized structures, including gonopores, strongly suggest

1000 that true sexual organs exist in Scyphozoa (interpreted broadly to include Cubozoa and

1001 Staurozoa), even though they presented observations on only a single species of coronate

1002 scyphozoan. The homology between gametoducts in Staurozoa and gonopores in *Periphylla*

1003 *periphylla* remains to be tested. Indeed, recent research is beginning to uncover more complex

1004 reproductive systems in different cnidarians (Cartwright & Nawrocki, 2010; Schiariti et al.,

1005 2012), especially some species belonging to the class Cubozoa (Garm, Lebouvier & Tolunay,

1006 2015; Marques, García & Ames 2015). Although plesiomorphic external fertilization would be

1007 expected in adult medusae (Marques & Collins, 2004), certain cubomedusae can present

1008 courtship behavior, specialized internal fertilization, and sperm storage (Lewis & Long, 2005;

1009 Garm, Lebouvier & Tolunay, 2015; Marques, García & Ames 2015), which demonstrate the

1010   importance to highlight different cnidarian reproductive strategies in order to study their

1011   evolution.

1012   However, a recent review concluded that Cnidaria has no specialization in the

1013   reproductive system, such as genital ducts, generally used for storing, transporting, or extruding

1014   gametic products (Extavour, 2007). Our results and data in Tiemann & Jarms (2010) refute this

1015   interpretation. That said, gonoducts in Bilateria generally take gonadal elements directly to the

1016   outside of the animal (Dewel, 2000; Extavour, 2007), in contrast to the structures of Staurozoa

1017   and *P. periphylla* (Tiemann & Jarms, 2010). Staurozoan gametoducts release gametes into the

1018   gastrovascular cavity, after which the gametes are then expelled to the outside through the mouth

1019   (Otto, 1976). In addition, staurozoan gametoduct structures are perhaps unlikely to be

1020   homologous with bilaterian gonoducts because of their different origins, the latter generally

1021   mesodermal (Extavour, 2007; Nielsen, 2008).

1022   Convergent evolution may have produced different morphological solutions to the

1023   problems posed by sexual reproduction (Extavour, 2007), although it is possible that similarities

1024   in the underlying molecular pathways may exist. Consequently, further investigation of the

1025   occurrence of gonopores or gametoducts in other cnidarians, as well as additional developmental

1026   data, particularly on gene expression, could uncover possible homologies of these specialized

1027   structures. Such knowledge will likely have important implications for understanding the

1028   evolution of reproductive systems across Eumetazoa.

1029

1030   **7. Anchors and primary tentacles**

1031   During the early metamorphosis of a stauropolyp, eight primary tentacles develop, four

1032   perradial and four interradial (Wietrzykowski, 1912; Hirano, 1986; Kikinger & Salvini-Plawen,

1033   1995), which may have four different fates in the stauromedusa stage: 1) they disappear by

1034   resorption (in *L. quadricornis*, Berrill, 1963); 2) they metamorphose into adhesive structures

1035   called anchors (in species of *Haliclystus*, Hirano, 1986); 3) they remain as primary tentacles,

1036   although with a modified shape (in *Calvadosia tsingtaoensis* and *C. cruciformis*; Ling, 1937); 4)

1037   they are originally rather filiform, but transform into capitate tentacles and cluster together with

1038   secondary tentacles (in species of *Stylocoronella*, Kikinger & Salvini-Plawen, 1995).

1039   Anchors are apparently restricted to Haliclystidae (Fig. 59; Table 3; Miranda et al., 2016),

1040   and their shapes have been broadly used to distinguish species of *Haliclystus* (Miranda,

1041   Morandini & Marques, 2009; Kahn et al., 2010). However, the use of this character for

1042   differentiating species can cause taxonomic problems because of ontogenetic variation (Miranda,

1043   Morandini & Marques, 2009).

1044   Primary tentacles and anchors are hollow structures, composed of an internal layer of

1045   gastrodermis and an external layer of epidermis, with mesoglea between them (Figs 9, 10).

1046   Perradial primary tentacles/anchors are directly connected to the gastrodermis of the gastric

1047   radial pockets (or accessory radial pockets in animals with claustra) (Fig. 9). Interradial primary

1048   tentacles/anchors are connected to the gastrovascular cavity by means of small interradial ostia

1049   (Fig. 10) that connect adjacent gastric radial pockets (or accessory radial pockets in the animals

1050   with claustra).

1051   We agree that anchors (or rhopalioids) and rhopalia, present in Staurozoa, Cubozoa, and

1052   Scyphozoa, are probably homologous marginal structures because they all result from

1053   metamorphosis of primary tentacles (Uchida, 1929; Thiel, 1966). However, whereas the rhopalia

1054   in Cubozoa and Scyphozoa have a sensorial function (Nakanishi et al., 2010), the rhopalioids in

1055   Staurozoa likely have a role in substrate attachment (Larson, 1988). The epidermis of the anchor

1056   is formed by tall supporting cells and glandular cells, providing evidence for an adhesive

1057   function that contributes to small movements of the animals, mainly when the peduncle is

1058   detached from the substrate (Miranda, Collins & Marques, 2013). Nematocysts are generally not

1059   observed in the anchors, but they are visible in species with a knobbed remnant of primary

1060   tentacles, such as in *M. uchidai*, corroborating their tentacular nature. The primary tentacles of *C.*

1061   *cruciformis* also have an external layer of nematocysts (Fig. 9L), and they probably also help in

1062   the locomotion (adhesive function) of the stauromedusa.

1063

1064   **8. Ostia**

1065   The presence of an ostium between two adjacent gastric radial pockets has been recorded

1066   before for a small number of staurozoan species, such as *H. salpinx*, *Manania atlantica* (Berrill,

1067   1963), and *H. antarcticus* (Miranda, Collins & Marques, 2013). The ostium connects the

1068   gastrodermis of the interradial anchor with that of the calyx (Fig. 10). In species with claustra

1069   this connection occurs in the accessory radial pockets. The main hypothesis to explain the

1070   presence of these ostia is that they might permit a nutritional extension into the four interradial

1071   anchors (Berrill, 1963: 742). However, they are small that they might not allow for effective

1072   circulation of fluids between two adjacent radial pockets (Berrill, 1963). Based on this

1073   hypothesis, species without anchors would not need an ostium connecting adjacent gastric radial

1074   pockets if ostia really only serve to allow for the connection of the anchor/primary tentacle to the

1075   calyx (Miranda, Collins & Marques, 2013).

1076   However, all species analyzed, both with and without anchors/primary tentacles, have an

1077   ostium connecting two adjacent gastric radial pockets (Fig. 10). Therefore, two main hypotheses

1078   emerge: (1) the ostia, that probably provided gastrodermal extension to the primary interradial

1079   tentacles in the stauropolyp stage, were simply retained after the disappearance of primary

1080   tentacles in the stauromedusa stage (species without anchors/primary tentacles); (2) ostia are

1081   important in the communication of radial pockets, and probably have other function(s) besides

1082   providing nutritional extension to the four interradial anchors/primary tentacles.

1083   Comparable structures, such as the septal ostium or connecting canal, have been observed

1084   in Scyphozoa (Korschelt & Heider, 1895; Chapman, 1966) and Cubozoa (Conant, 1898: 18, 19),

1085   but further detailed studies are necessary to assess their homology across these taxa (see also Fig.

1086   59; Table 3).

1087

1088   **9. Pad-like adhesive structures**

1089   Pad-like structures can be present individually in the outermost secondary tentacles of the

1090   tentacular cluster (Larson & Fautin, 1989), or as a broad structure on the tip of each arm (Fig. 24;

1091   Larson, 1980; Miranda et al., 2012). We found individual pad-like adhesive structures in the

1092   outermost secondary tentacles in *C. convolvulus*, *M. uchidai*, *C. cruciformis*, and *C. vanhoeffeni*.

1093   These structures are a simple lateral projection in the tentacular stem, with an epidermal

1094   thickening (Fig. 24L-N). The only examined species with pads at the tips of arms was *C. corbini*

1095   (Fig. 24A-K). This more complex structure is an exumbrellar lateral projection with thick

1096   epidermis, mesoglea, and internal hollow gastrodermal canals, connected to the gastrovascular

1097   cavity of arms.

1098   Individual adhesive glandular pads at the outermost secondary tentacles are widespread in

1099   the class (Miranda et al., 2016), a putative synapomorphy for the class (Fig. 59; Table 3),

1100   whereas the broad pad-like adhesive structure on the tip of each arms is probably a

1101   synapomorphy of a clade within *Calvadosia* (Miranda et al., 2016, figure 16). The pad-like

1102   adhesive structures of the outermost secondary tentacles and at the tips of the arms were

1103   hypothesized to be homologous by Corbin (1978), and the broad adhesive pad-like structure on

1104   the tip of each arm was suggested to be the result of fusion of several outermost secondary

1105   tentacles (Larson, 1980). Indeed, cross sections of the pads on the tips of arms show many

1106   hollow gastrodermal canals, which could be interpreted as the "merging" of several stem canals

1107   of the secondary tentacles. However, the thin gastrodermis of the pads in the arms contrasts with

1108   the thick and glandular gastrodermis of the secondary tentacles (Figs 17, 24A-K), but this could

1109   be a secondary differentiation related to a different function assumed by the pads.

1110   Adhesive pads help the animals to adhere to its substrate (Larson, 1980). They have been

1111   hypothesized to serve to temporarily reattach the stauromedusae when the peduncle is detached

1112   (Larson, 1988). Their internal anatomy, with epidermis composed of tall glandular and

1113   supporting cells, like all other adhesive regions (viz. secondary tentacles, anchors, peduncle and

1114   pedal disk) of a stauromedusa, corroborates this hypothesis (Miranda, Collins & Marques, 2013).

1115

1116   **CONCLUSIONS**

1117   We have presented the internal anatomy of nine species of Staurozoa. Histological and

1118   taxonomic characters, such as the longitudinal interradial muscles, claustra, and chambers in

1119   peduncle were reviewed based on the recently proposed phylogenetic hypothesis for the class

1120   (Miranda et al., 2016). Characters rarely cited in the literature were also assessed. We found a

1121   general occurrence of intertentacular lobules in Staurozoa (putative synapomorphy for the class),

1122   contrary to the restricted occurrence of "U-shaped" space in some species of *Haliclystus*. Ostia

1123   between radial pockets are present in all observed species, even in those without interradial

1124   anchors/primary tentacles. Additionally, the functional and evolutionary aspects of key internal

1125   structures were discussed, such as the complex gonads in Staurozoa, and possibly in other

1126   cnidarians, with regionalization of mature and immature gametes and the presence of

1127   gametoducts (putative synapomorphy for the class, although more information for other

1128   cnidarian classes is necessary), both in males and females, thereby elucidating gamete release.

1129   Two different nematogenesis regions were observed in most species examined: 1) in the

1130   subumbrellar epidermis of infundibula, which supplies nematocysts to secondary tentacles, and

1131   2) at the peripheral region of white spots, supplying nematocysts exclusively to the white spots.

1132   The new evidence that white spots have an opening through which the nematocysts can be

1133   released to the environment is consistent with the hypothesis that the white nematocyst spots (a

1134   putative synapomorphy of Staurozoa) are structures for defense of the gonads and attack,

1135   warranting more direct studies of their function. Future histological studies should include

1136   genera not addressed in this study (*Depastromorpha*, *Depastrum*, *Halimocyathus*, *Kyopoda,*

1137   *Lipkea*, and *Stylocoronella*) in order to access important information on the universality of many

1138   characters discussed here, such as the anatomy of the claustrum.

1139   The challenge to homologize structures of Staurozoa and other cnidarian classes is due to

1140   the fact that a single stauromedusa has characters found in both medusae and polyps of other

1141   medusozoans. Therefore, comprehensive histological surveys associated with robust

1142   phylogenetic frameworks are important for providing a better understanding of the evolution of

1143   Cnidaria. In this context, comparative analyses including different life history stages are also

1144   essential to address the morphological evolution within the phylum.

1145

1146   **ACKNOWLEDGEMENTS**

1147   The authors are grateful to André C. Morandini (IB-USP) for discussions on the

1148   morphology and anatomy of Medusozoa and to Enio Mattos (IB-USP), José Eduardo A. R.

1149   Marian (IB-USP), and Amanda Ferreira e Cunha (IB-USP) for their kind assistance with the

1150   histological procedures and analyses. We are also grateful to James Reimer, Marymegan Daly,

1151   and an anonymous reviewer who helped to improve the quality of the manuscript.

1152

1153   **REFERENCES**

1154   Arai MN. 1997. *A functional biology of Scyphozoa*. London: Chapman & Hall.

1155   Berrill M. 1963. Comparative functional morphology of the Stauromedusae. *Canadian Journal*

1156   *of Zoology* 41:741-752.

1157   Browne ET. 1910. *Reports of the natural history results of the voyage of the SS Discovery in the*

1158   *Antarctic regions in 1901, under Captain R F Scott RN. Coelentera. V. Medusae.* London:

1159   London British Museum (Natural History).

1160   Carlgren O. 1935. Über eine neue Südafrikanische Lucernariidae, *Depastromorpha africana* n.

1161   gen., n. sp., nebst Bemerkungen über den Bau und die Systematik dieser Tiergruppe.

1162   *Kungliga Svenska Vetenskapsakademiens Handlingar*15:1-24.

1163   Carlgren O. 1938. Eine neue südafrikanische Lucernariidae, *Lucernariopsis capensis*. *Kungliga*

1164   *Fysiografiska Sällskapets i Lund Förhandlingar* 8:1-6.

1165   Cartwright P, Nawrocki AM. 2010. Character evolution in Hydrozoa (phylum Cnidaria).

1166   *Integrative and Comparative Biology* 50:456-472.

1167   Chapman DM. 1966. Evolution of the scyphistoma. In: Rees WJ, ed. *The Cnidaria and their*

1168   *Evolution*. Symposia of the Zoological Society of London. London and New York:

1169   Zoological Society of London, Academic Press, 51-75.

1170   Clark HJ. 1863. Prodromus of the history, structure, and physiology of the order Lucernariae.

1171   *Journal of the Boston Society of Natural History* 7:531-567.

1172   Clark HJ. 1878. Lucernariae and their allies. A memoir on the anatomy and physiology of

1173   *Haliclystus auricula* and other Lucernarians, with a discussion of their relations to other

1174   Acalephae; to Beroids, and polypi. *Smithsonian Contributions to Knowledge* 242:1-130.

1175   Collins AG. 2002. Phylogeny of Medusozoa and the evolution of cnidarians life cycles. *Journal*

1176   *of Evolutionary Biology* 15:418-432.

1177   Collins AG, Daly M. 2005. A new deepwater species of Stauromedusae, *Lucernaria janetae*

1178   (Cnidaria, Staurozoa, Lucernariidae), and a preliminary investigation of stauromedusan

1179   phylogeny based on nuclear and mitochondrial rDNA data. *Biological Bulletin* 228:221-230.

1180   Collins AG, Schuchert P, Marques AC, Jankowski T, Medina M, Schierwater B. 2006.

1181   Medusozoan phylogeny and character evolution clarified by large and small subunit rDNA

1182   data and an assessment of the utility of phylogenetic mixture models. *Systematic Biology*

1183   55:97-115.

1184   Conant FS. 1898. The Cubomedusae. *Memoirs of the Biological Laboratory of the Johns*

1185   *Hopkins University* 4:1-61.

1186   Corbin PG. 1978. A new species of the stauromedusan genus *Lucernariopsis* (Coelenterata:

1187   Scyphomedusae). *Journal of the Marine Biological Association of the United Kingdom*

1188   58:285-290.

1189   Davenport J. 1998. Note on the trophic relationships of the stauromedusa *Haliclystus antarcticus*

1190   from subantarctic South Georgia. *Journal of the Marine Biological Association of the United*

1191   *Kingdom* 78:663-664.

1192   Dewel RA. 2000. Colonial origin for Eumetazoa: major morphological transitions and the origin

1193   of Bilaterian complexity. *Journal of Morphology* 243:35-74.

1194   Eckelbarger KJ. 1994. Oocyte nutrition in the lower Metazoa: the Scyphozoa. In: Wilson WH,

1195   Stricker SA, Shinn GL, eds. *Reproduction and development of marine invertebrates*.

1196   Baltimore: John Hopkins University Press, 15-28.

1197   Eckelbarger KJ, Larson RJ. 1993. Ultrastructural study of the ovary of the sessile scyphozoan,

1198   *Haliclystus octoradiatus* (Cnidaria: Stauromedusae). *Journal of Morphology* 218:225-236.

1199   Edmondson CH. 1930. New Hawaiian medusae. Bernice P. *Bishop Museum Occasional Papers*

1200   9:1-16.

1201   Extavour CGM. 2007. Gray anatomy: phylogenetic patterns of somatic gonad structures and

1202   reproductive strategies across the Bilateria. *Integrative and Comparative Biology* 47:420-426.

1203   Garm A, Lebouvier M, Tolunay D. 2015. Mating in the box jellyfish *Copula sivickisi* – novel

1204   function of cnidocytes. *Journal of Morphology* 276:1055-1064.

1205   Goloboff P, Farris J, Nixon K. 2008. TNT, a free program for phylogenetic analysis. *Cladistics*

1206   24:774-786.

1207   Gosse PH. 1860. On the *Lucernaria cyathiformis* of Sars. *The Annals and Magazine of Natural*

1208   *History* 5:480-481.

1209   Gross I. 1900. Zur Anatomie der Lucernariden. *Jenaischen Zeitschrift für Naturwissenschaft*

1210   33:611-624.

1211   Gwilliam GF. 1956. Studies on West Coast Stauromedusae. PhD. Dissertation. Berkeley:

1212   University of California.

1213   Gwilliam GF. 1960. Neuromuscular physiology of a sessile scyphozoan. *Biological Bulletin*

1214   119:454-473.

1215 Haeckel E. 1879. *Das system der medusen. I, 2: System der Acraspeden. Zweite Hälfte des*

1216   *Systems der Medusen*. Jena: Gustav Fischer.

1217 Haeckel E. 1882. Report on the deep-sea medusae dredged by H.M.S. Challenger during the

1218   years 1873-1876. *Report on the scientific results of the voyage H.M.S. Challenger during the*

1219   *years 1873-1876, Zoology* 4:1-154.

1220 Hand C. 1966. On the evolution of the Actiniaria. In: Rees WJ, ed. *The Cnidaria and their*

1221   *Evolution*. London and New York: Zoological Society of London, Academic Press, 135-146.

1222 Hirano YM. 1986. Species of Stauromedusae from Hokkaido, with notes on their

1223   metamorphosis. *Journal of the Faculty of Science, Hokkaido University, Zoology* 24:182-201.

1224 Hirano YM. 1997. A review of a supposedly circumboreal species of stauromedusa, *Haliclystus*

1225   *auricula* (Rathke, 1806). In: den Hartog JC, ed. *Proceedings of the 6th International*

1226   *Conference on Coelenterate Biology*. The Netherlands. Leiden: Nationaal Naturhistorisch

1227   Museum, Noordwijkerhout, 247-252.

1228 Humason GL. 1962. *Animal tissue techniques*. San Francisco: W. H. Freeman and Company.

1229 Hyman LH. 1940. Observations and experiments on the physiology of medusae. *Biological*

1230   *Bulletin* 79:282-296.

1231 Johnston G. 1835. Illustrations in British zoology. *The Magazine of Natural History, and Journal*

1232   *of Zoology, Botany, Mineralogy, Geology, and Meteorology* 8:59-61.

1233 Johnston G. 1847. *A history of the British Zoophytes*. Second Edition, Volume I. London: John

1234   Van Voorst, Paternoster Row.

1235 Kahn AS, Matsumoto GI, Hirano YM, Collins AG. 2010. *Haliclystus californiensis*, a "new"

1236   species of stauromedusa (Cnidaria: Staurozoa) from the northeast Pacific, with a key to the

1237   species of *Haliclystus*. *Zootaxa* 2518:49-59.

1238   Kassianow N. 1901. Studien über das Nervensystem der Lucernariden nebst sonstigen

1239   histologischen Beobachtungen über diese Gruppe. *Zeitschrift für Wisssenschaftliche Zoologie*

1240   69:287-377.

1241   Kier WM. 2012. The diversity of hydrostatic skeletons. *Journal of Experimental Biology*

1242   215:1247-1257.

1243   Kikinger R, Salvini-Plawen LV. 1995. Development from polyp to stauromedusa in

1244   *Stylocoronella* (Cnidaria: Scyphozoa). *Journal of the Marine Biological Association of the*

1245   *United Kingdom* 75:899-912.

1246   Kishinouye K. 1910. Some medusae of Japanese waters. *The Journal of the College of Science,*

1247   *Imperial University of Tokyo* 27:1-35.

1248   Kling O. 1879. Ueber *Craterolophus tethys*. Ein Beitrag zur Anatomie und Histologie der

1249   Lucernarien. *Morphologisches Jahrbuch* 5:141-166.

1250   Korschelt E, Heider K. 1895. *Text-book of the embryology of invertebrates*. Part I: Porifera,

1251   Cnidaria, Ctenophora, Vermes, Enteropneusta, Echinodermata. London: Swan Sonnenschein

1252   & Co., Ld.; New York: Macmillan & Co..

1253   Kramp PL. 1961. Synopsis of the medusae of the world. *Journal of the Marine Biological*

1254   *Association of the United Kingdom* 40:292-303.

1255   Larson RJ. 1980. A new stauromedusa, *Kishinouyea corbini* (Scyphozoa, Stauromedusae) from

1256   the tropical western Atlantic. *Bulletin of Marine Science* 30:102-107.

1257   Larson RJ. 1988. *Kyopoda lamberti* gen.nov., sp.nov., an atypical stauromedusa (Scyphozoa,

1258   Cnidaria) from the eastern Pacific, representing a new family. *Canadian Journal of Zoology*

1259   66:2301-2303.

1260 Larson RJ, Fautin DG. 1989. Stauromedusae of the genus *Manania* (= *Thaumatoscyphus*)

1261 (Cnidaria, Scyphozoa) in the northeast Pacific, including descriptions of new species

1262 *Manania gwilliami* and *Manania handi*. *Canadian Journal of Zoology* 67:1543-1549.

1263 Leuschel H. 1932. Beiträge zur Histologie und Physiologie der Lucernariden. *Zoologische*

1264 *Jahrbücher* 52:338-388.

1265 Lewis C, Long TAF. 2005. Courtship and reproduction in *Carybdea sivickisi* (Cnidaria:

1266 Cubozoa). *Marine Biology* 147:477-483.

1267 Ling SW. 1937. Studies on Chinese Stauromedusae. I. Stauromedusae from Tsingtao. *Amoy*

1268 *Marine Biological Bulletin* 3:1-35.

1269 Ling SW. 1939. Studies on Chinese stauromedusae. II. Further studies on some stauromedusae

1270 from China. *Lingnan Science Journal* 18:281-291, 495-503.

1271 Mahoney R. 1966. *Laboratory techniques in Zoology*. London: Butterworth & Co..

1272 Marques AC, Collins AG. 2004. Cladistic analysis of Medusozoa and cnidarian evolution.

1273 *Invertebrate Biology* 123:32-42.

1274 Marques AC, García J, Ames CL. 2015. Internal fertilization and sperm storage in cnidarians: a

1275 response to Orr and Brennan. *Trends in Ecology and Evolution* 30:435-436.

1276 Mayer AG. 1910. *Medusae of the world*. Volume III. Scyphomedusae. Washington: Carnegie

1277 Institution Publishing, Publication 109.

1278 Mills CE, Hirano YM. 2007. Stauromedusae. In: Denny MW, Gaines SD, eds. *Encyclopedia of*

1279 *tidepools and rocky shores*. Berkeley: University of California Press, 541-543.

1280 Miranda LS, Morandini AC, Marques AC. 2009. Taxonomic review of *Haliclystus antarcticus*

1281 Pfeffer, 1889 (Stauromedusae, Staurozoa, Cnidaria), with remarks on the genus *Haliclystus*

1282 Clark, 1863. *Polar Biology* 32:1507-1519.

1283   Miranda LS, Collins AG, Marques AC. 2010. Molecules clarify a cnidarian life cycle – the

1284   "hydrozoan" *Microhydrula limopsicola* is an early life stage of the staurozoan *Haliclystus*

1285   *antarcticus*. *PLoS ONE* 5:e10182.

1286   Miranda LS, Haddad MA, Mills CE, Marques AC. 2012. *Lucernariopsis capensis* Carlgren,

1287   1938 (Cnidaria, Staurozoa) in Brazil: first record outside its type locality in South Africa.

1288   *Zootaxa* 3158:60-64.

1289   Miranda LS, Collins AG, Marques AC. 2013. Internal anatomy of *Haliclystus antarcticus*

1290   (Cnidaria, Staurozoa) with a discussion on histological features used in staurozoan taxonomy.

1291   *Journal of Morphology* 274:1365-1383.

1292   Miranda LS, Collins AG, Marques AC. 2015. Is *Haootia quadriformis* related to extant

1293   Staurozoa (Cnidaria)? Evidence from the muscular system reconsidered. *Proceedings of the*

1294   *Royal Society B, Biological Sciences* 282:20142396.

1295   Miranda LS, Hirano YM, Mills CE, Falconer A, Fenwick D, Marques AC, Collins AG. 2016.

1296   Systematics of stalked jellyfishes (Cnidaria: Staurozoa). *PeerJ* 4:e1951.

1297   Müller OF. 1776. *Zoologiae Danicae Prodromus, seu animalium Daniae et Norvegiae*

1298   *indigenarum, Characteres, Nomina et Synonyma imprimis popularium*. Havniae: Typis

1299   Hallageriis.

1300   Nakanishi N, Yuan D, Hartenstein V, Jacobs DK. 2010. Evolutionary origin of rhopalia: insights

1301   from cellular-level analyses of Otx and POU expression patterns in the developing rhopalial

1302   nervous system. *Evolution & Development* 12:404-415.

1303   Naumov DV. 1961. Stsifoidnye meduzy morei SSSR (Scyphozoan medusae in the sea of USSR).

1304   *Opredeliteli po Faune SSSR* 75:1-98.

1305 Nielsen C. 2008. Six major steps in animal evolution: are we derived sponge larvae? *Evolution &*

1306   *Development* 10:241-257.

1307 Okubo T. 1917. Preliminary note on a new genus of Stauromedusae from Hokkaido. *Zoological*

1308   *Magazine, Tokyo* 29:317-322.

1309 Otto JJ. 1976. Early development and planula movement in *Haliclystus* (Scyphozoa,

1310   Stauromedusae. In: Mackie GO, ed. *Coelenterate Ecology and Behavior*. New York: Plenum

1311   Press, 319-329.

1312 Pisani V, Otero-Ferrer F, Lotto S, Maurel P, Goy J. 2007. *Lipkea ruspoliana* Vogt, 1887

1313   (Stauromedusae, Scyphozoa, Cnidaria) dans les aquariums du Musée Océanographique de

1314   Monaco. *Bulletin de la Société Zoologique de France* 132:183-190.

1315 Prell H. 1910. Beiträge zur Kenntnis der Lebensweise einiger Pantopoden. *Bergens Museums*

1316   *Aarbog* 10:1-30.

1317 Redikorzev V. 1925. Die Lucernose des Weißen Meeres. *Zoologischer Anzeiger* 62:155-157.

1318 Satterlie RA, Thomas KS, Gray GC. 2005. Muscle organization of the cubozoan jellyfish

1319   *Tripedalia cystophora* Conant 1897. *Biological Bulletin* 209:154-163.

1320 Schiariti A, Christiansen E, Morandini AC, da Silveira FL, Giberto DA, Mianzan HW. 2012.

1321   Reproductive biology of *Lychnorhiza lucerna* (Cnidaria: Scyphozoa: Rhizostomeae):

1322   individual traits related to sexual reproduction. *Marine Biology Research* 8:255-264.

1323 Stangl K, Salvini-Plawen LV, Holstein TW. 2002. Staging and induction of medusa

1324   metamorphosis in *Carybdea marsupialis* (Cnidaria, Cubozoa). *Vie Milieu* 52:131-140.

1325 Thiel H. 1966. The evolution of Scyphozoa: a review. In: Rees WJ, ed. *The Cnidaria and their*

1326   *Evolution*. London and New York: Zoological Society of London, Academic Press, 77-118.

1327 Tiemann H, Jarms G. 2010. Organ-like gonads, complex oocyte formation, and long-term

1328   spawning in *Periphylla periphylla* (Cnidaria, Scyphozoa, Coronatae). *Marine Biology*

1329   157:527-535.

1330 Uchida T. 1929. Studies on the Stauromedusae and Cubomedusae, with special reference to their

1331   metamorphosis. *Japanese Journal of Zoology* 2:103-193.

1332 Uchida T, Hanaoka K-I. 1933. On the morphology of a stalked medusa, *Thaumatoscyphus*

1333   *distinctus* Kishinouye. *Journal of the Faculty of Science, Hokkaido Imperial University,*

1334   *Series VI, Zoology* 2:135-153.

1335 Uchida T, Hanaoka K-I. 1934. Anatomy of two stalked medusae with remarks on the distribution

1336   of the Stauromedusae in Japan. *Journal of the Faculty of Science, Hokkaido Imperial*

1337   *University, Series VI, Zoology* 2:209-219.

1338 Van Iten H, Leme JM, Simões MG, Marques AC, Collins AG. 2006. Reassessment of the

1339   phylogenetic position of Conulariids (?Ediacaran-Triassic) within the subphylum Medusozoa

1340   (phylum Cnidaria). *Journal of Systematic Palaeontology* 4:109-118.

1341 Weill R. 1925. Foyers de formation et voies de migration des nématocystes de *Halyclistus* [SIC]

1342   *octoradiatus* Clark. Existence, sur leur parcours, de réservoirs sélectifs. *Comptes Rendus*

1343   *Hebdomadaires des Séances de l'Académie des* Sciences 180:327-330.

1344 Weill R. 1935. Les "réservoirs sélectifs" et la maturation des nématocystes de *Lucernaria*

1345   *campanulata* Lam. *Comptes Rendus Hebdomadaires des Séances de l'Académie des Sciences*

1346   120:774-777.

1347 Wietrzykowski W. 1911. Seconde note sur le développement des Lucernaires. *Archives de*

1348   *Zoologie Expérimentale et Générale, 5th Series* 6:49-52.

1349   Wietrzykowski W. 1912. Recherches sur le développement des Lucernaires. *Archives de*

1350   *Zoologie Expérimentale et Générale, 5th Series* 10:1-95.

Species of Staurozoa analyzed in this study, with respective localities, voucher catalog numbers, and slides catalog numbers.

LEM: Laboratory of Marine Evolution of the Institute of Biosciences, University of São Paulo;

MZUSP: Museum of Zoology of the University of São Paulo, Brazil; USNM: National Museum of

Natural History, Smithsonian Institution, USA.

Family	Species	Locality	Voucher catalog number	Slides catalog number
Haliclystidae	*Haliclystus tenuis*	Muroran, Hokkaido, Japan	USNM 1106652	LEM 09
	Manania uchidai	Muroran, Hokkaido, Japan	USNM 1106645	LEM 10
Lucernariidae	*Lucernaria quadricornis*	Chupa Inlet, Kandalaksha Bay, Russia	USNM 1106240	LEM 11
	Lucernaria bathyphila	Nicolskaya Inlet, Kandalaksha Bay, Russia	USNM 1106643	LEM 12
	Lucernaria sainthilairei	Cross Islands, close to the Biological Station of Moscow State University, Russia	USNM 1102446	LEM 13
Kishinouyeidae	*Calvadosia corbini*	Aracruz, Espírito Santo, Brazil	MZUSP 1563	LEM 14
	Calvadosia cruciformis	Muroran, Hokkaido, Japan	USNM 1106656	LEM 15
	Calvadosia vanhoeffeni	Janus Island, Palmer Archipelago, Antarctica	USNM 79939	LEM 16
Craterolophidae	*Craterolophus convolvulus*	Woods Hole , Massachusetts, USA	USNM 54321	LEM 17

Abbreviations of structures reported in the figures.

Abbreviations	Structures
ac	axial canal
am	arm
an	anchor
ar	accessory radial pocket
AR	adradii
ax	auxiliary radial pocket
bn	battery of nematocysts
ci	cilium
cl	calyx
cm	coronal muscle
cs	claustrum
ep	epidermis
ex	exumbrella
fc	follicle cells
ga	gametoduct
gd	gonad
gf	gastric filament
gp	gastric radial pocket
gt	gastrodermis
gvc	gastrovascular cavity
il	intertentacular lobules
in	infundibulum
IR	interradii
ito	immature oocytes
iv	invagination
kb	knob
mc	manubrial corner
mn	manubrium
mnm	mature nematocysts
ms	mesoglea
mto	mature oocytes
mu	interradial longitudinal muscle/longitudinal muscle
nm	nematocyst
nmb	nematoblast
oo	oocytes
ot	ostia
pa	pads
pam	paired arms
pc	perradial chamber
pd	pedal disk
pe	peduncle
pr	principal radial pocket
PR	perradii
pt	primary tentacle

sb	subumbrella
sc	spermatocytes
sp	septum
st	stem
sz	spermatozoa
tc	tentacles
usp	"U-shaped" space
vs	vesicle
ws	white spots of nematocysts

Matrix of internal anatomy characters for the staurozoan genera.

Information from Gosse (1860), Clark (1863), Mayer (1910), Uchida (1929), Uchida & Hanaoka (1933, 1934), Carlgren (1935), Ling (1937), Kramp (1961), Larson (1980, 1988), Hirano (1986, 1997), Larson & Fautin (1989), Kikinger & Salvini-Plawen (1995), Marques & Collins (2004), Collins & Daly (2005), Collins et al. (2006), Van Iten et al. (2006), Pisani et al. (2007), Miranda et al. (2016), and this study. Information that was not available (or not confirmed) was coded as a question mark (?) and non-comparable structures were coded in the matrix as N. Polymorphic characters have states indicated. **1: Longitudinal muscles in peduncle.** (0) present; (1) absent. Four interradial, intramesogleal longitudinal muscles associated with infundibula were considered symplesiomorphic for Staurozoa, shared by staurozoan ancestor with some other medusozoans (Collins et al., 2006; Miranda et al., 2016). **2: Coronal muscle.** (0) entire; (1) divided. Coronal muscle may be divided into eight sections by the adradial arms or entire (Miranda et al., 2016). Coronal muscle entire would be a putative symplesiomorphy of Staurozoa (Miranda et al., 2016). *Haliclystus inabai* has been described with entire coronal muscle (Hirano, 1986). It is not clear in the original description if the coronal muscle of *Halimocyathus platypus* is entire or divided (Clark, 1863). *Stylocoronella* has vestigial coronal muscle (Kikinger & Salvini-Plawen, 1995). **3: Number of chambers in peduncle.** (0) peduncle one-chambered; (1) peduncle four-chambered; (2) peduncle 4/1 chambered. The peduncle four-chambered is hypothesized as a synapomorphy of Staurozoa, as the four perradial chambers in the peduncle of stauromedusae are not found in any other cnidarian (Collins & Daly, 2005; Miranda et al., 2016). The species with 4/1-chambered peduncle have four chambers basally and one chamber at the middle of the peduncle (Miranda et al., 2016). Some species of *Manania* have also been described with one chamber throughout the peduncle or one chamber basally and 4 chambers in the middle of the peduncle, and this character should be investigated in detail for the genus (see Uchida, 1929; Hirano, 1986; and Miranda et al., 2016 for discussion on changes during development).

Kyopoda has a unique peduncular anatomy, containing the stomach and gonads (see Larson, 1988), and more detailed information is necessary to code this state. **4: Claustrum.** (0) absent; (1) present. The claustrum as a potential symplesiomorphy of Staurozoa (Thiel, 1966; Collins & Daly, 2005) is equivocal (Miranda et al., 2016), and detailed histological studies of the outgroup taxa are need to ground homology hypotheses. **5: White spots of nematocysts.** (0) absent; (1) present. White spots of nematocysts is a putative synapomorphy of Staurozoa (see text for further details). Some species of *Haliclystus* (*H. auricula* and *H. antarcticus*) do not have white spots (see Hirano, 1997; Miranda, Morandini & Marques, 2009). **6: Internal tips of arms (intertentacular lobules X U-shaped space).** (0) absent; (1) internal tips of arms with intertentacular lobules; (2) internal tips of arms with U-shaped-space. Intertentacular lobules in the internal tips of arms is a putative synapomorphy of Staurozoa (see text). Some species of *Haliclystus* (*H. tenuis*, *H. borealis*, and *H. californiensis*) have a U-shaped space in the internal tips of arms (Hirano, 1997). Coding is uncertain for *Depastromorpha*, but according to the illustrations of the original description *D. africana* (single species of the genus) seems to have intertentacular lobules (Carlgren, 1935). This character is probably not applicable in *Lipkea* because marginal lobes (or lappets) cannot be undoubtedly homologized with arms or anchors (Miranda et al., 2016). **7: Gametoduct.** (0) absent; (1) present. Gametoduct is a putative synapomorphy of Staurozoa (although additional information about the presence of this structure in other cnidarians is still necessary; see Tiemann & Jarms, 2010). **8: Anchors.** (0) absent; (1) present. Anchors are metamorphosed eight primary tentacles (perradial and interradial) (Wietrzykowski, 1912). Polyp primary tentacles are a potential symplesiomorphy of Staurozoa (Collins et al., 2006; Miranda et al., 2016). Some species of *Calvadosia* retain primary tentacles, with a modified shape (*C. cruciformis*, *C. tsingtaoensis*; Ling, 1937, 1939). Anchors have a swollen, adhesive base, but can retain a remnant of primary tentacle (Larson & Fautin, 1989; Kahn et al. 2010). **9: Ostia.** (0) present; (1) absent. Stauromedusae have an interradial ostium between two adjacent gastric radial pockets (or accessory radial pockets in species with claustra). Comparable structures, such as the septal ostium or connecting canal,

have been observed in Scyphozoa (Korschelt & Heider, 1895; Chapman, 1966) and Cubozoa (Conant, 1898). Although further detailed studies are necessary to assess homology across taxa, we consider ostia between adjacent gastric radial pockets a symplesiomorphy of Staurozoa. **10: Pad-like adhesive structures.** (0) absent; (1) presence of pads in the outermost tentacles; (2) presence of pads on the tips of arms, connected to the stem of secondary tentacles; (3) presence of pads on the tips of arms, externally separated from the stem of the secondary tentacles. The presence of pad-like adhesive structures in the outermost secondary tentacles is a putative synapomorphy of Staurozoa (see text). Some species of *Calvadosia* (*C. capensis*, *C. corbini*, *C. hawaiiensis*, and *C. tasmaniensis*) have broad pads on the tips of arms (Miranda et al., 2016). *Calvadosia cruxmelitensis* has a particular adhesive pad-like structure on the tip of each arm, in which the secondary tentacles arise directly from this structure (Corbin, 1978; Miranda et al., 2016). This character is probably not applicable in *Lipkea* because marginal lobes (or lappets) cannot be undoubtedly homologized with arms or anchors, and capitate secondary tentacles cannot be recognized (Pisani et al., 2007; Miranda et al., 2016).

Staurozoan genera	1	2	3	4	5	6	7	8	9	10
Calvadosia	1	1	2	0	1	1	1	0	0	1
Craterolophus	1	1	1	1	1	1	1	0	0	1
Depastromorpha	0	0	1	1	1	1(?)	?	1	?	1
Depastrum	0	0	1	1	1	?	?	0	?	0
Haliclystus	0	0/1	1	0	0/1	1/2	1	1	0	0/1
Halimocyathus	0	?	1	1	1	?	?	1	?	1
Kyopoda	0	0	?	0	1	?	?	1	?	1
Lipkea	0	0	0	0	1	N(?)	?	0	?	N(?)
Lucernaria	0	1	0	0	1	1	1	0	0	0
Manania	0	0	1	1	1	1	1	1	0	1
Stylocoronella	0	?	0	0	1	?	?	0	?	0

Figure 1

Molecular phylogenetic hypothesis (based on markers COI, 16S, ITS, 18S, and 28S) of relationship between species of Staurozoa, with its derived classification (Miranda et al., 2016).

*Species included in this histological study. "?" Groups not included in the molecular analysis, classified according to morphological evidence. EPR, East Pacific Rise; UK, The United Kingdom; USA, The United States of America.
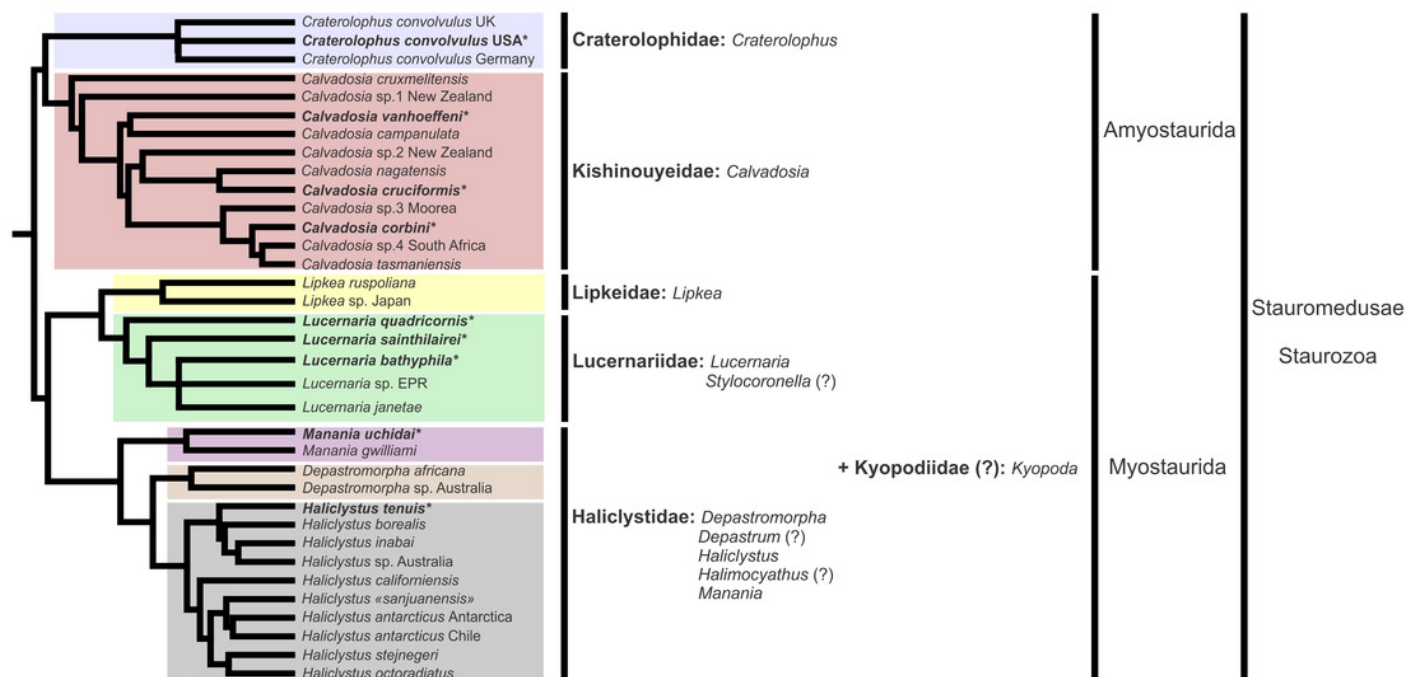
Figure 2

General organization of the body plan of stalked jellyfishes.

A) Scheme of a longitudinal section at interradii; B) scheme of a longitudinal section at perradii (species without claustrum); C) scheme of a longitudinal section at adradii (species without claustrum; the species with claustra do not have adrarial gonads); D) scheme of a longitudinal section at perradii (species with claustra) (modified from Miranda, Collins & Marques, 2013); *Haliclystus tenuis*: E) lateral view (exumbrellar); F) oral view (subumbrellar); *Calvadosia cruciformis*: G) basal view (exumbrellar); H) oral view (subumbrellar); *Manania uchidai*: I) lateral view (exumbrellar); J) margin of subumbrella. Legend (A-D): black, epidermis; blue, longitudinal muscle; gray, mesoglea; green, gonads; red, gastrodermis. See Table 2 for abbreviations.
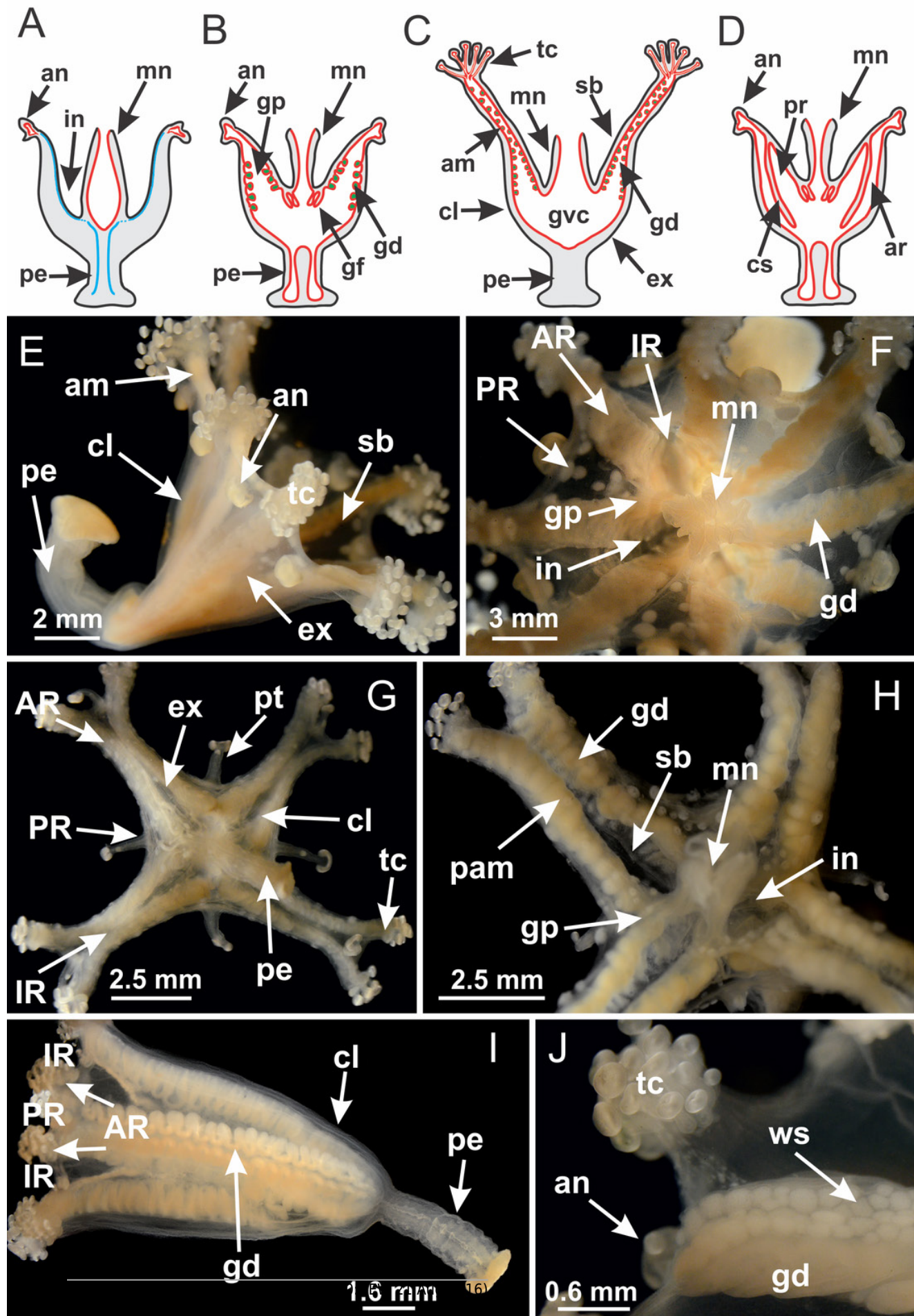
Figure 3

General view of *Haliclystus tenuis.*

A) General view of body; B, C) detail of calyx and peduncle; D) gonad and arms in calyx; E) anchor, coronal muscle, and white spots; F) general view of the subumbrella showing gonads and tentacles; G) detail of gonads and white spots; H) detail of manubrium; I) tentacular cluster. See Table 2 for abbreviations.
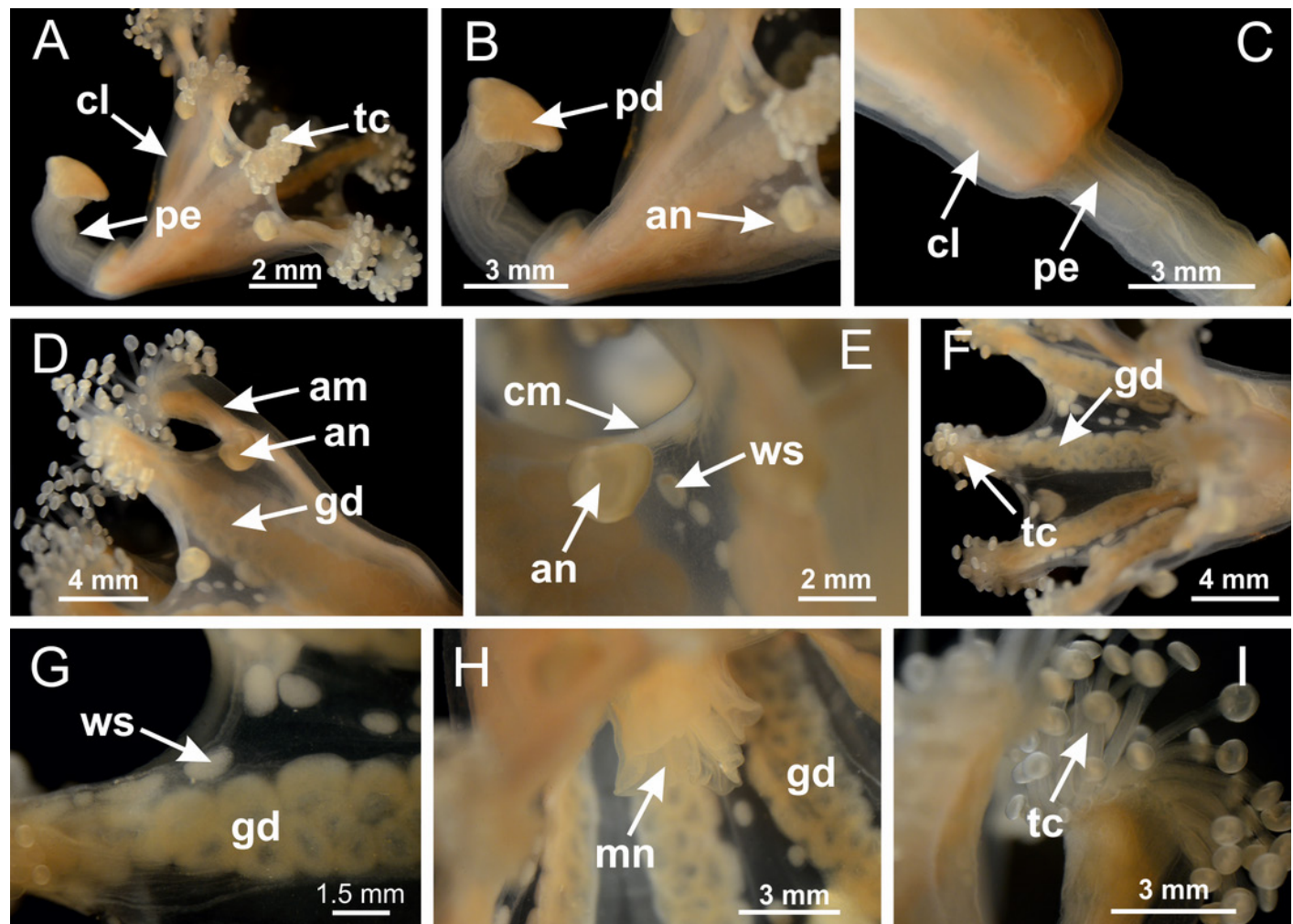
Figure 4

Peduncle and septa of *Haliclystus tenuis* (from base moving upward in A-J).

A-C) Organization of four perradial chambers and four interradial longitudinal muscles in peduncle; D-G) connection of the four perradial chambers in the region between peduncle and calyx, defining one central chamber; H) gastrodermis envelops interradial longitudinal muscle (indicated by black arrow), defining septum; I, J) detail of septum, with infundibulum delimited by epidermis, lateral gonads and gastric filaments. A-J: cross sections. See Table 2 for abbreviations.
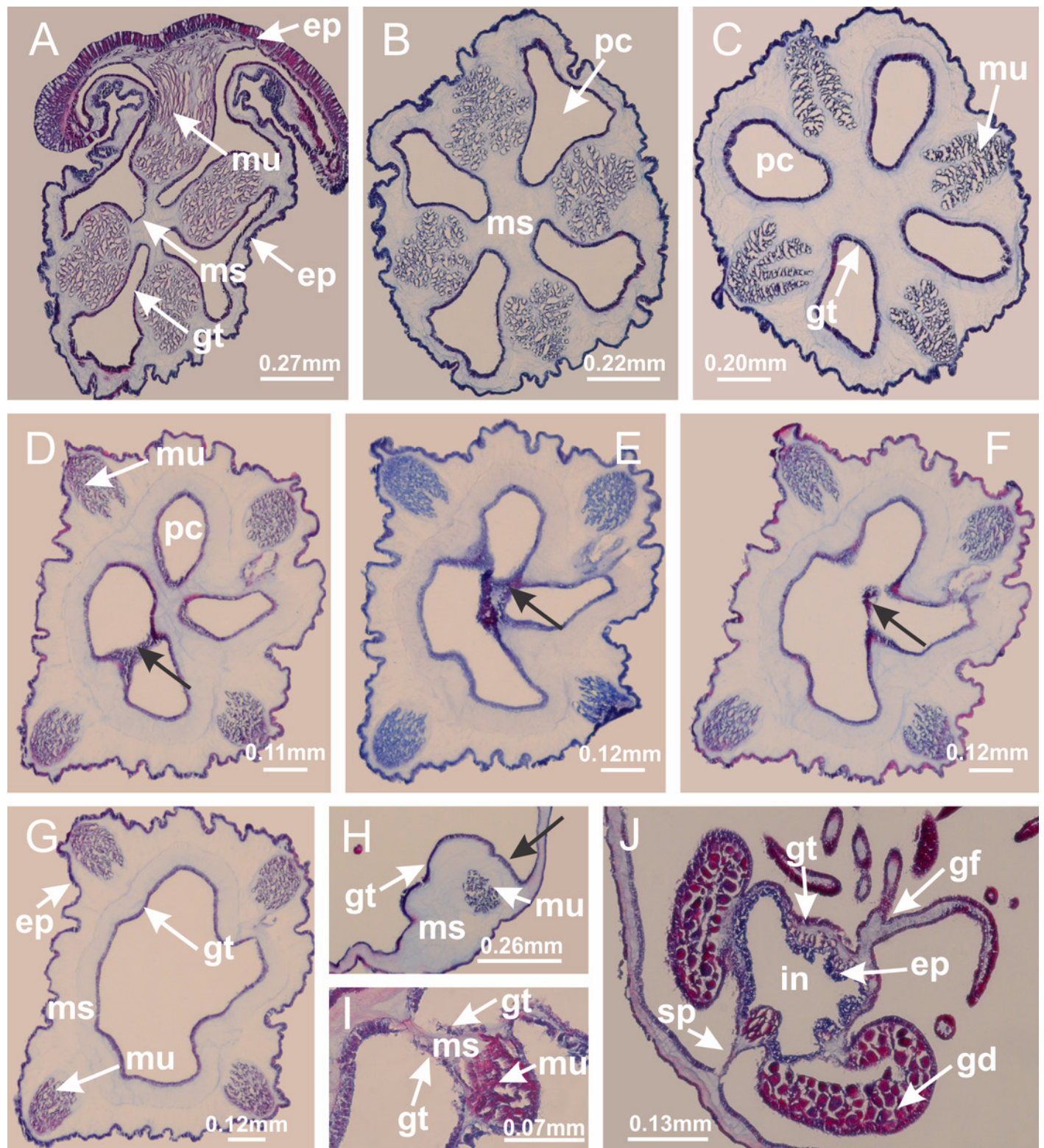
Figure 5

Muscular system.

Manania uchidai: A, B) interradial longitudinal muscles in peduncle; ***Lucernaria sainthilairei***: C) interradial longitudinal muscle in peduncle; D) interradial longitudinal muscle in calyx; ***Calvadosia vanhoeffeni***: E) absence of interradial longitudinal muscle in peduncle (indicated by black arrow); F) interradial longitudinal muscle associated with septum at peduncle/calyx connection; G) interradial longitudinal muscle associated with septum at base of calyx; H) interradial longitudinal muscle in calyx, divided into two bands; ***Calvadosia corbini***: I) absence of interradial longitudinal muscle in peduncle; J) interradial longitudinal muscle associated with septum at peduncle/calyx connection; K) interradial longitudinal muscle associated with septum at base of calyx; L) interradial longitudinal muscle in calyx, divided into two bands; ***Haliclystus tenuis***: M) organization of muscular system in the region between calyx and arms (division of arms at perradial region occurs first than at interradial region; one band of longitudinal muscle toward each arm); ***M. uchidai***: N) coronal muscle at the margin of calyx; ***C. corbini***: O) detail of coronal muscle; P) detail of interradial longitudinal muscle; ***H. tenuis***: Q) muscular organization in arms (one central band of longitudinal muscle, and two lateral bands of coronal muscle); ***C. vanhoeffeni***: R, S) longitudinal muscle toward secondary tentacles; ***C. corbini***: T) longitudinal muscle toward secondary tentacles, U) longitudinal muscle in the stem of secondary tentacles; ***H. tenuis***: V) longitudinal muscle in the stem of secondary tentacles. A-U: cross sections; V: longitudinal section. See Table 2 for abbreviations.
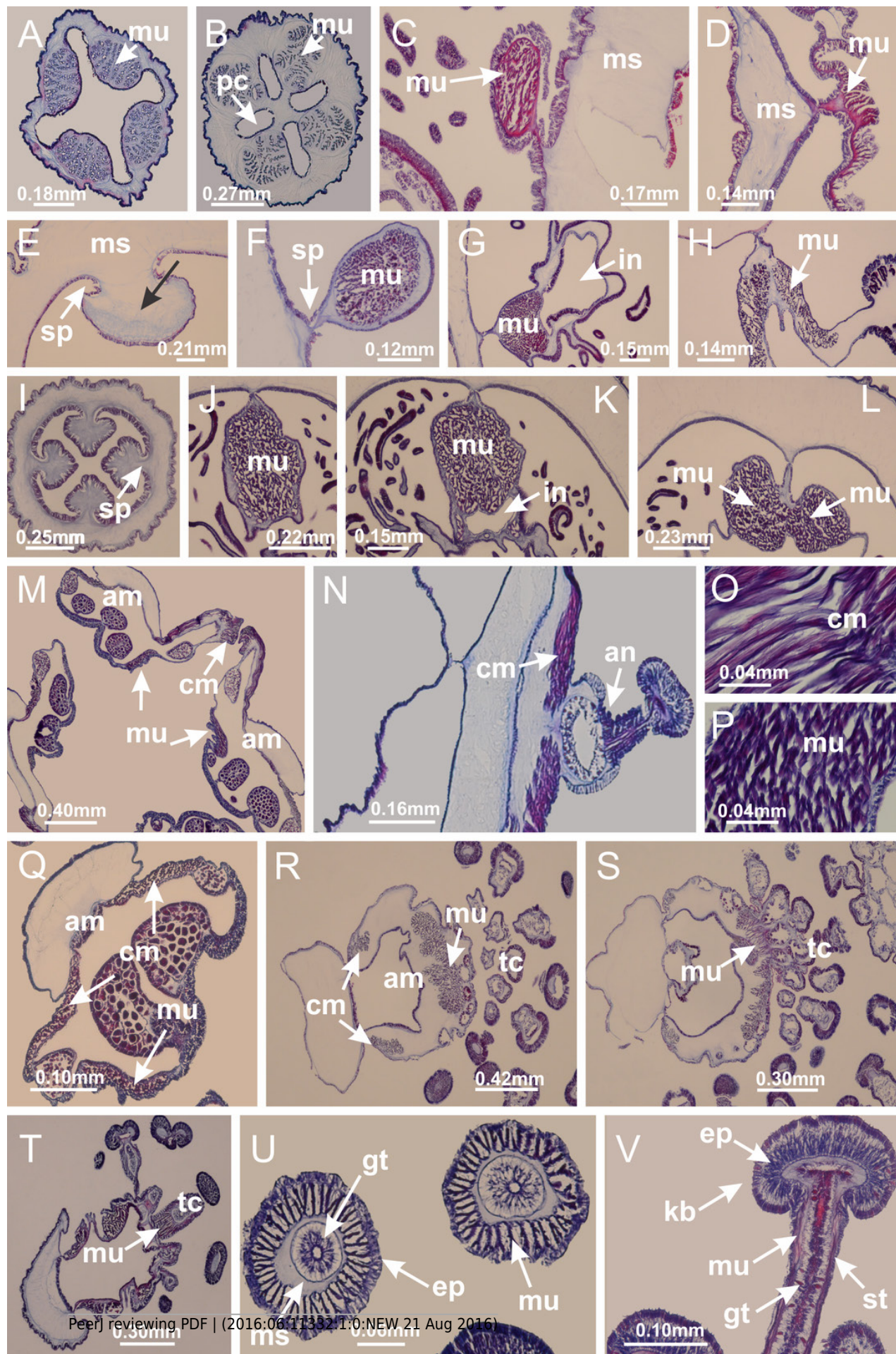
Figure 6

Manubrium and gastric radial pockets.

Haliclystus tenuis: A) internal organization at calyx base, below manubrium delimitation; B-D) gastrodermis of adjacent septa gradually merges (indicated by black arrows), delimiting gastrodermis of manubrium and gastrodermis of gastric radial pockets; E-G) epidermis of adjacent septa (infundibula) gradually merges (indicated by black arrows), delimiting epidermis of manubrium and epidermis of gastric radial pockets; H) internal organization at base of manubrium; I-N) manubrium and gastric radial pockets with gonads; gastric radial pockets separated by interradial septa; O) internal organization of manubrium completely delimited; P) manubrium corner. A-P: cross sections. See Table 2 for abbreviations.
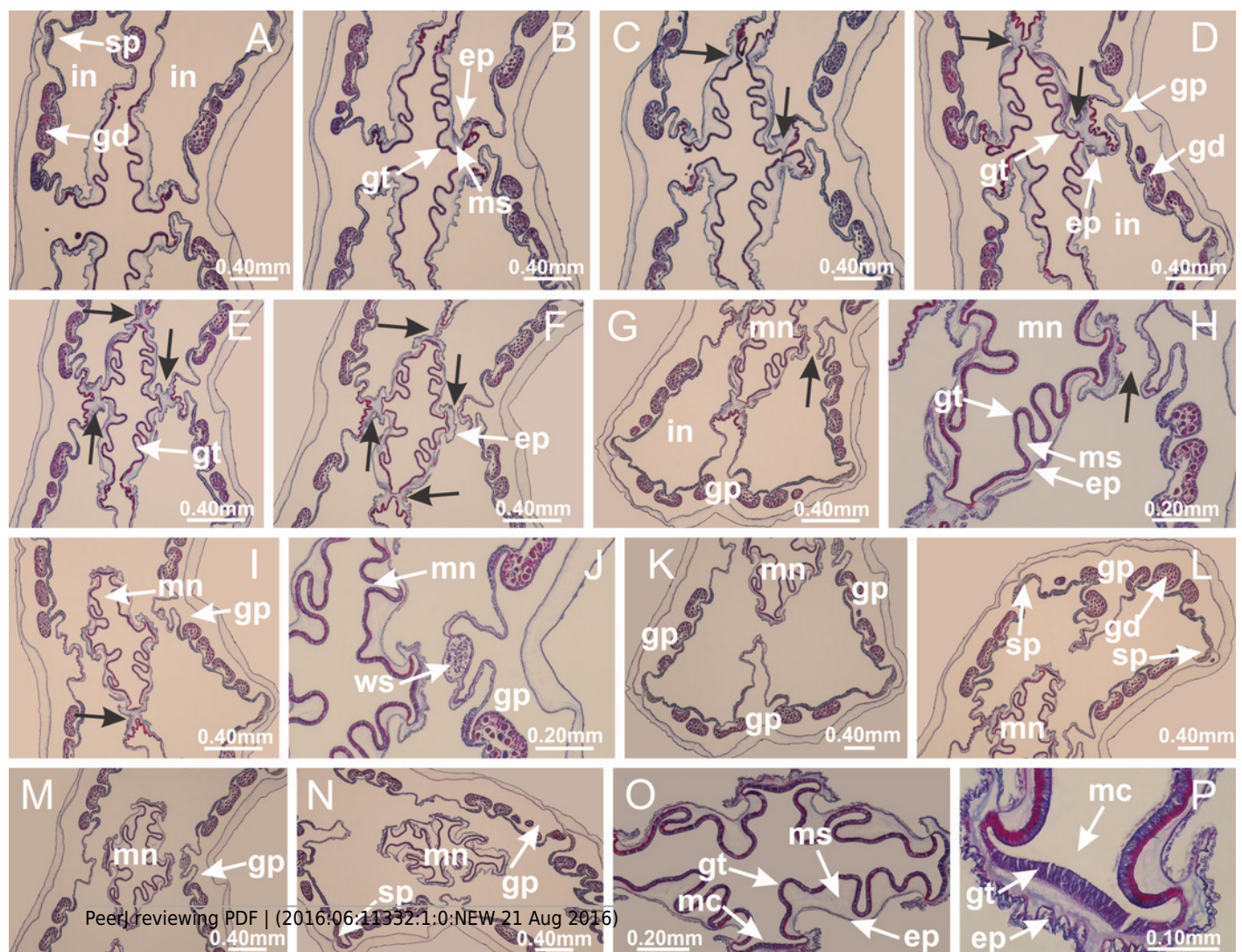
Figure 7

Gastric filaments.

Calvadosia corbini: A-C) formation of gastric filaments through lateral evagination of septal gastrodermis; D-F) gastric filaments associated with gastric radial pockets; ***Lucernaria quadricornis***: G) formation of gastric filaments through lateral evagination of septal gastrodermis; ***Calvadosia vanhoeffeni***: H) formation of gastric filaments through lateral evagination of septal gastrodermis; ***Manania uchidai***: I) gastric filaments; ***Craterolophus convolvulus***: J) gastric filaments. A-J: cross sections. See Table 2 for abbreviations.
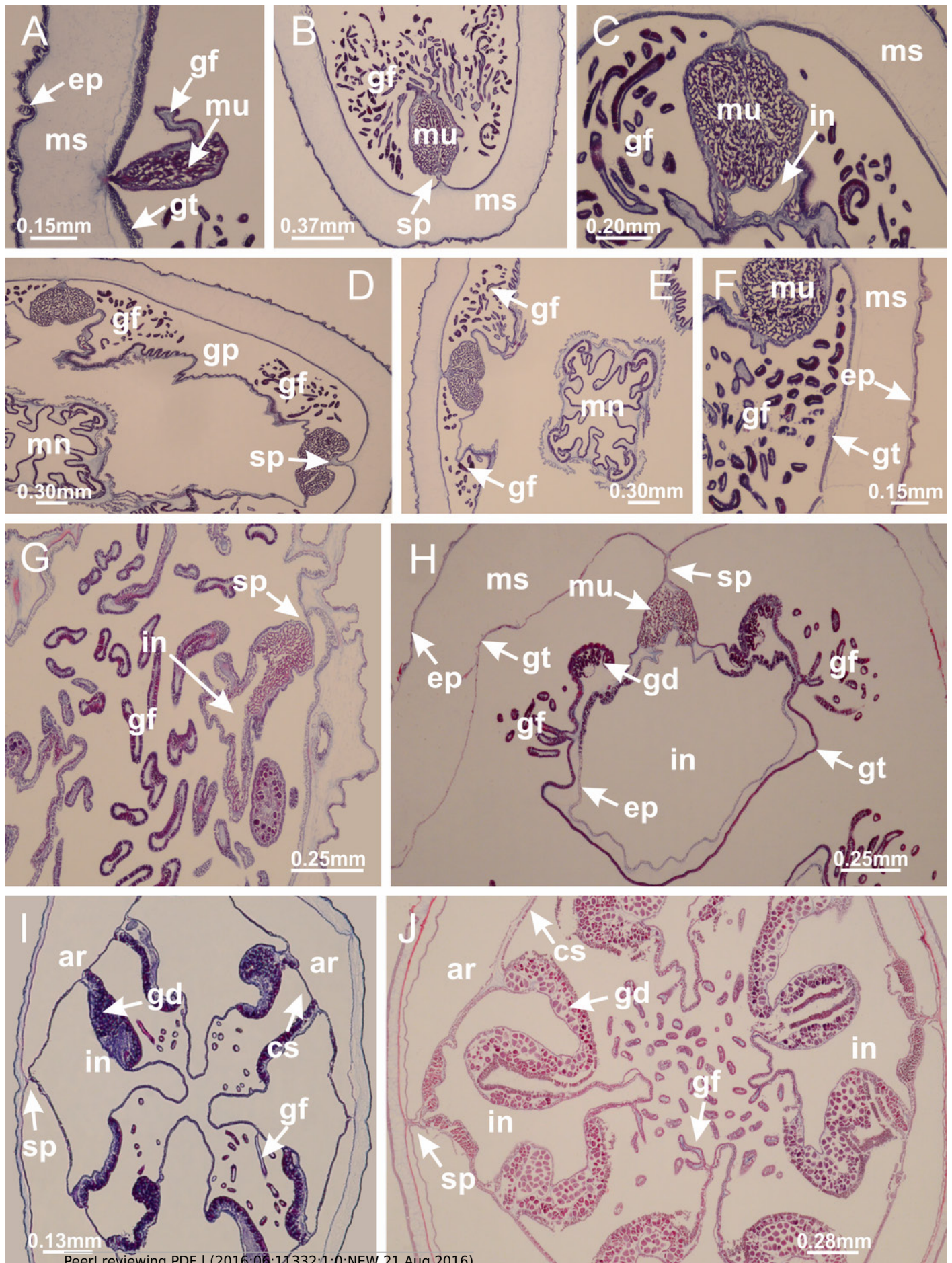
Figure 8

Gonads and gametoduct of *Haliclystus tenuis.*

A) Female vesicle, with peripheral layer of immature oocytes, adjacent to gastrodermis, and a central layer of mature oocytes, adjacent to epidermis; B) general view of vesicles inside gastric radial pockets; C) detail of immature and mature oocytes; D-G) sequence of gametoduct connecting the mature oocytes with gastrovascular cavity; H-M) sequence of gametoduct connecting the mature oocytes with gastrovascular cavity, in two adjacent vesicles; N, O) detail of gametoduct. A-N: cross sections; O: longitudinal section. See Table 2 for abbreviations.
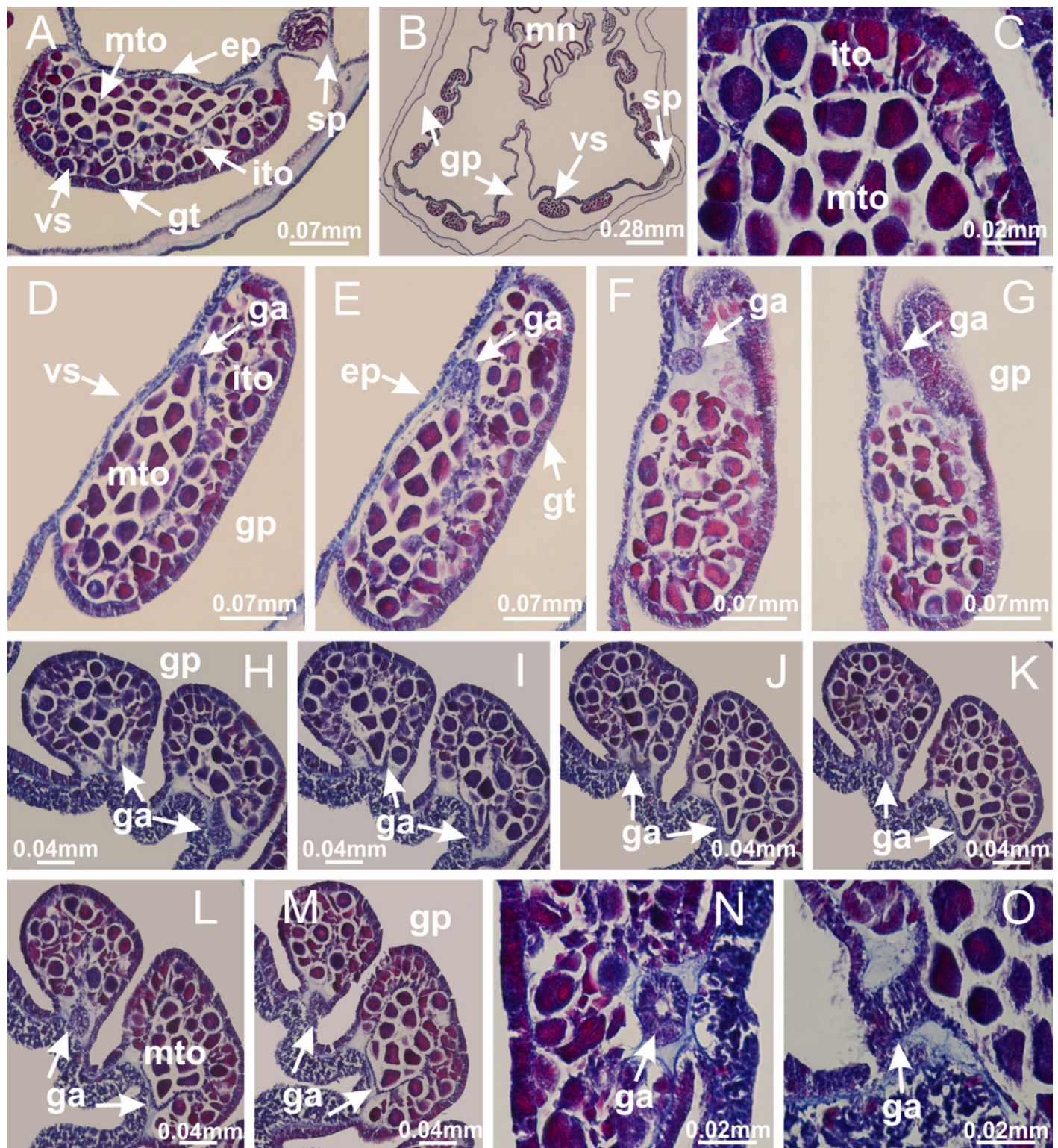
Figure 9

Perradial anchors and perradial primary tentacles.

Haliclystus tenuis: A-H) gastrodermis of the hollow perradial anchor connecting with gastrodermis of calyx, through the stem of anchor (indicated by black arrows); I) general view of anchor at calyx margin; **Calvadosia cruciformis**: J-S) gastrodermis of the hollow perradial primary tentacle connecting with gastrodermis of calyx, through the stem of primary tentacle (indicated by black arrows); L) detail of the nematocysts present in the knob of primary tentacle. A-S: longitudinal sections of anchors and primary tentacles (cross sections of animals). See Table 2 for abbreviations.
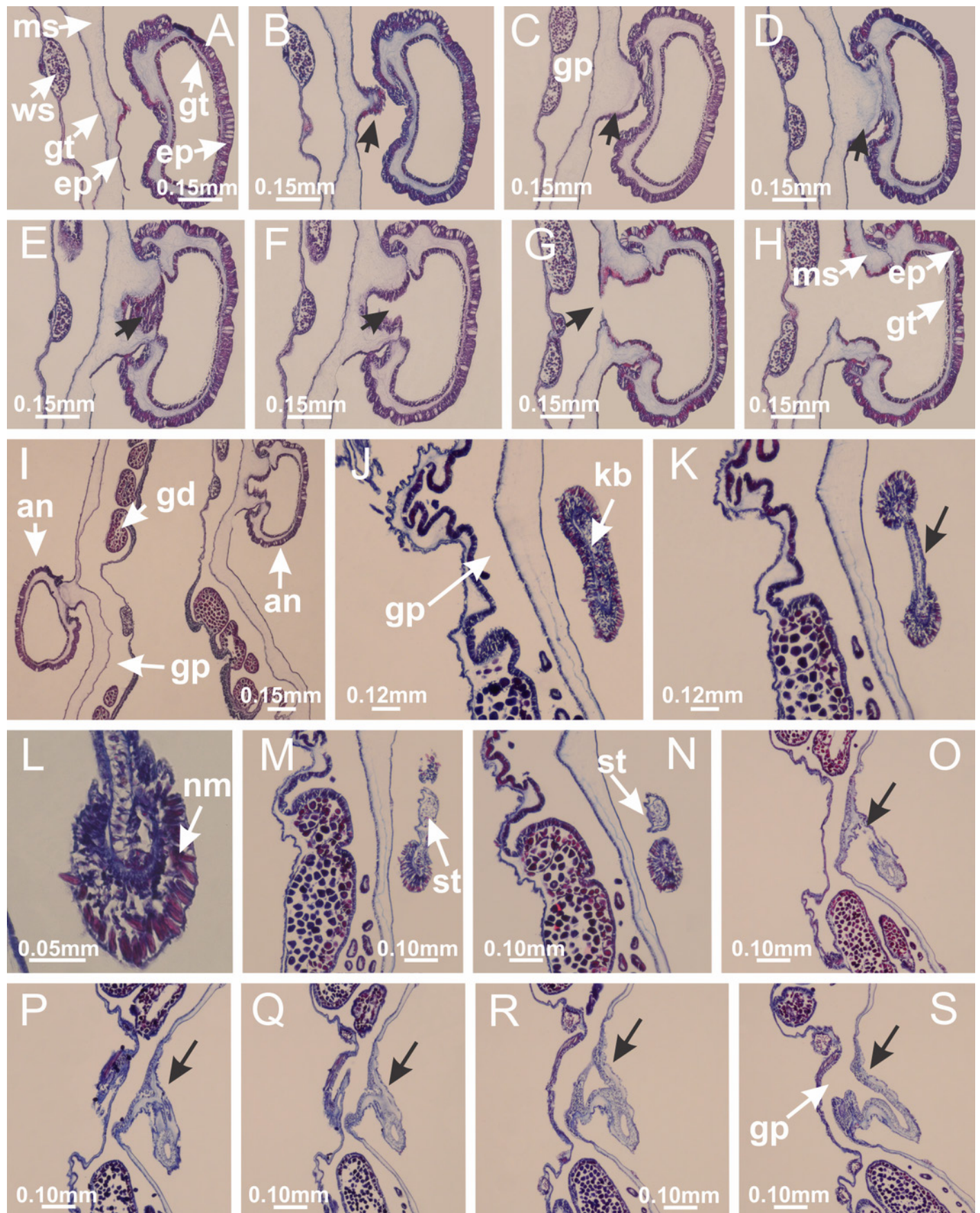
Figure 10

Interradial anchors, interradial primary tentacles, and ostia.

Haliclystus tenuis: A-F) gastrodermis of hollow interradial anchor connecting with gastrodermis of calyx (indicated by black arrow), through the stem of anchor, by means of small ostium; **Calvadosia cruciformis**: G-L) gastrodermis of hollow interradial primary tentacle connecting with gastrodermis of calyx (indicated by black arrow), through the stem of primary tentacle, by means of small ostium; **Calvadosia vanhoeffeni**: M-O) septum detaches from layer of gastrodermis of calyx, forming an ostium, connecting two adjacent gastric radial pockets; **Calvadosia corbini**: P-U) septum detaches from layer of gastrodermis of calyx, forming an ostium, connecting two adjacent gastric radial pockets (indicated by black arrows). A-U: cross sections (A-L: longitudinal sections of anchors and primary tentacles). See Table 2 for abbreviations.
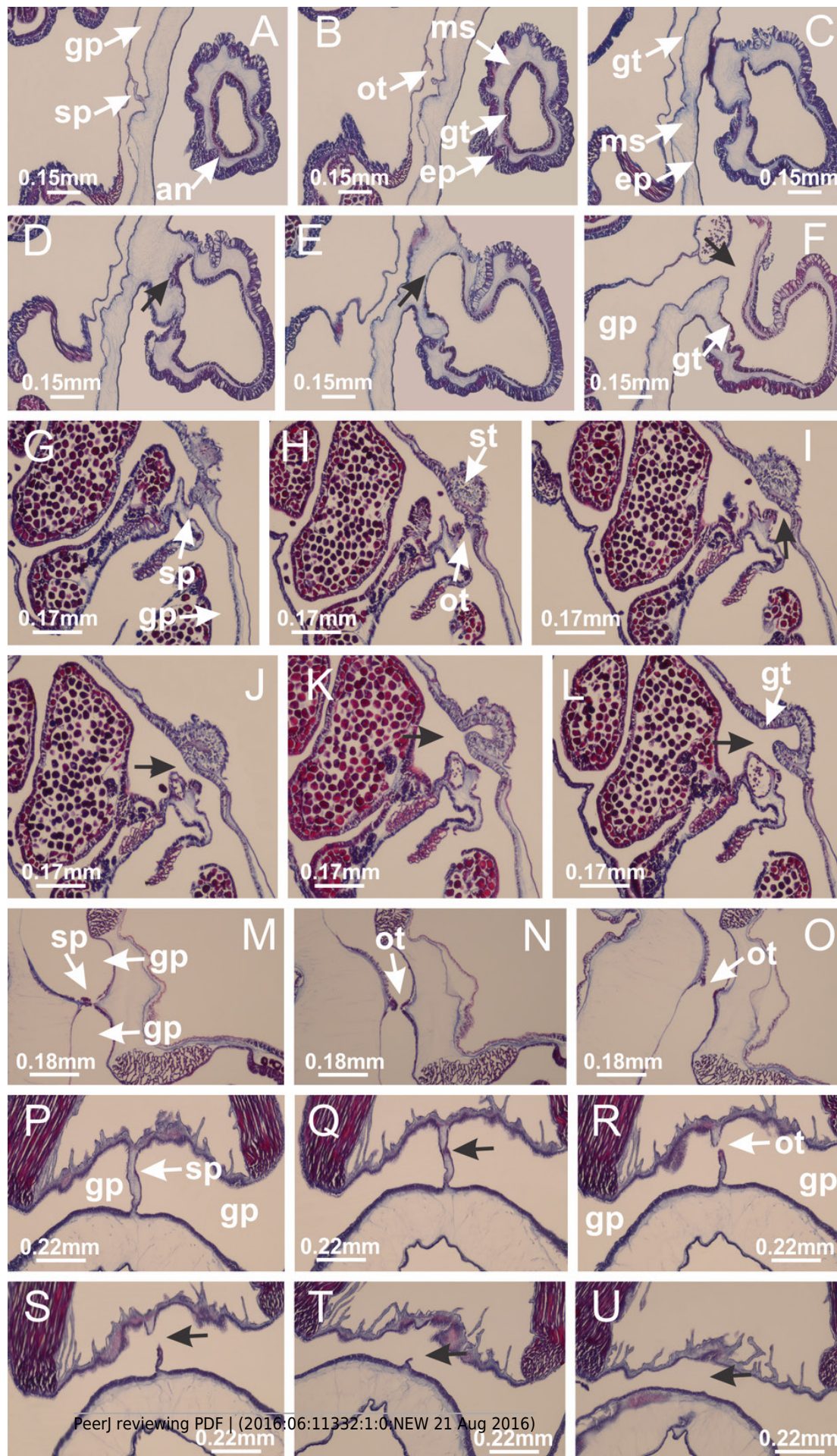
Figure 11

Arms delimitation.

Haliclystus tenuis: A) general view of the calyx margin, with perradial notches separated;
B-G) progressive separation of interradial notches (indicated by black arrows) through fusion
of gastrodermis and epidermis of subumbrella and exumbrella, delimiting the arms; H) arm,
composed of one central band of longitudinal muscle and two lateral bands of coronal
muscle; **Calvadosia vanhoeffeni**: I-K) progressive separation of interradial notches
(indicated by black arrows) through fusion of gastrodermis and epidermis of subumbrella and
exumbrella, delimiting the arms; L) arm, composed of one central band of longitudinal
muscle and two lateral bands of coronal muscle. A-L: cross sections. See Table 2 for
abbreviations.
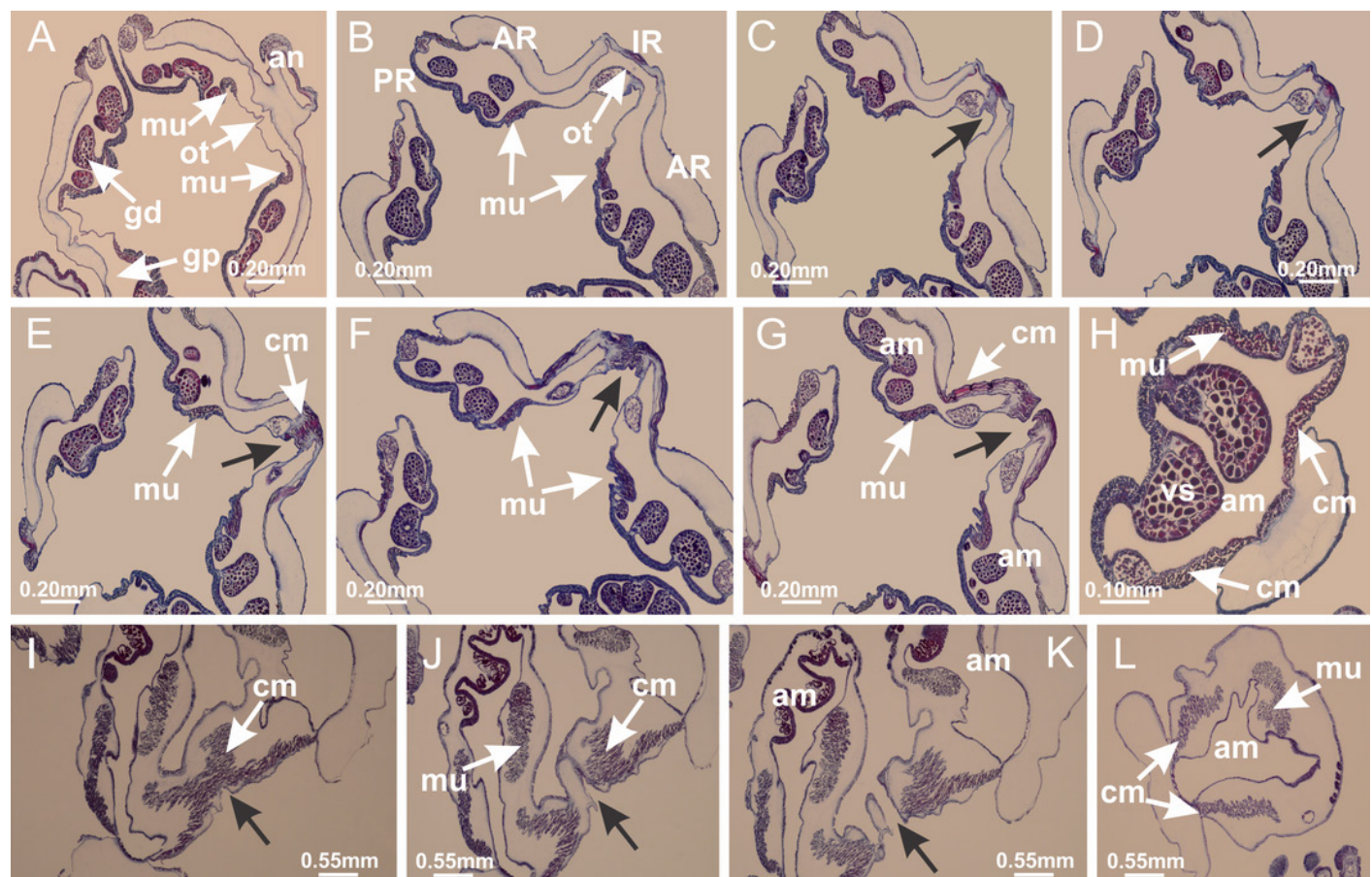
Figure 12

White spots of nematocysts.

Haliclystus tenuis: A) general view of perradial white spot of nematocysts; B) internal organization, with central mature nematocysts and a peripheral layer of nematoblasts; C) central thickening of epidermis of white spot (indicated by black arrow); **Manania uchidai**: D) white spots, associated with principal radial pocket and gonads; E) central thickening of epidermis of white spot (indicated by black arrow); **Calvadosia vanhoeffeni**: F) central thickening of epidermis of white spot (indicated by black arrow); **Calvadosia cruciformis**: G, H) central thickening of epidermis of white spots (indicated by black arrows); **Lucernaria sainthilairei**: I) possible communication of mature nematocysts with the outside (indicated by black arrow); **Calvadosia corbini**: J) internal organization, with central mature nematocysts and a peripheral layer of nematoblasts; K) central thickening of epidermis of white spot (indicated by black arrow); L, M) detail of internal organization, with central mature nematocysts and a peripheral layer of nematoblasts, and central thickening of epidermis of white spot (indicated by black arrow). A-M: longitudinal sections of white spots of nematocysts (cross sections of animals). See Table 2 for abbreviations.
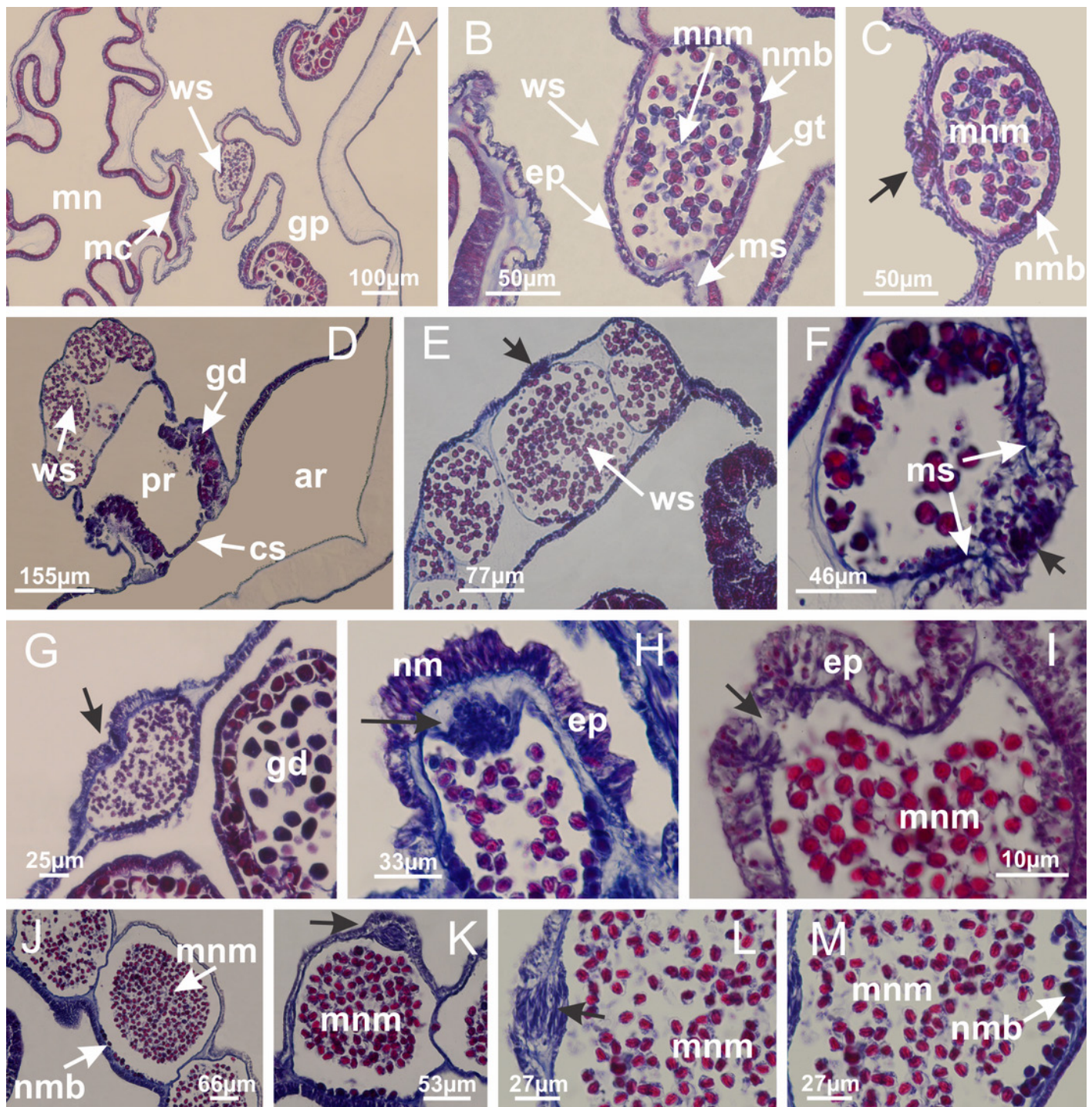
Figure 13

Batteries of nematocysts.

Manania uchidai: A, B) batteries of nematocysts in the epidermis of exumbrella; ***Haliclystus tenuis***: C) batteries of nematocysts in the epidermis of exumbrella; ***Calvadosia cruciformis***: D) batteries of nematocysts in the epidermis of exumbrella; ***Calvadosia vanhoeffeni***: E, F) nematocysts sparsely distributed in the epidermis of exumbrella of pedal disk; G) batteries of nematocysts in the epidermis of exumbrella of calyx; ***Calvadosia corbini***: H-K) batteries of nematocysts in the epidermis of exumbrella; L, M) batteries of nematocysts in the epidermis of subumbrella, associated with gonads. A-M: cross sections. See Table 2 for abbreviations.
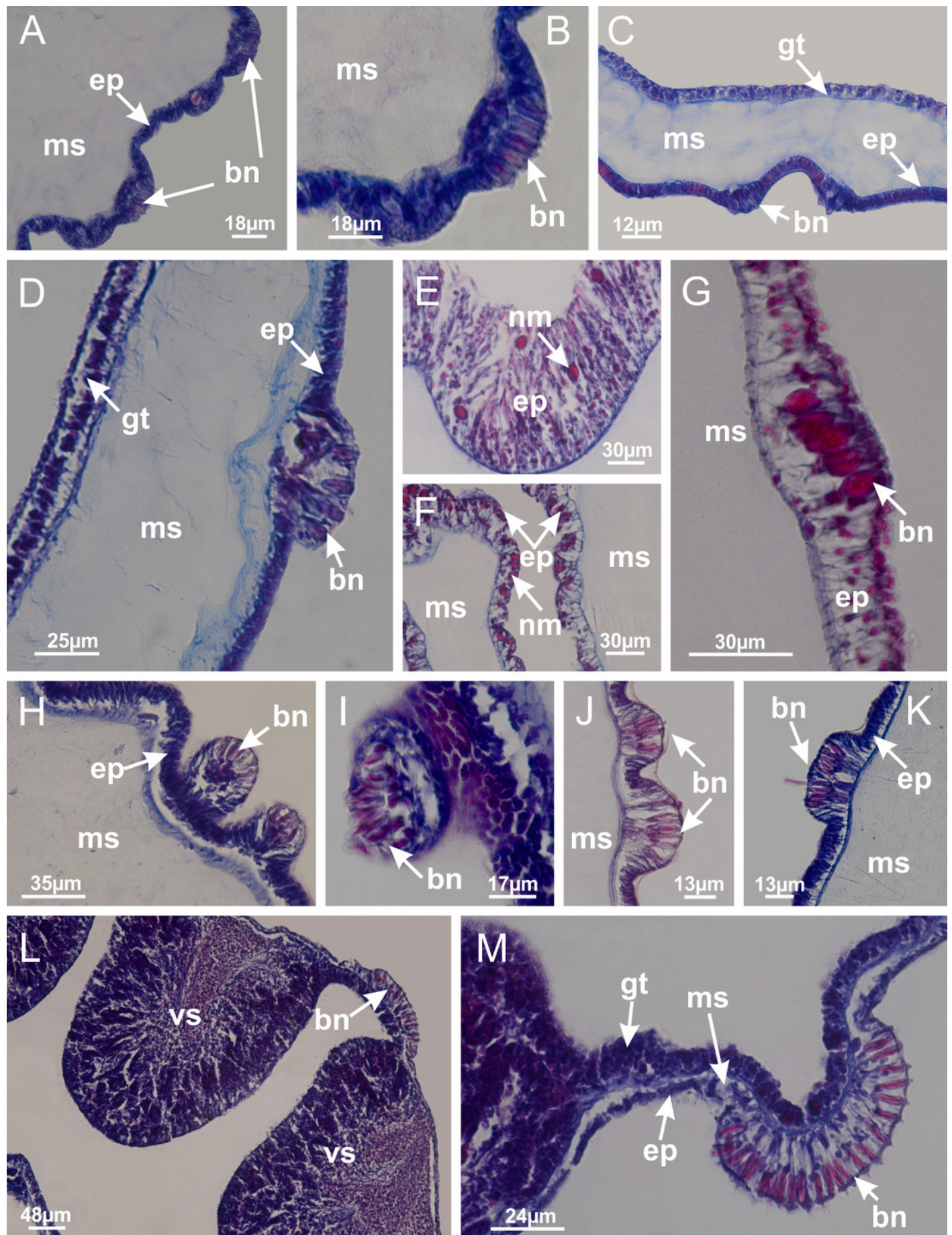
Figure 14

"U-shaped" space of *Haliclystus tenuis.*

A-C) General view of tip of arm, at the internal base of tentacles, with a platform or "U-shaped" space; D-U) sequence of longitudinal sections of arms, showing the "U-shaped" space (delimitation indicated by black arrows): a double layer of gastrodermis with a central layer of mesoglea; V, W) general view of "U-shaped" space. A-W: longitudinal sections. See Table 2 for abbreviations.
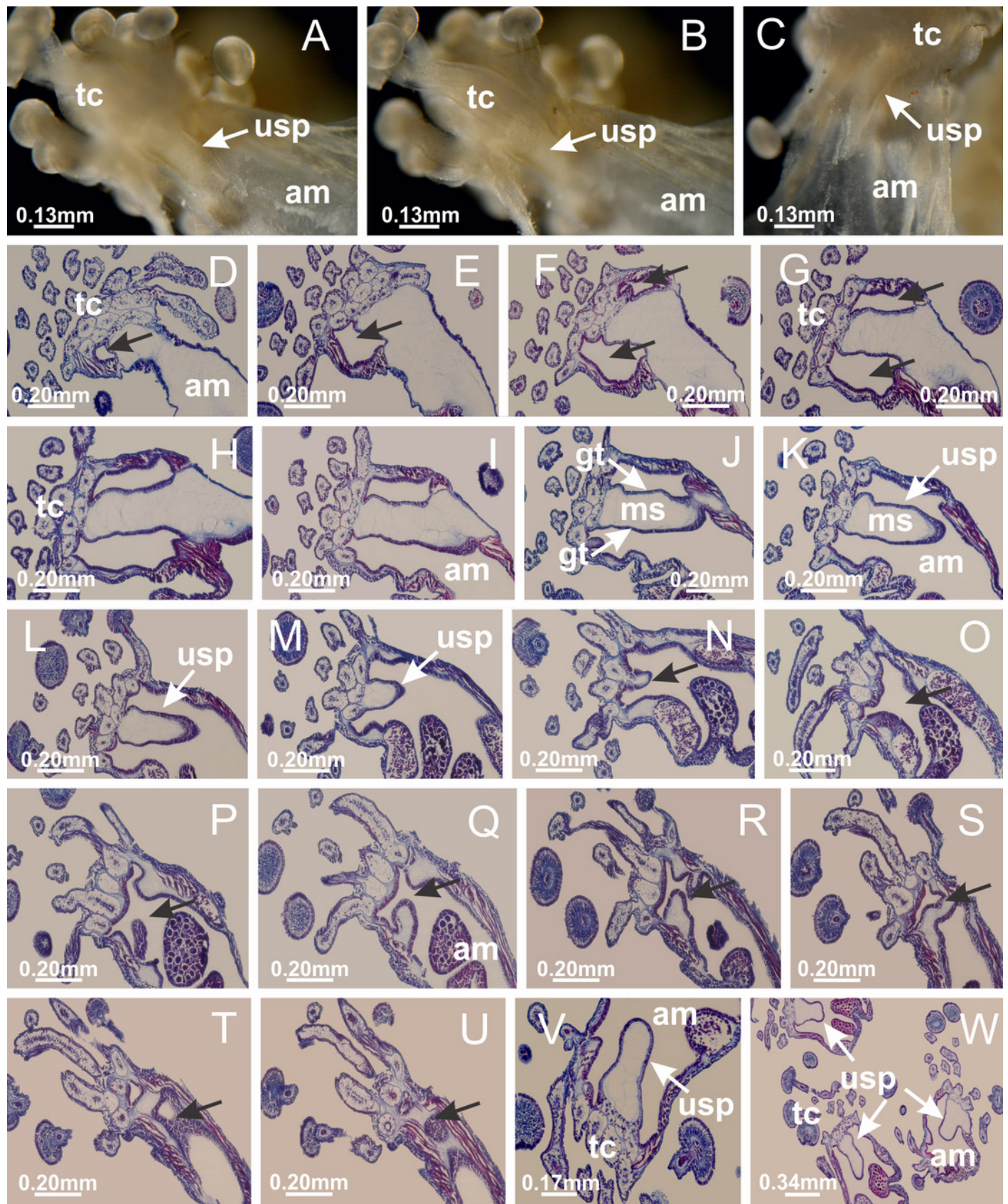
Figure 15

Internal subumbrellar layer of nematocysts.

Calvadosia vanhoeffeni: A-H) layer of nematocysts in the epidermis of the base of infundibula; **_Haliclystus tenuis_**: I-L) layer of nematocysts in the epidermis of infundibula; M-P) layer of nematocysts in the subumbrellar epidermis of calyx, associated with gastric radial pockets; Q) layer of nematocysts in the subumbrellar epidermis of arms; **_Calvadosia corbini_**: R) layer of nematocysts in the subumbrellar epidermis of arms; S) layer of nematocysts in the subumbrellar epidermis of arms associated with secondary tentacles. A-S: cross sections. See Table 2 for abbreviations.
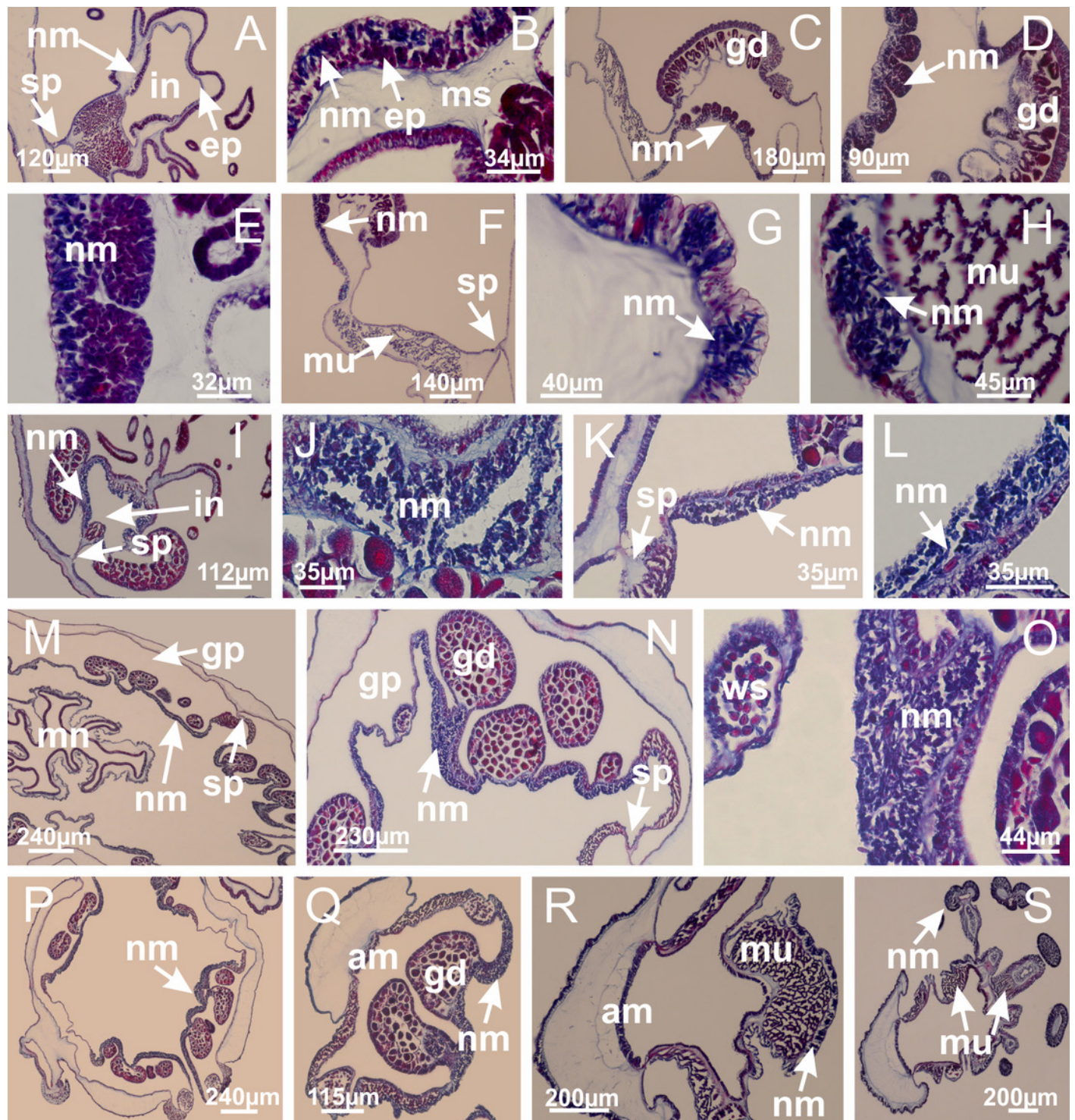
Figure 16

Internal layer of nematocysts in the secondary tentacles.

Calvadosia vanhoeffeni: A) general view of tips of arms and secondary tentacles; B, C) accumulation of nematocysts in the epidermis of secondary tentacles (base of stem); **Lucernaria quadricornis**: D) general view of tips of arms and secondary tentacles; E-H) accumulation of nematocysts in the epidermis of secondary tentacles; **Calvadosia corbini**: I) accumulation of nematocysts in the epidermis of secondary tentacles (base of stem); **Lucernaria sainthilairei**: J) general view of secondary tentacle; K) detail of nematocysts in the epidermis of tentacular stem; L) detail of the unorganized internal group of nematocysts, in the epidermis of tentacular stem base. A-L: longitudinal sections. See Table 2 for abbreviations.
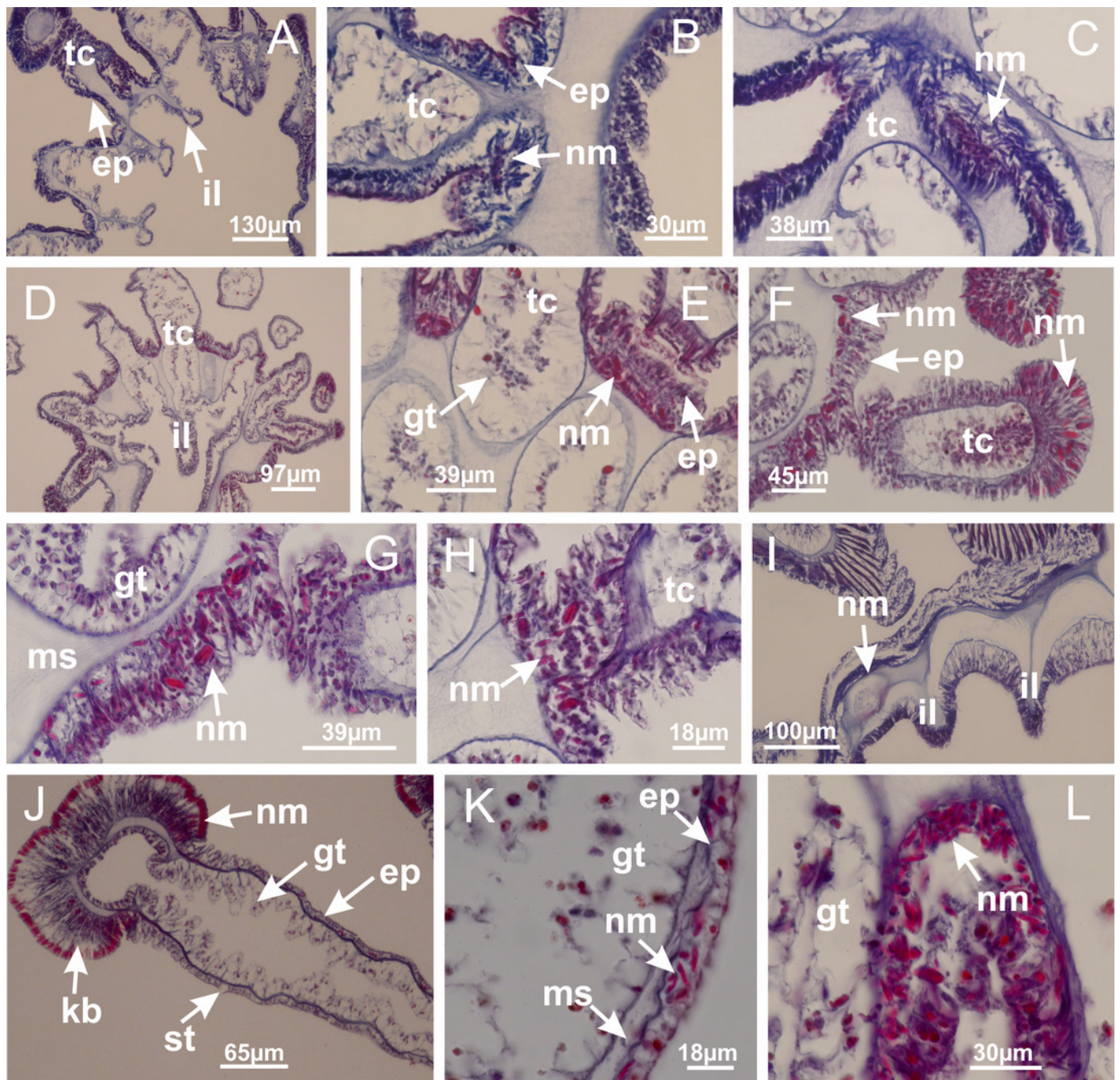
Figure 17

Secondary tentacles.

Calvadosia corbini: A, B) general organization of secondary tentacles; C) tentacular stem base highlighting the longitudinal muscle associated with epidermis, and gastrodermis with vacuolated cells; *Lucernaria quadricornis*: D) intertentacular lobules and tentacular stem base; E) intertentacular lobules; F) tentacular stem base; *Lucernaria bathyphila*: G) general organization of secondary tentacles; H) tentacular knob with tall epidermis and nematocysts on its apex; *Lucernaria sainthilairei*: I) general organization of secondary tentacles; J) tentacular knob with tall epidermis and nematocysts on its apex; *Manania uchidai*: K) general organization of secondary tentacles; L) tentacular knob with tall epidermis and nematocysts on its apex; M) intertentacular lobules; *Haliclystus tenuis*: N) general organization of secondary tentacles; O) detail of longitudinal muscle of tentacular stem; P, Q) tentacular knob with tall epidermis and nematocysts on its apex; *Craterolophus convolvulus*: R) general organization of secondary tentacles; S) tentacular stem base highlighting the longitudinal muscle associated with epidermis, and gastrodermis with vacuolated cells; T, U) tentacular knob with tall epidermis and nematocysts on its apex. A, B, G, I, K, L, N-P, R, T: longitudinal sections; C-F, H, J, M, Q, S, U: cross sections. See Table 2 for abbreviations.
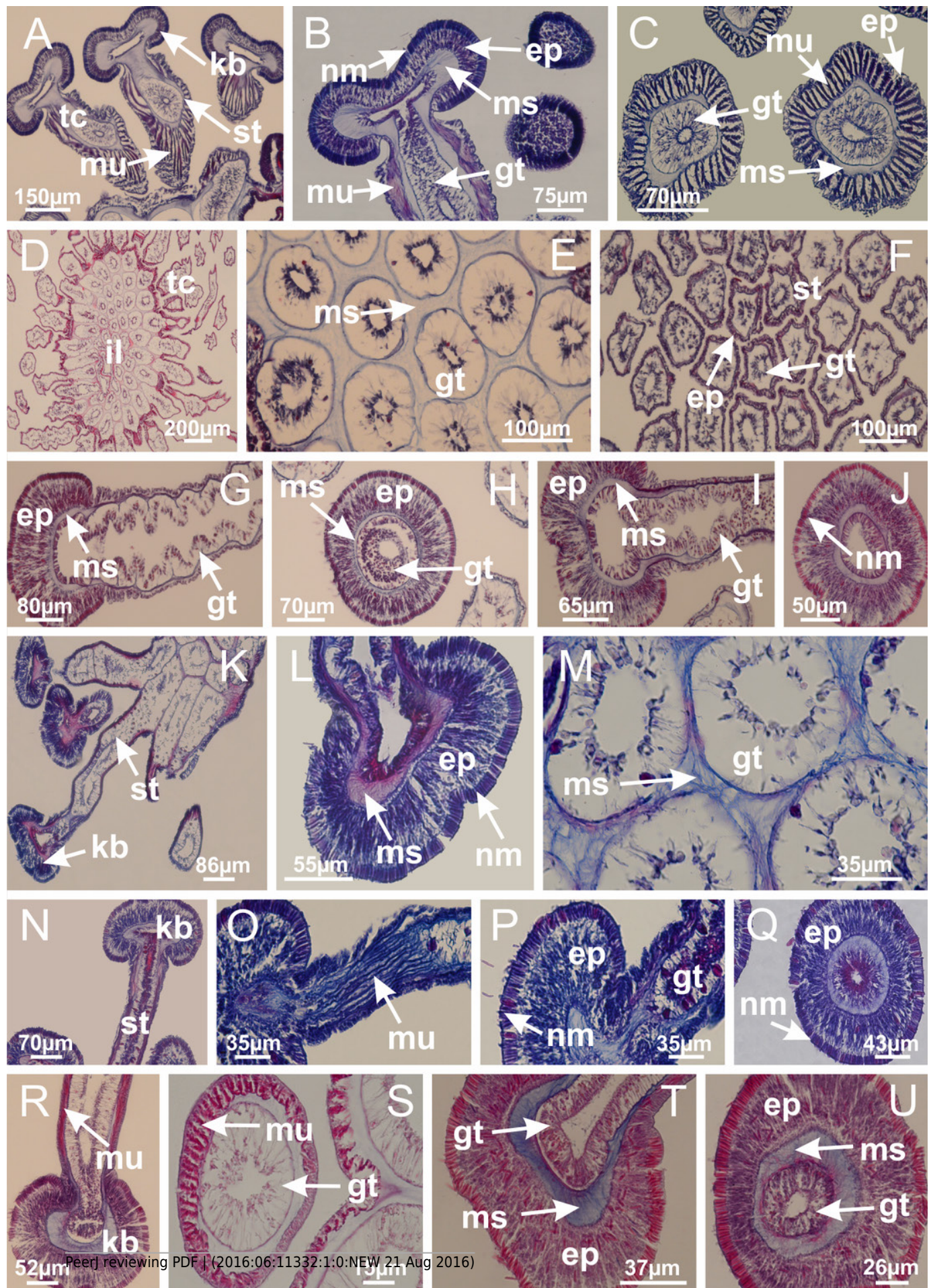
Figure 18

General view of *Manania uchidai.*

A) General view of calyx; B-D) apical region of calyx, with continuous coronal muscle; E) detail of anchor, with a knobbed remnant of primary tentacle, and a swollen base (indicated by black arrow); F, G) peduncle and pedal disk; H) subumbrellar view, with manubrium and gonads; I, J) white spots, associated with perradial gonads; K, L) exumbrellar coronal muscle (external to anchors) and tentacular cluster, with pad-like adhesive structures in the outermost secondary tentacles. See Table 2 for abbreviations.
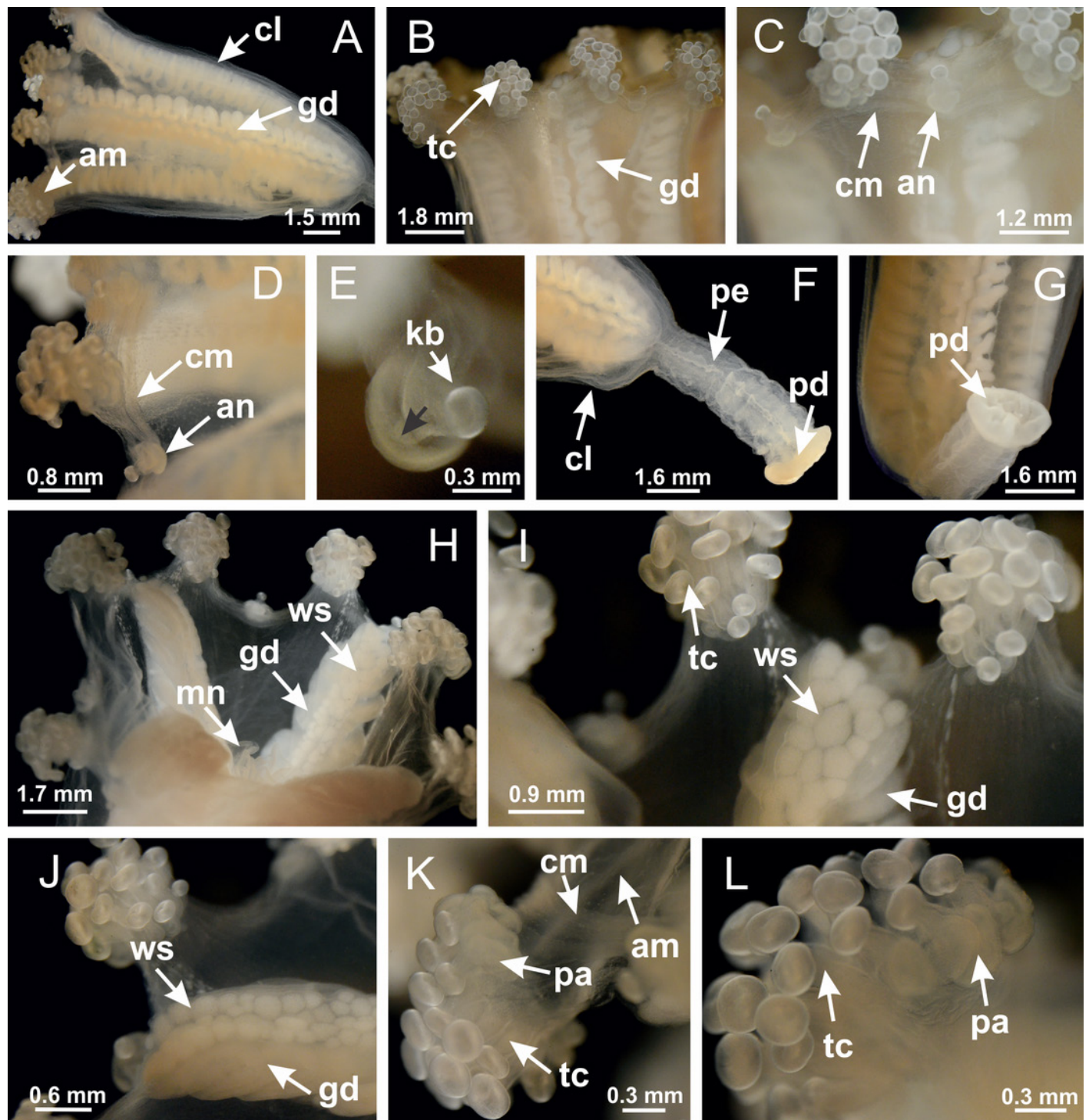
Figure 19

Peduncle and septa of *Manania uchidai* (from base moving upward in A-T).

A) Base of peduncle with one chamber delimited by gastrodermis and four interradial longitudinal muscles; B-G) variation in shape and size of the central chamber; H-L) gradual division of central chamber in four perradial chambers (indicated by black arrows); M-S) variation in shape and size of four perradial chambers; T) four interradial septa, with infundibula delimited by epidermis, connected by a central mesoglea. A-T: cross sections. See Table 2 for abbreviations.
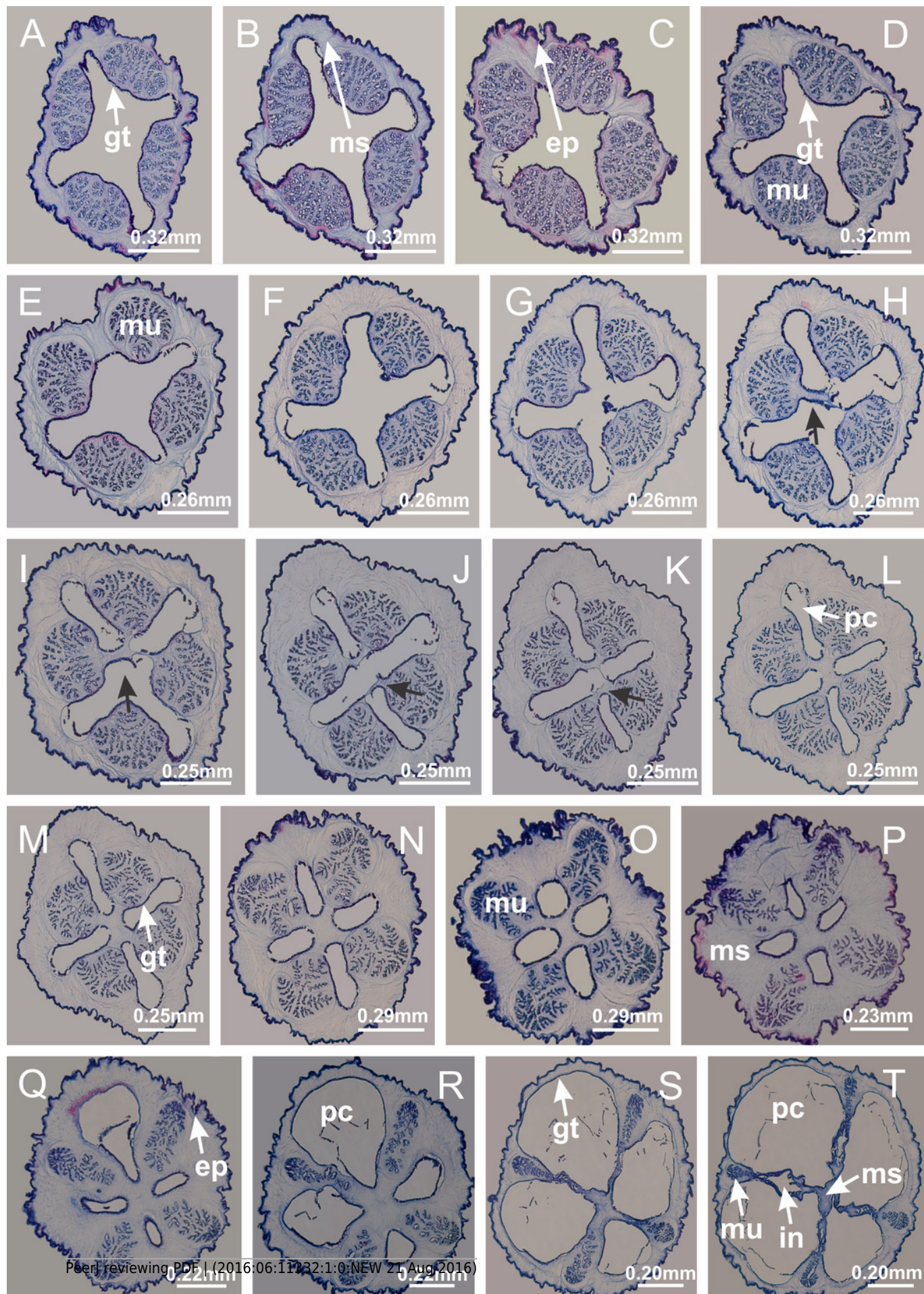
Figure 20

Claustra in *Manania uchidai.*

A-F) Claustra delimitation (lateral projections of adjacent septa, indicated by black arrows); G, H) claustra completely delimited, dividing the gastrovascular cavity, forming accessory radial pockets; I, J) fusion of gastrodermis and epidermis of adjacent septa (indicated by black arrow), delimiting manubrium and principal radial pocket; K, L) principal radial pocket, associated with gonads and white spots of nematocysts; M) detail of principal radial pocket. A-M: cross sections. See Table 2 for abbreviations.
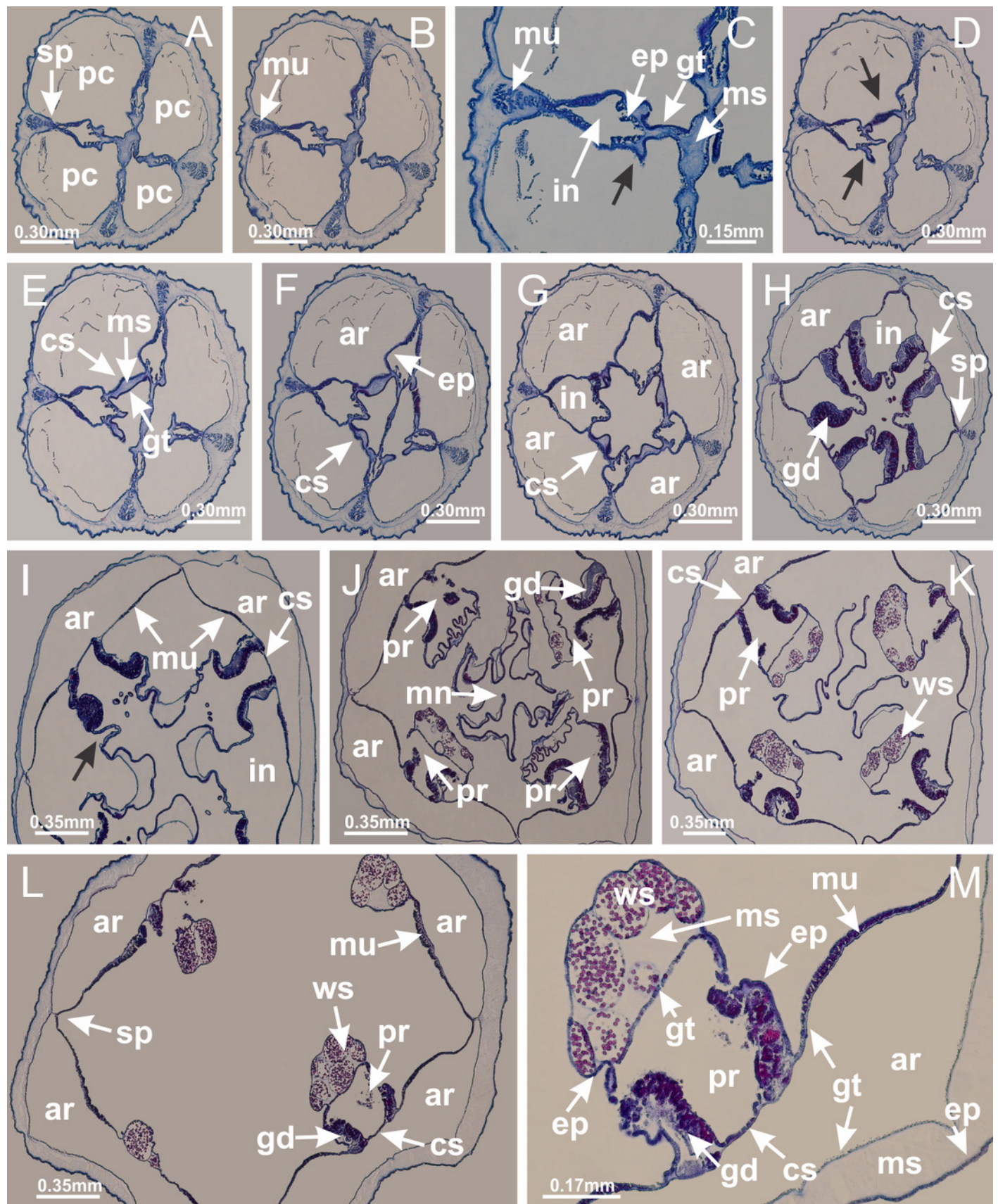
Figure 21

Position of interradial longitudinal muscle.

Haliclystus tenuis: A) interradial longitudinal muscle internal in relation to septa; **Manania uchidai**: B) interradial longitudinal muscle external in relation to septa. A, B: cross sections. See Table 2 for abbreviations.
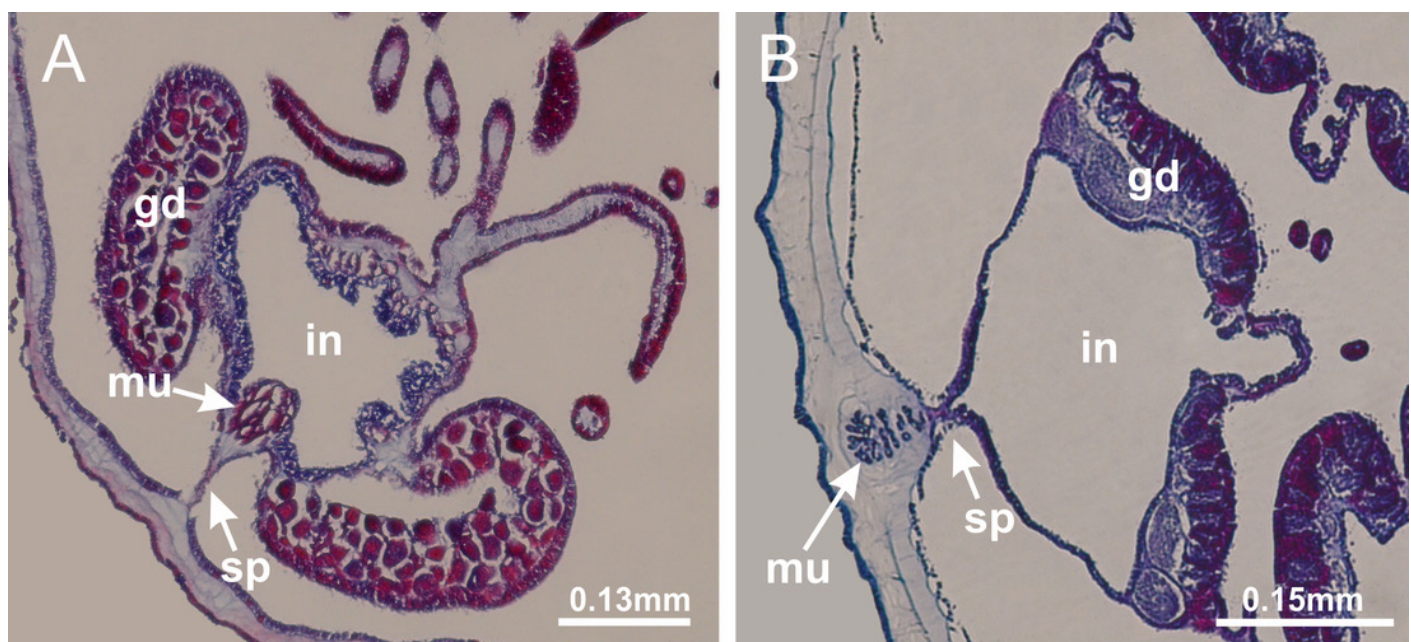
Figure 22

Gonads and gametoduct of *Manania uchidai.*

A) General view of septa (calyx base) with gonadal content, below delimitation of principal radial pockets; B) gonadal content between a layer of gastrodermis (adjacent to spermatocytes) and epidermis (adjacent to spermatozoa); C) detail of gonad adjacent to claustrum; D-H) organization of male gonad, with spermatocytes and spermatozoa; I-N) sequence of gametoduct connecting the spermatozoa with the gastrovascular cavity of principal radial pocket. A-N: cross sections. See Table 2 for abbreviations.
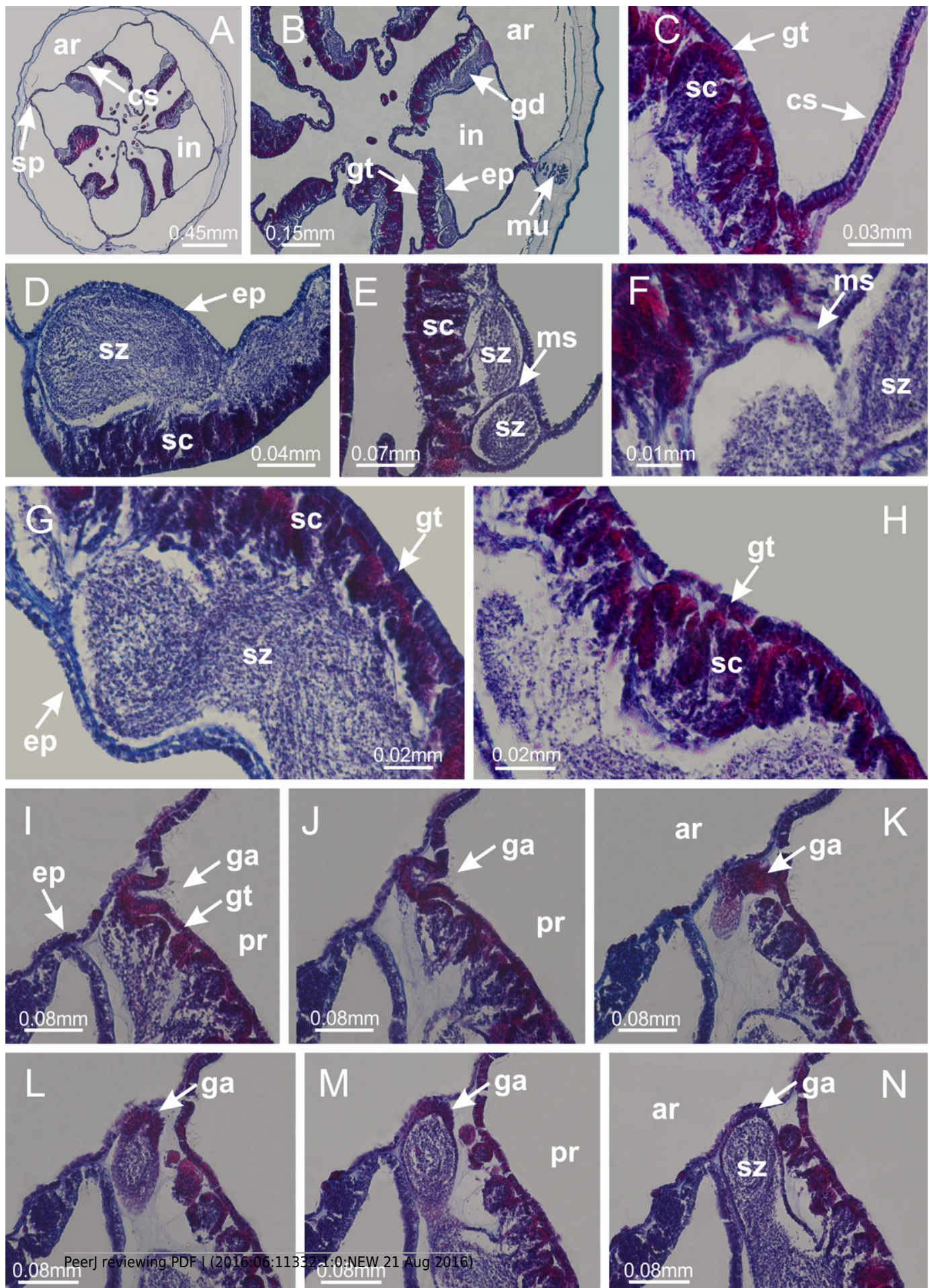
Figure 23

Intertentacular lobules of *Manania uchidai.*

A) Tip of arm; B-F) delimitation of intertentacular lobules (indicated by black arrows; connection of secondary tentacles with gastrovascular cavity in arm); G-J) intertentacular lobules, structures composed of a double layer of gastrodermis (of adjacent tentacles) and a central layer of mesoglea. A-J: longitudinal sections. See Table 2 for abbreviations.
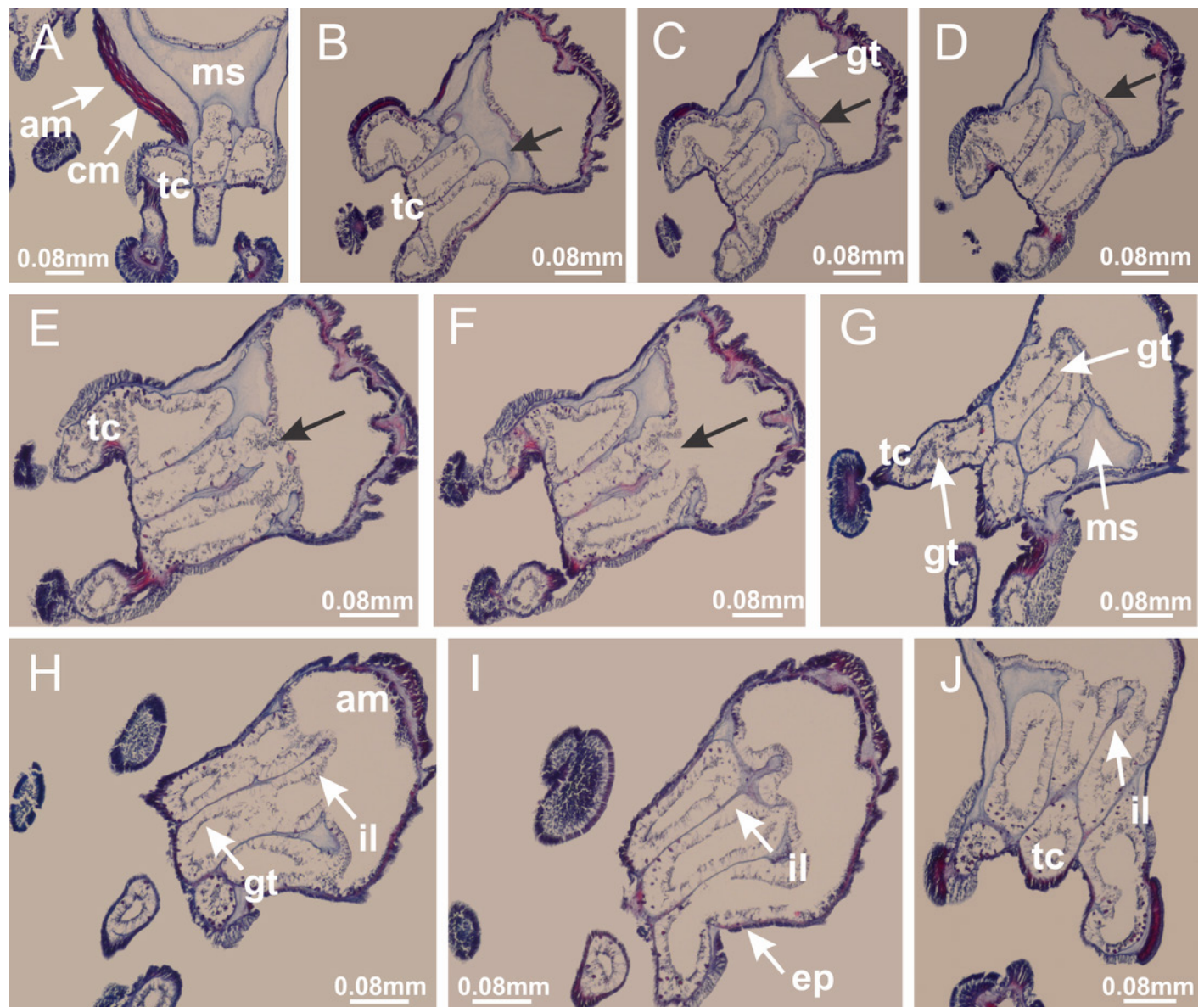
Figure 24

Pad-like adhesive structures.

Calvadosia corbini: A) general view of pad-like adhesive structure at the tip of arm; B-E) details of pad-like adhesive structure, with hollow canals (connection of canals indicated by black arrows) delimited by a thin layer of gastrodermis; F-K) connection of pad-like adhesive structure with the tip of arms (indicated by black arrows); ***Manania uchidai***: L, M) general view of pad-like adhesive structure in outermost secondary tentacle; N) detail of pad in outermost secondary tentacle, with tall epidermis. A-K: cross sections; L-N: longitudinal sections. See Table 2 for abbreviations.
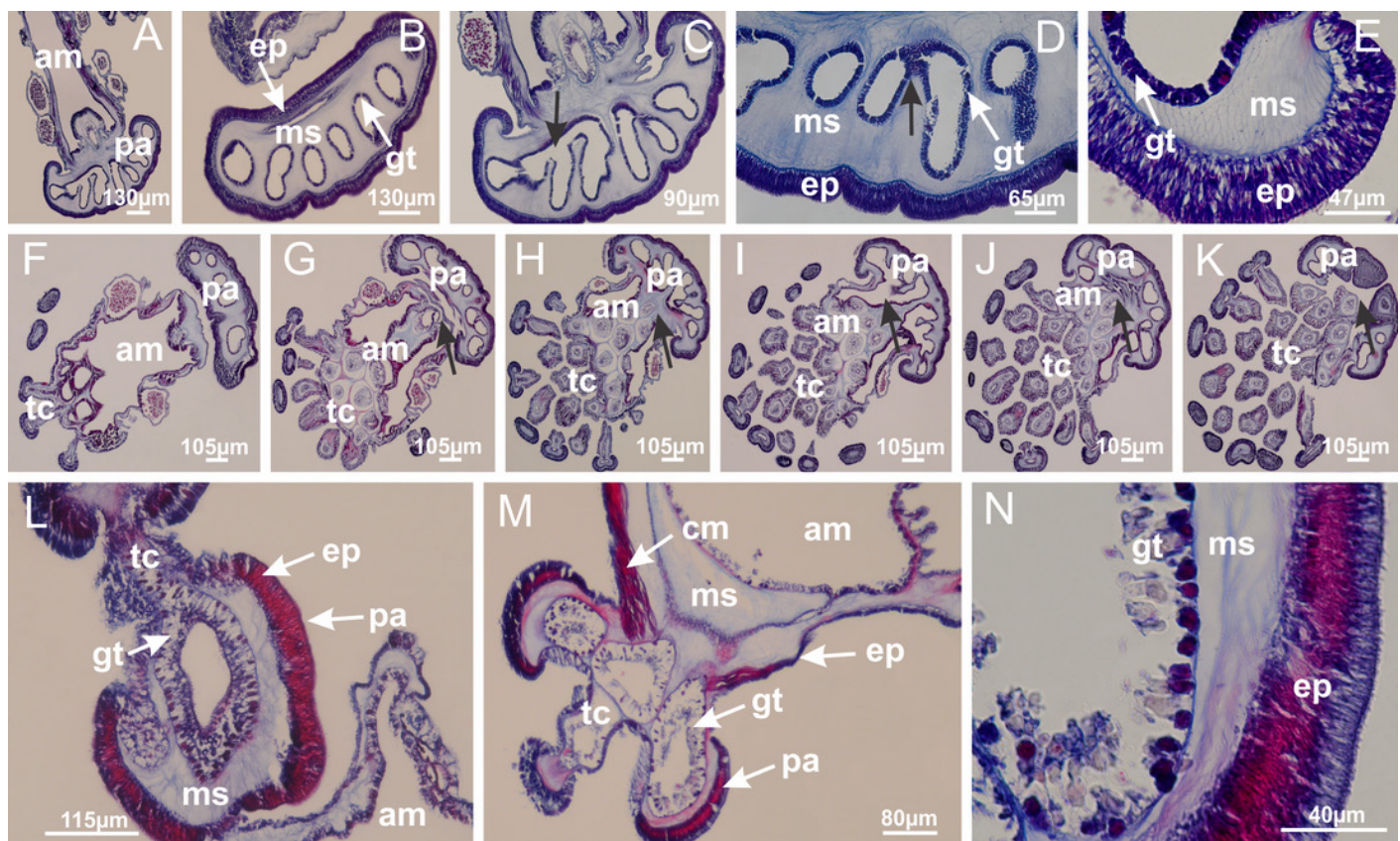
Figure 25

General view of *Lucernaria quadricornis.*

A) General view of body, with calyx and peduncle; B, C) detail of peduncle and pedal disk; D,
E) paired arms and tentacular clusters; F) detail of tentacular clusters; G) white spots of
nematocysts at margin of calyx (subumbrella); H) subumbrellar view of gonads; I)
manubrium. See Table 2 for abbreviations.
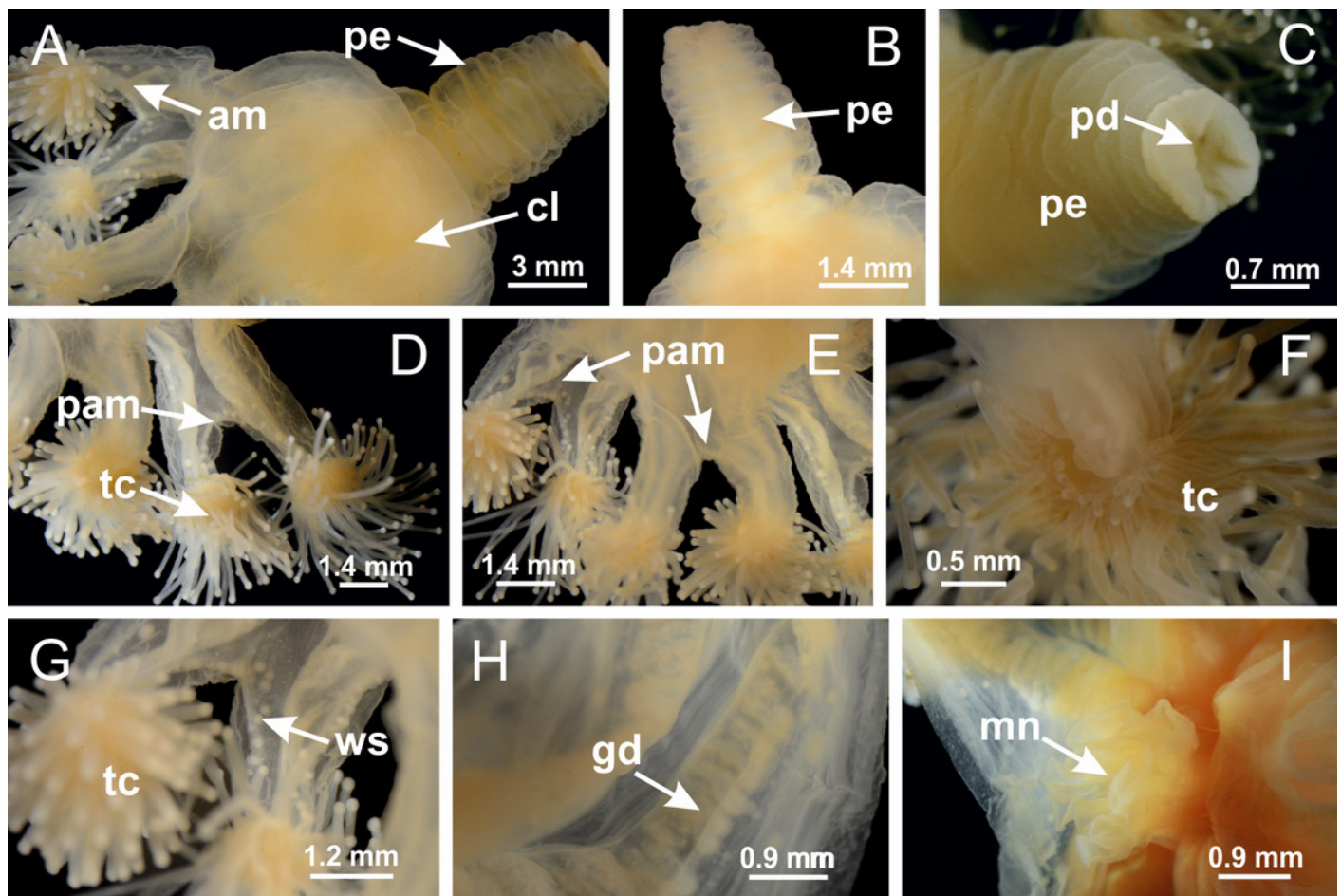
Figure 26

Peduncle and septa of *Lucernaria quadricornis* (from base moving upward in A-H).

A, B) Base of peduncle; C, D) delimitation of septa; E) interradial septa, with interradial longitudinal muscle and one central chamber in peduncle; F) detail of septum; G) formation of gastric filaments through lateral evagination of septal gastrodemis; H) septum at peduncle/calyx connection, with infundibulum (delimited by epidermis). A-H: cross sections. See Table 2 for abbreviations.
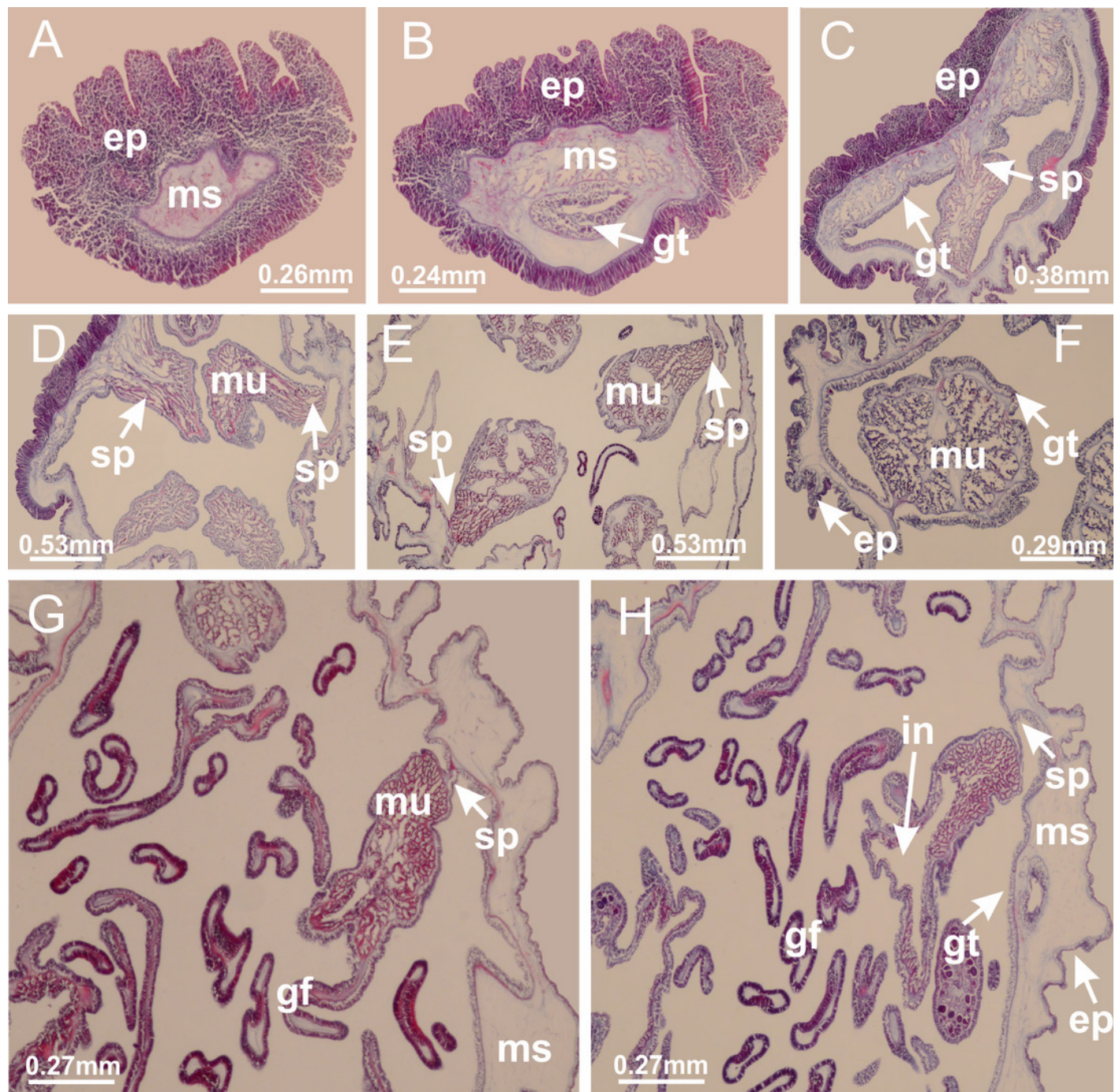
Figure 27

Gonads and gametoduct of *Lucernaria quadricornis.*

A) General view of gonad associated with septum; B, C) female gonadal content, delimited by a layer of gastrodermis and epidermis; D-G) sequence of gametoduct connecting oocytes with the gastrovascular cavity (indicated by black arrows); H, I) detail of gametoduct, with cilia. A-I: cross sections. See Table 2 for abbreviations.
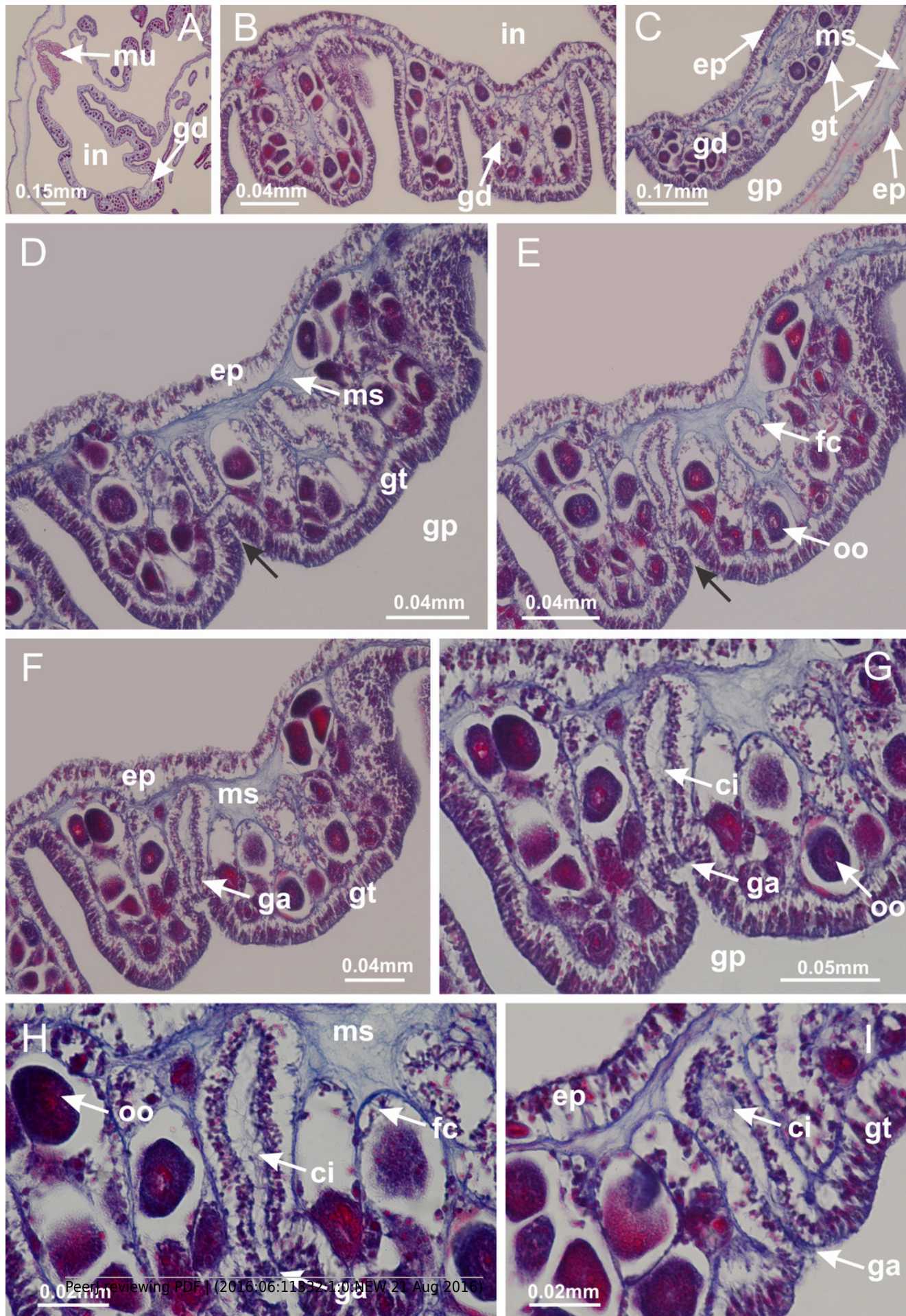
Figure 28

Intertentacular lobules of *Lucernaria quadricornis.*

A) General view of tip of arms and base of tentacles, with intertentacular lobules; B) internal base of tentacles; C) general view of tip of arms, and base of tentacles; D-H) tip of arms, in the region between intertentacular lobules and secondary tentacles; I) detail of intertentacular lobules, structures composed of a double layer of gastrodermis (of adjacent tentacles) and a central layer of mesoglea. A-I: longitudinal sections. See Table 2 for abbreviations.
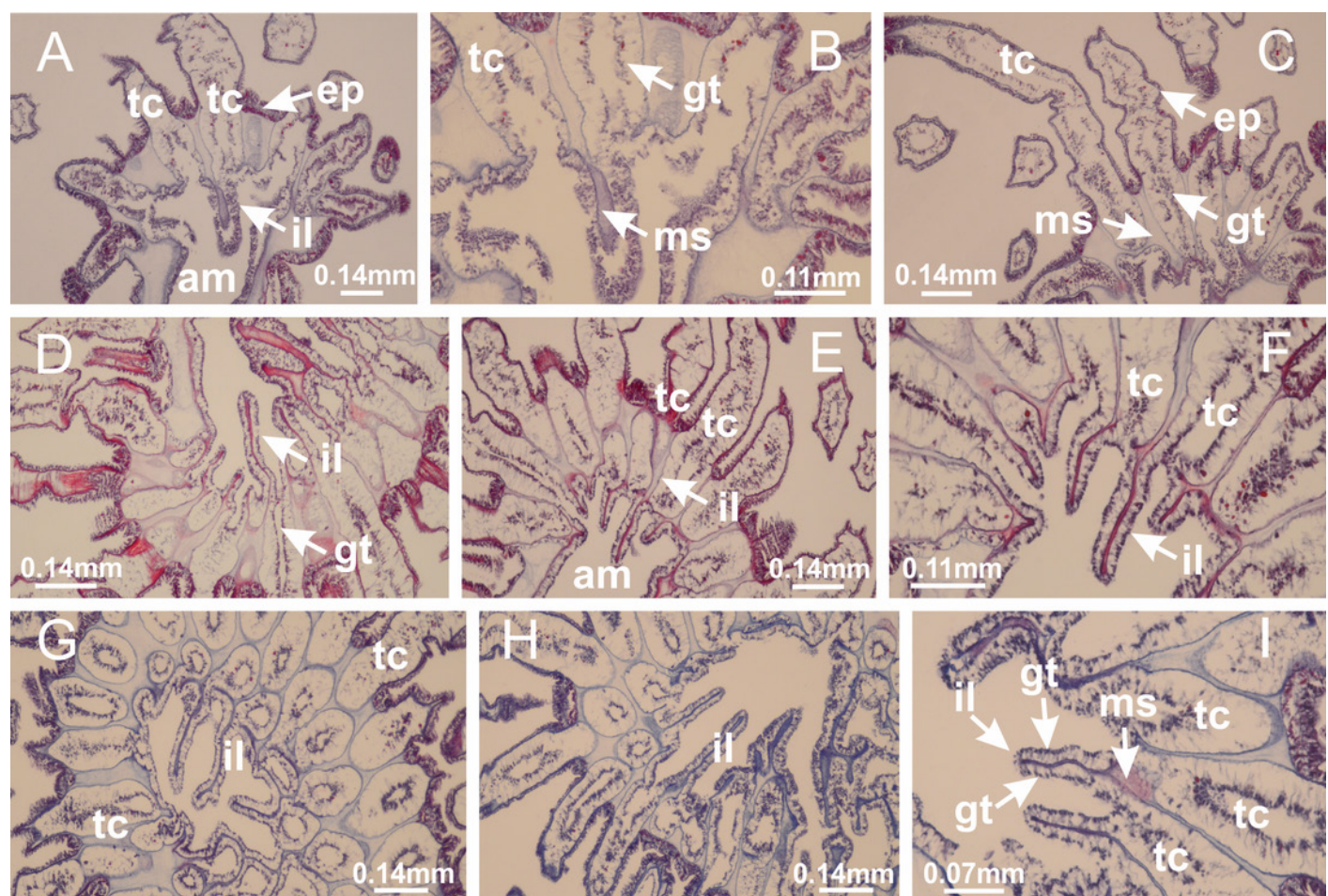
Figure 29

General view of *Lucernaria bathyphila.*

A, B) General view of peduncle and base of calyx; C) batteries of nematocysts in exumbrella; D) white spots of nematocysts on subumbrella (calyx); E) arms and tentacular clusters; F) detail of tentacles; G) manubrium and gonads; H) detail of white spots and gonads. See Table 2 for abbreviations.
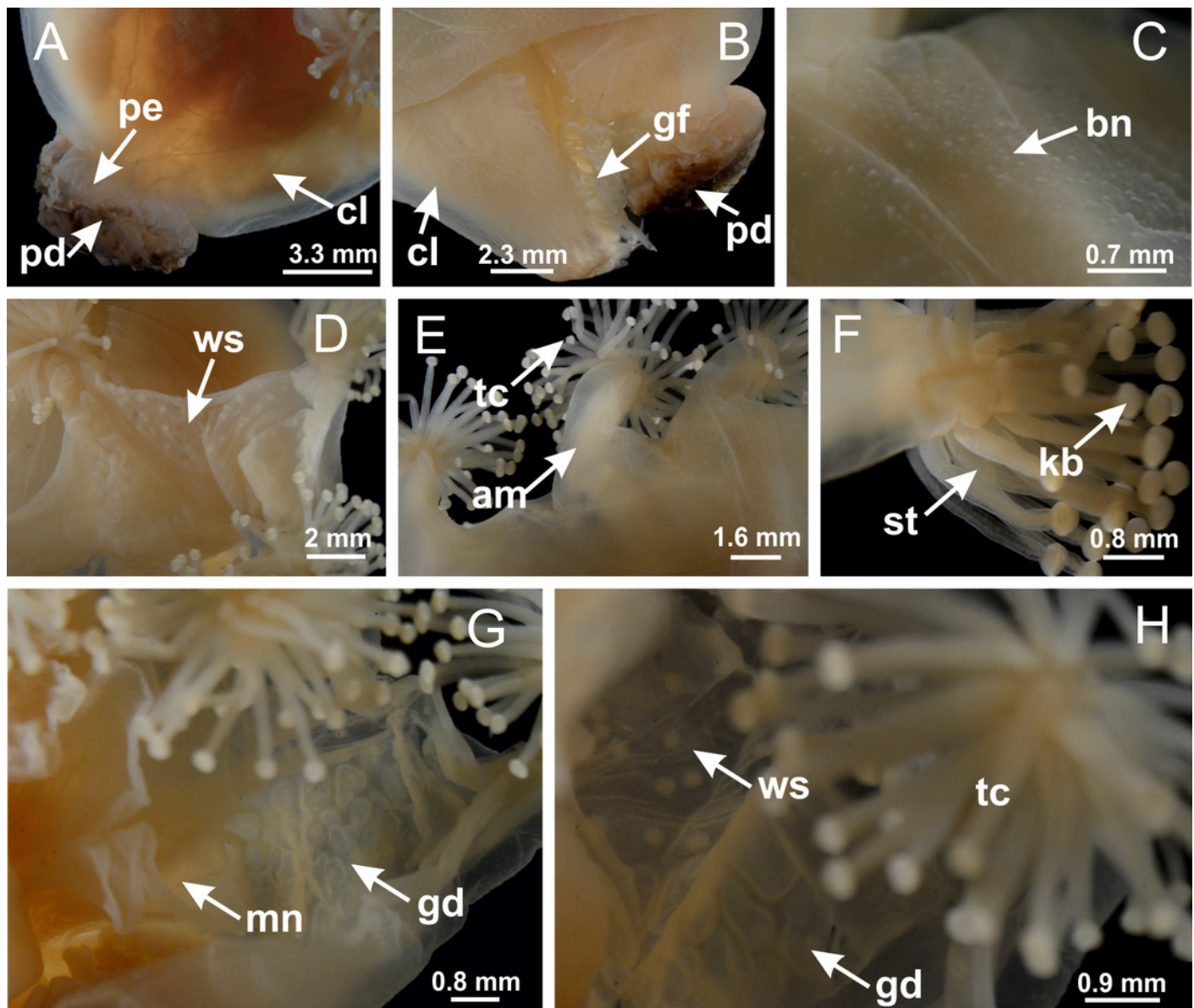
Figure 30

Peduncle and septa of *Lucernaria bathyphila* (from base moving upward in A-L).

A, B) Base of peduncle; C-F) delimitation of septa; G-I) interradial septa, with interradial longitudinal muscle, and one central chamber in peduncle; J) detail of septum; K) formation of gastric filaments through lateral evagination of septal gastrodermis; L) septum at the connection between calyx and peduncle, with lateral gonads, and central infundibulum (delimited by epidermis). A-L: cross sections. See Table 2 for abbreviations.
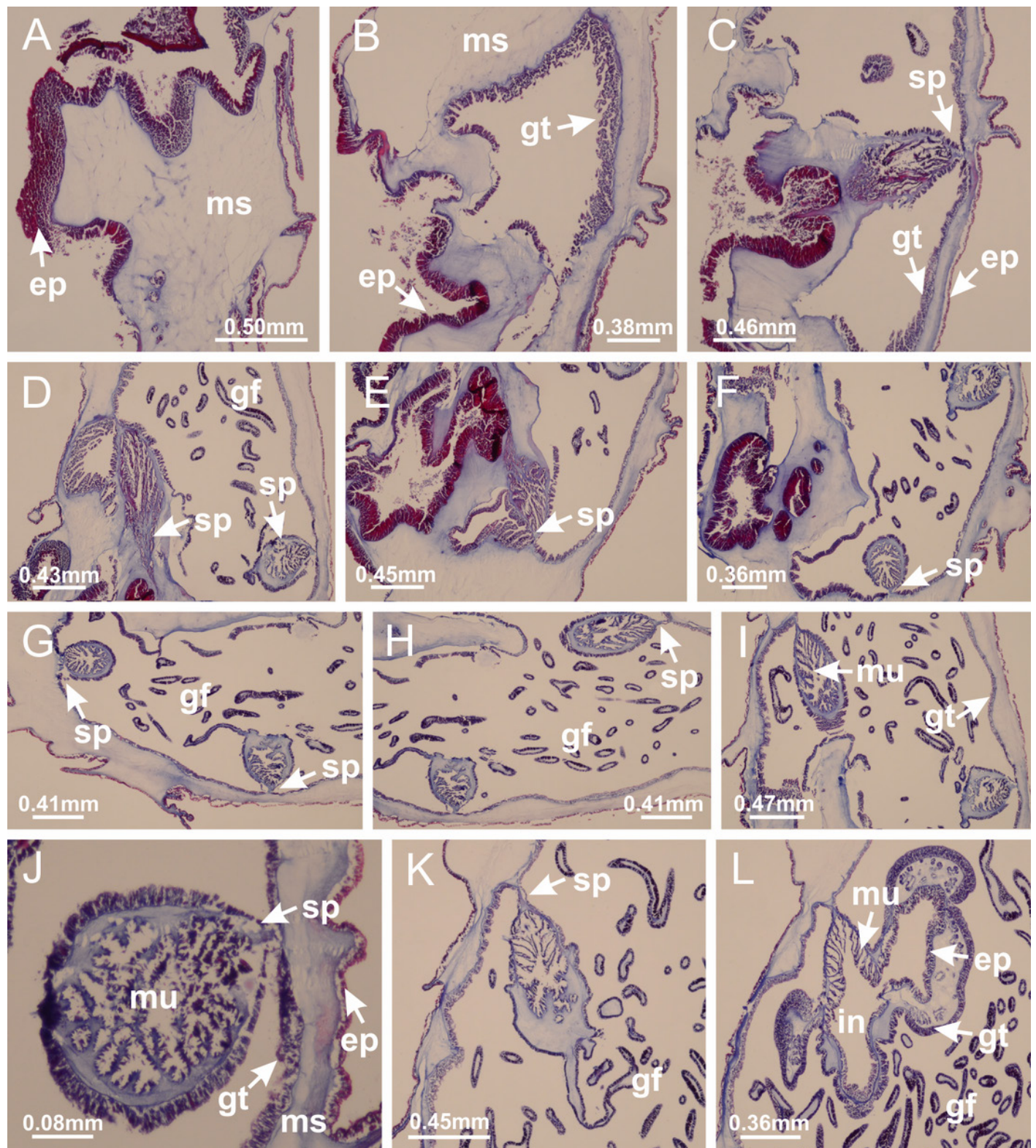
Figure 31

Gonads and gametoduct of *Lucernaria bathyphila.*

A) General view of gonad associated with septum; B) male gonadal content, delimited by a layer of gastrodermis and epidermis; C) gonads associated with gastric radial pockets; D, E) internal organization of gonads; F-J) sequence of gametoduct connecting the spermatocytes with the gastrovascular cavity (indicated by black arrows); K-P) sequence of gametoduct connecting the spermatocytes with the gastrovascular cavity (indicated by black arrows); Q) detail of gametoduct, with cilia. A-E: cross sections; F-Q: longitudinal sections of gonad (cross sections of animals). See Table 2 for abbreviations.
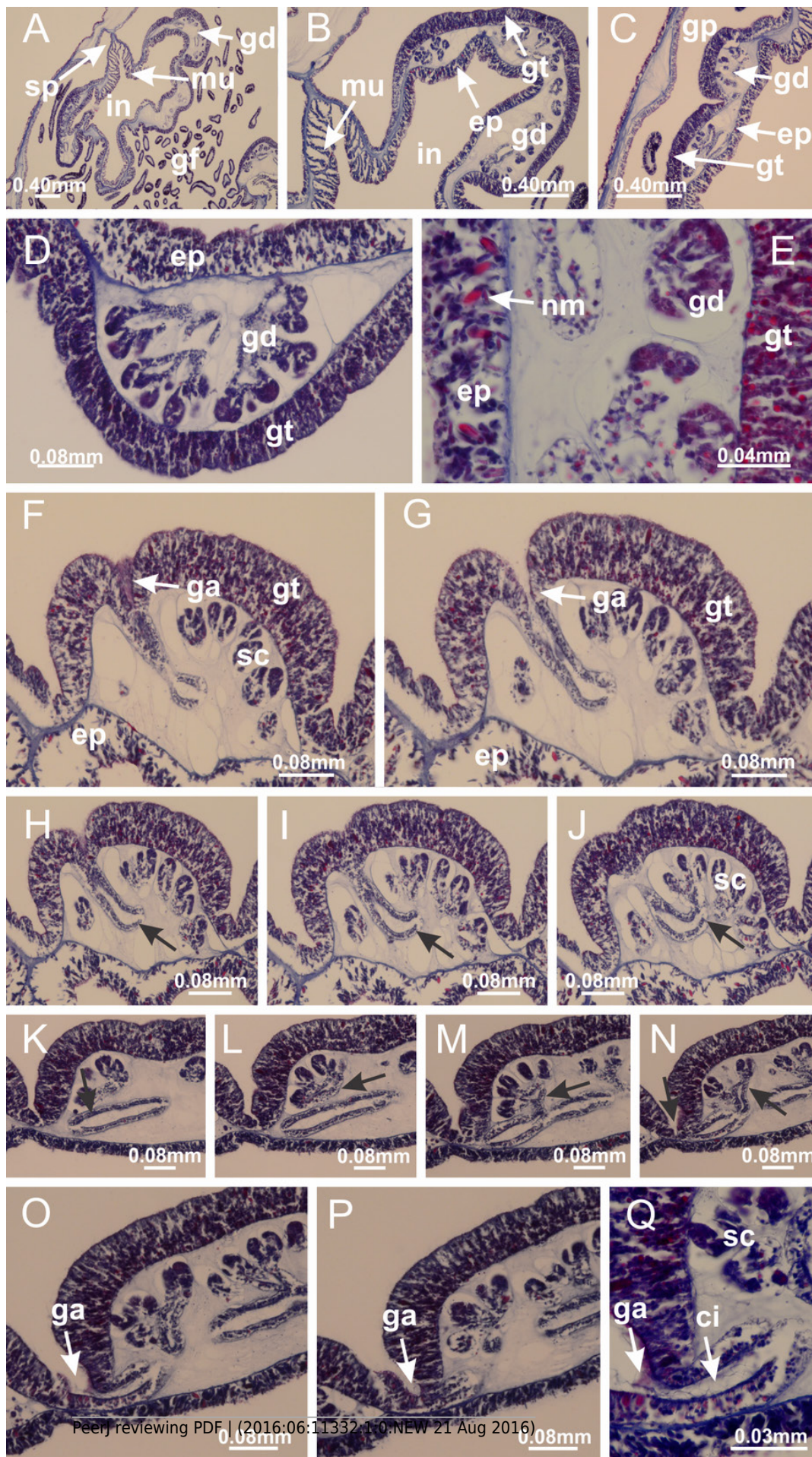
Figure 32

White spots of nematocysts.

Craterolophus convolvulus: A-F) gradual disconnection and posterior reconnection of a layer of mesoglea associated with the central thickening of epidermis; G-L) opening of white spots (indicated by black arrows), through a central pore, associated with thickening in epidermis; M) detail of central opening of white spots (indicated by black arrow); ***Lucernaria bathyphila***: N-P) central thickening of epidermis of white spots (indicated by black arrows); Q-V) opening of white spots of nematocysts (indicated by black arrows), through a central pore, associated with thickening in epidermis; W) detail of central opening of white spots (indicated by black arrow). A-W: longitudinal sections of white spots of nematocysts (cross sections of animals). See Table 2 for abbreviations.
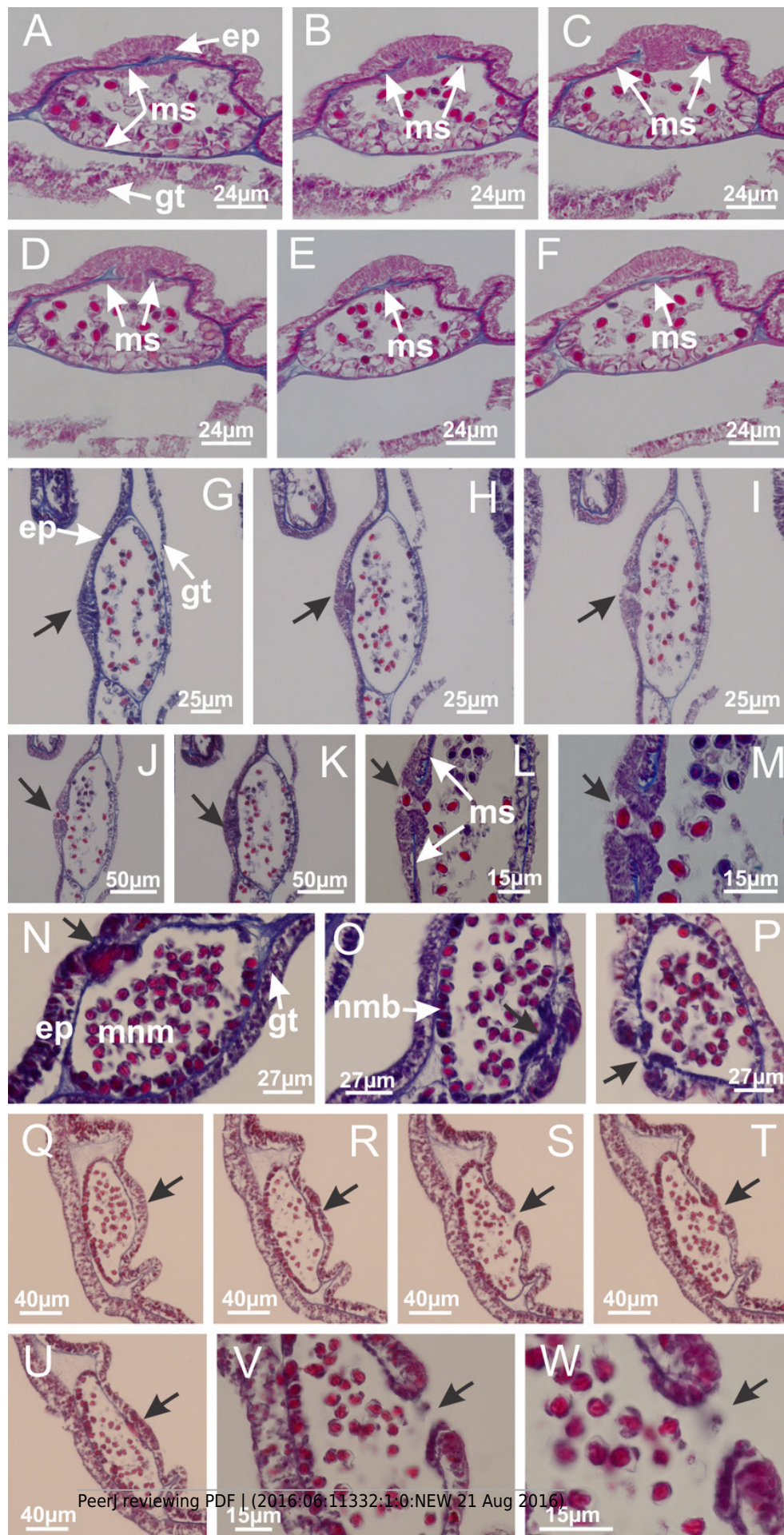
Figure 33

Intertentacular lobules of *Lucernaria bathyphila.*

A, B) General view of tip of arms and base of tentacles, with intertentacular lobules; C-E) internal organization of intertentacular lobules, structures composed of a double layer of gastrodermis (of adjacent tentacles) and a central layer of mesoglea; F) detail of intertentacular lobules. A-F: longitudinal sections. See Table 2 for abbreviations.
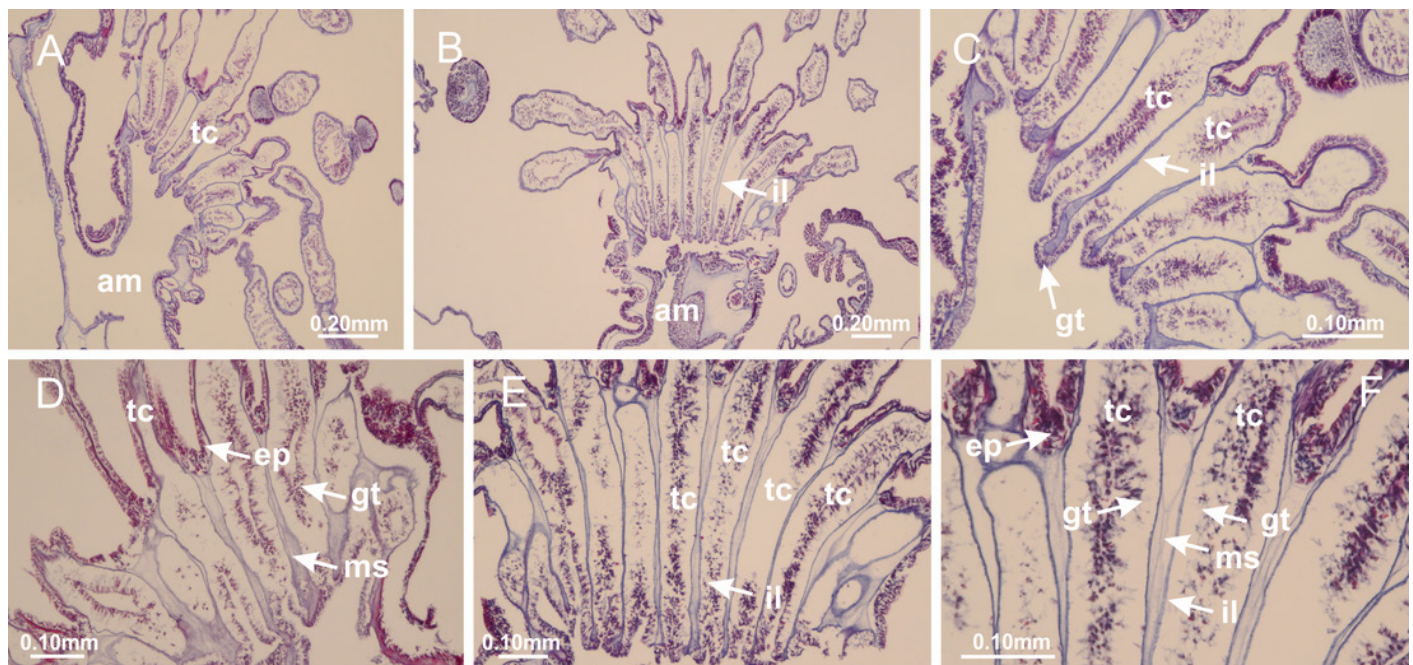
Figure 34

General view of *Lucernaria sainthilairei.*

A) General view of calyx; B) apical region of calyx, with arms and tentacular clusters; C) short peduncle; D) batteries of nematocysts in the exumbrella; E) general view of subumbrella of calyx, with manubrium; F) exumbrellar view of gonad and arms; G) manubrium and gonads; H) detail of gonad and white spots of nematocysts. See Table 2 for abbreviations.
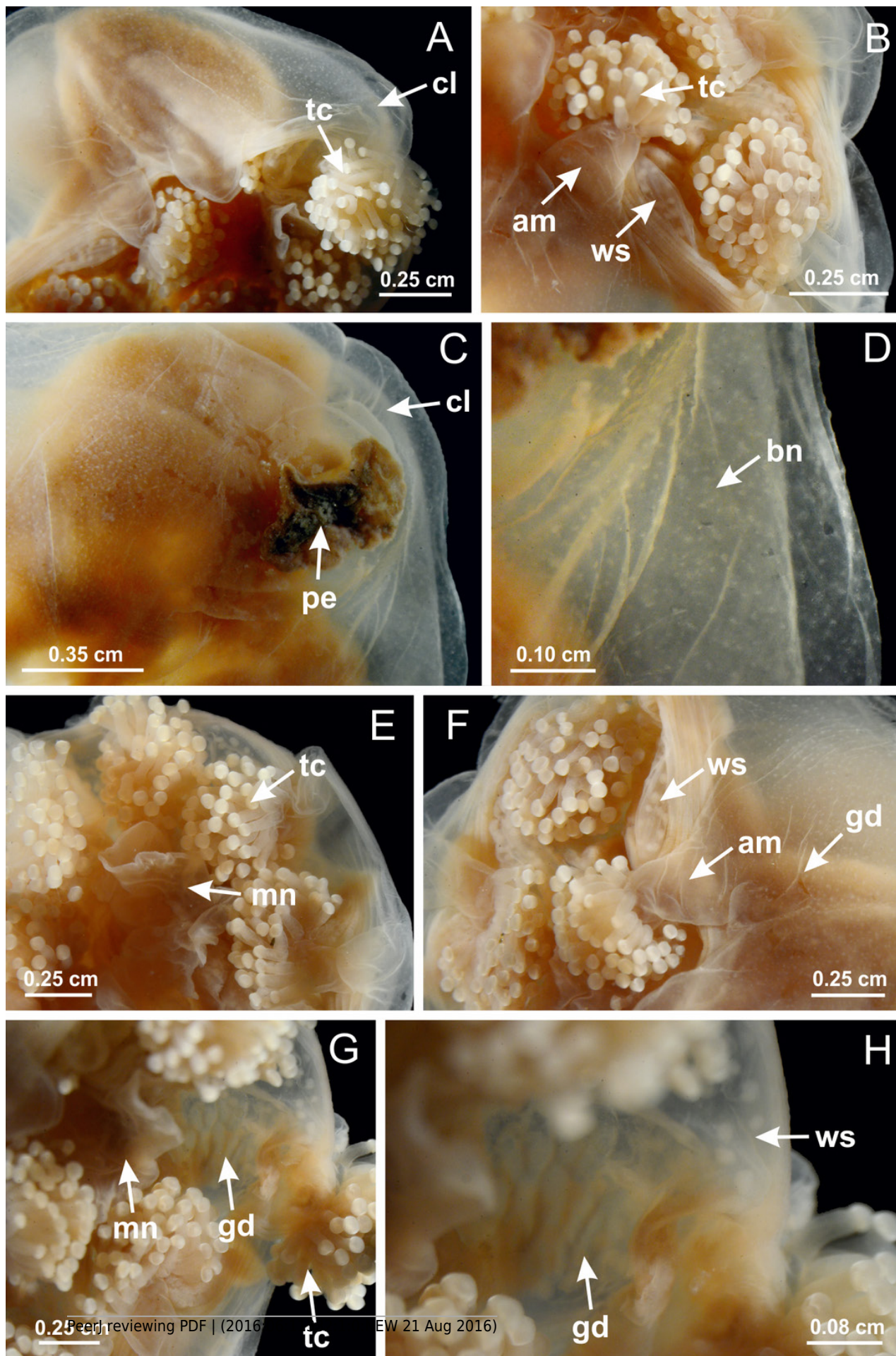
Figure 35

Peduncle and septa of *Lucernaria sainthilairei* (from base moving upward in A-D).

A) Base of peduncle; B, C) interradial septa, with interradial longitudinal muscles, and one central chamber in peduncle; D) septum at the peduncle/calyx connection, with infundibulum (delimited by epidermis). A-D: cross sections. See Table 2 for abbreviations.
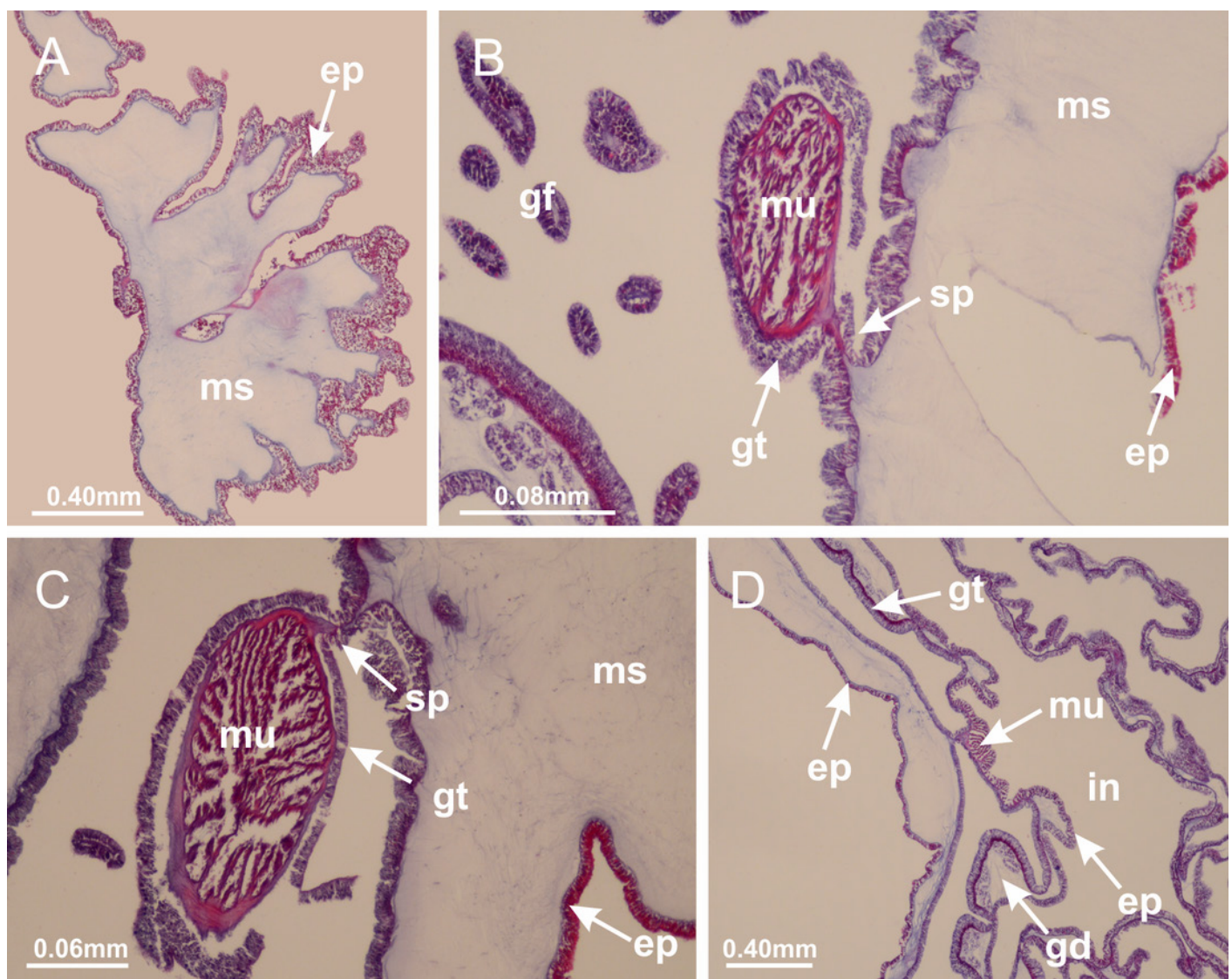
Figure 36

Gonads of *Lucernaria sainthilairei.*

A) General view of gonad delimited between a layer of gastrodermis and epidermis of septum; B-D) gonads associated with gastric radial pockets; E) detail of immature male gonadal content, with spermatocytes. A-E: cross sections. See Table 2 for abbreviations.
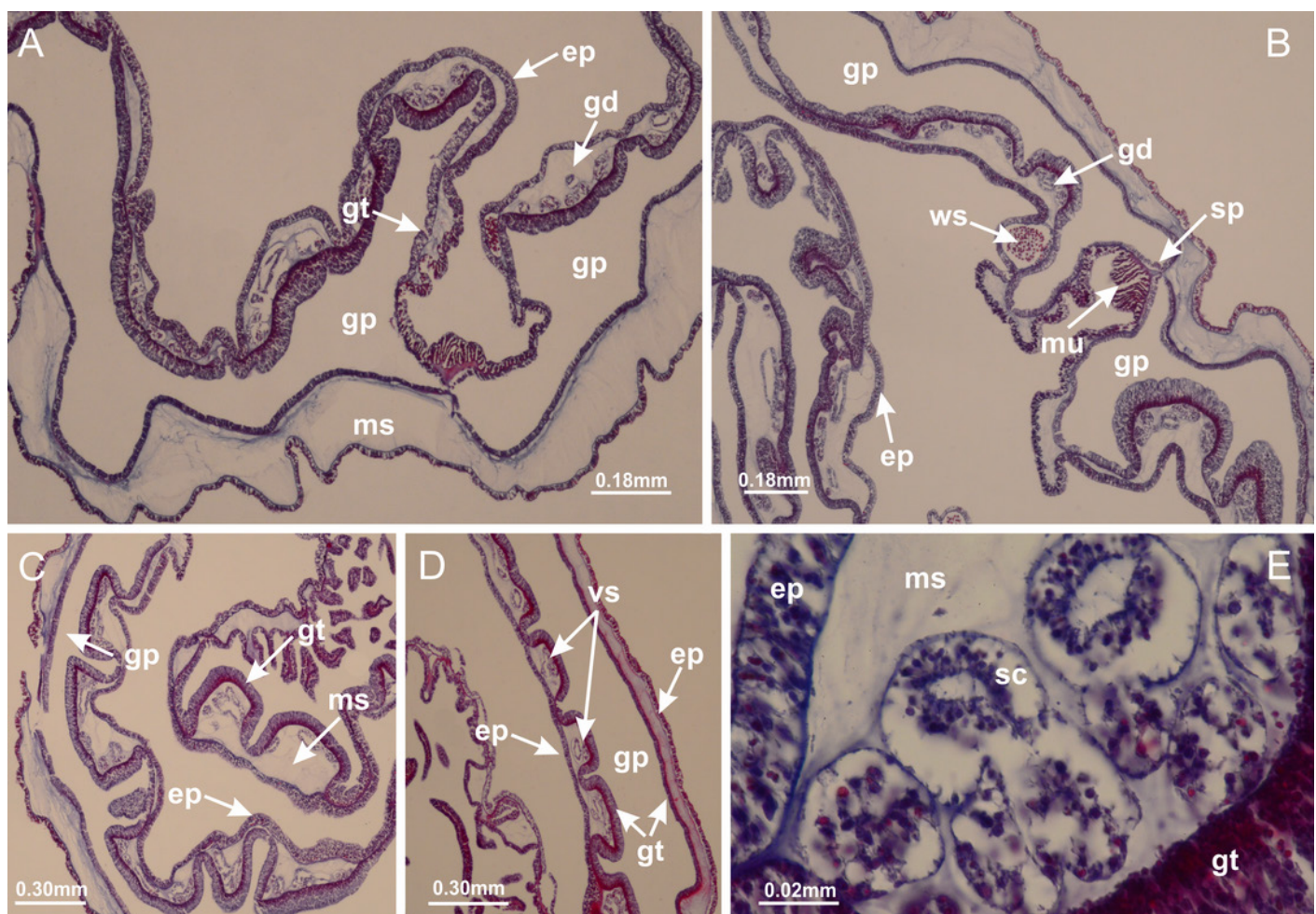
Figure 37

Intertentacular lobules of *Lucernaria sainthilairei.*

A, B) Tip of arms, in the region between intertentacular lobules and secondary tentacles; C) detail of intertentacular lobules, structures composed of a double layer of gastrodermis (of adjacent tentacles) and a central layer of mesoglea. A-C: longitudinal sections. See Table 2 for abbreviations.
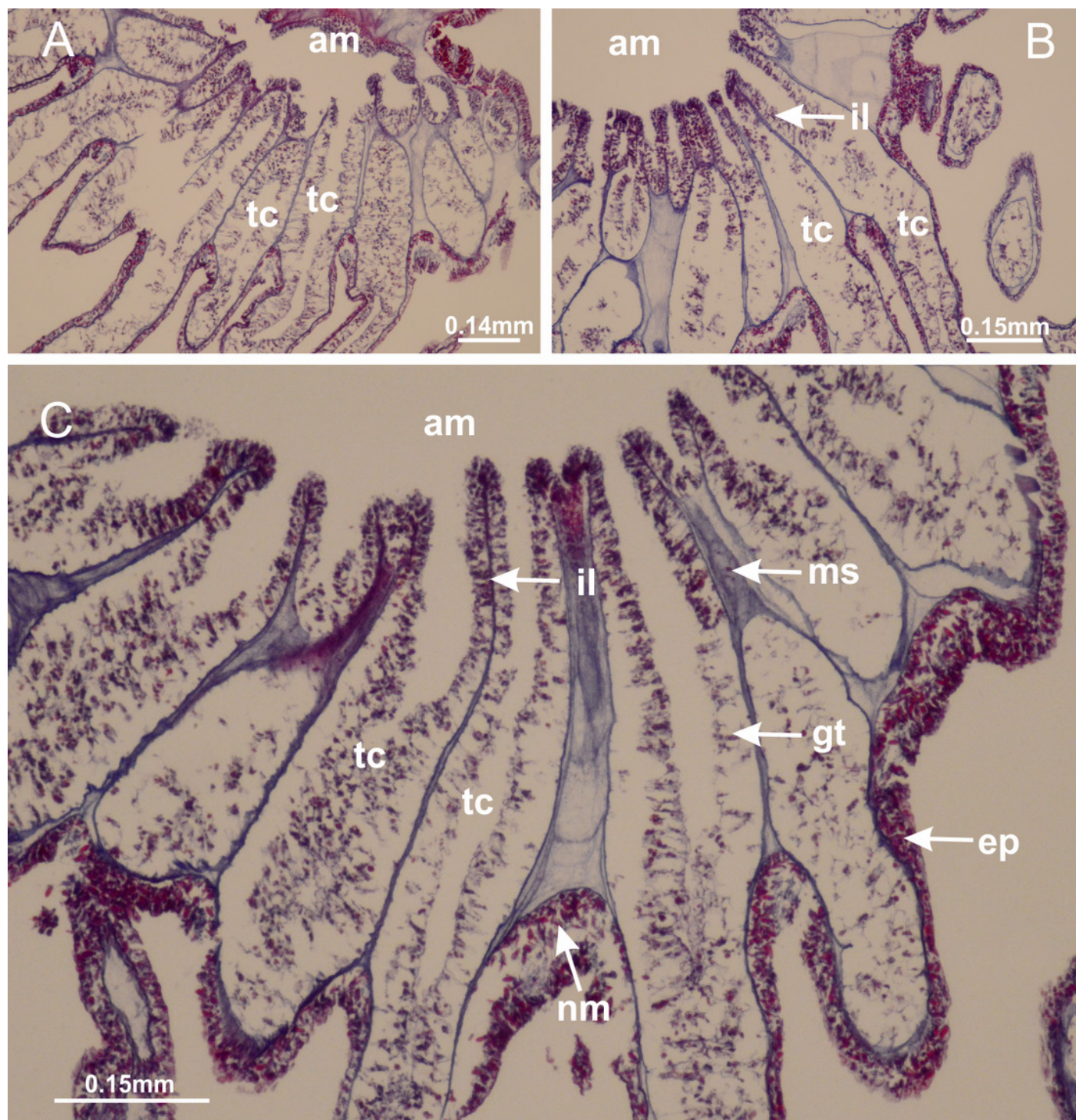
Figure 38

General view of *Calvadosia corbini.*

A, B) General view of body, with calyx and peduncle; C) pedal disk of peduncle; D) marginal coronal muscle; E) subumbrellar view of calyx, with central manubrium and gonads; F) detail of manubrium; G) white spots of nematocysts at calyx margin; H) detail of nodular gonads; I) subumbrellar view of paired arms; J) exumbrellar view of paired arms; K, L) pad-like adhesive structures at the tip of arms, and tentacular clusters. See Table 2 for abbreviations.
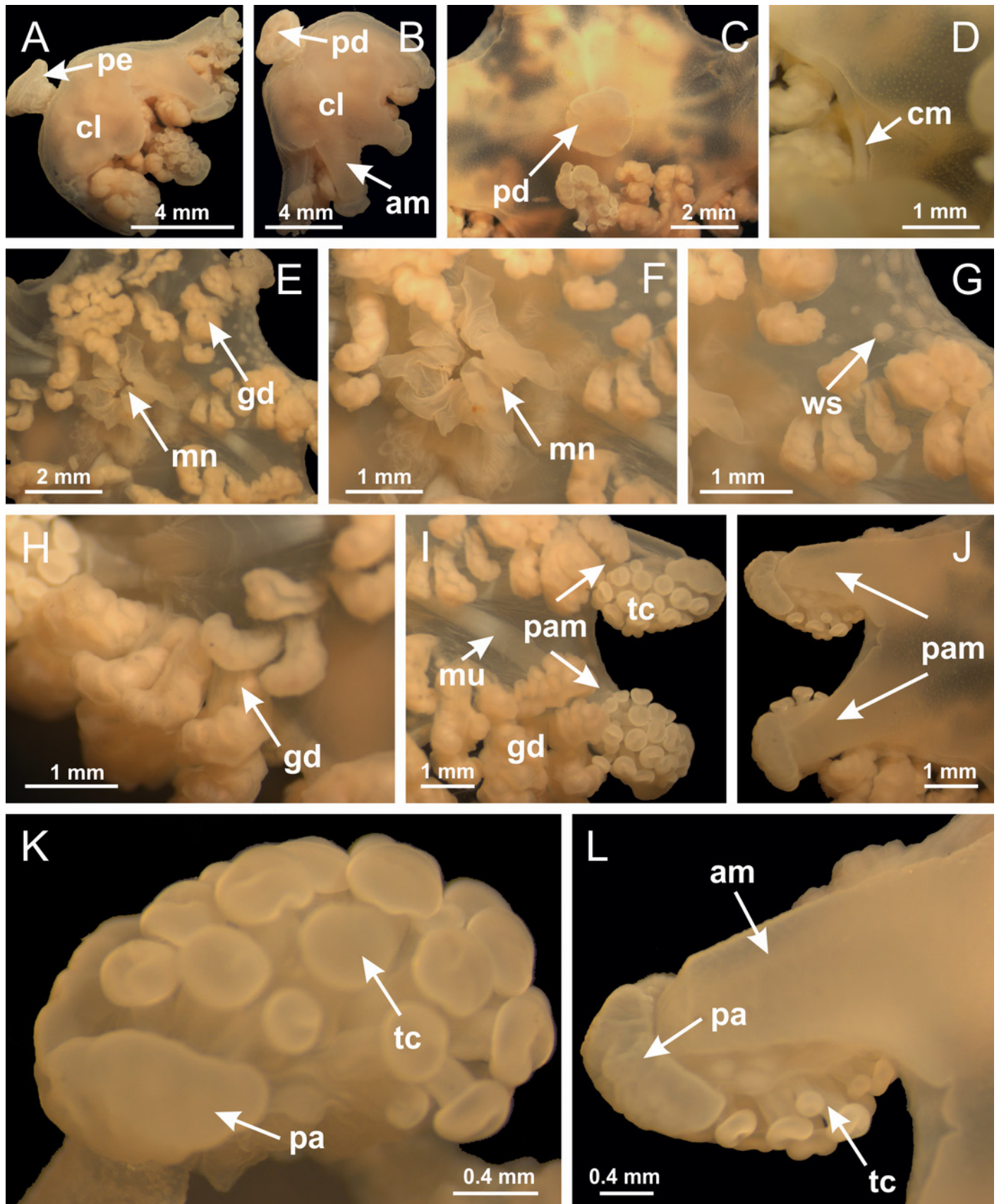
Figure 39

Peduncle and septa of *Calvadosia corbini* (from base moving upward in A-Y).

A) Base of peduncle; B-D) delimitation of four perradial chambers; E, F) fusion of four perradial chamber (indicated by black arrow), and delimitation of the four interradial septa; G) detail of interradial septum, without interradial longitudinal muscle; and evaginations in the gastrodermis of chamber; H) detail of evaginations in the gastrodermis; I) central cruciform chamber, delimited by gastrodermis, and four interradial septa, without interradial longitudinal muscle; J-Q) modification in shape and size of interradial septa and chamber; R-T) septa and chamber at the peduncle/calyx connection; U) interradial septa at calyx base, with interradial longitudinal muscle; V, W) gastric filaments as lateral evaginations of septal gastrodermis; X, Y) septa with infundibula delimited by epidermis, at calyx base. A-Y: cross sections. See Table 2 for abbreviations.
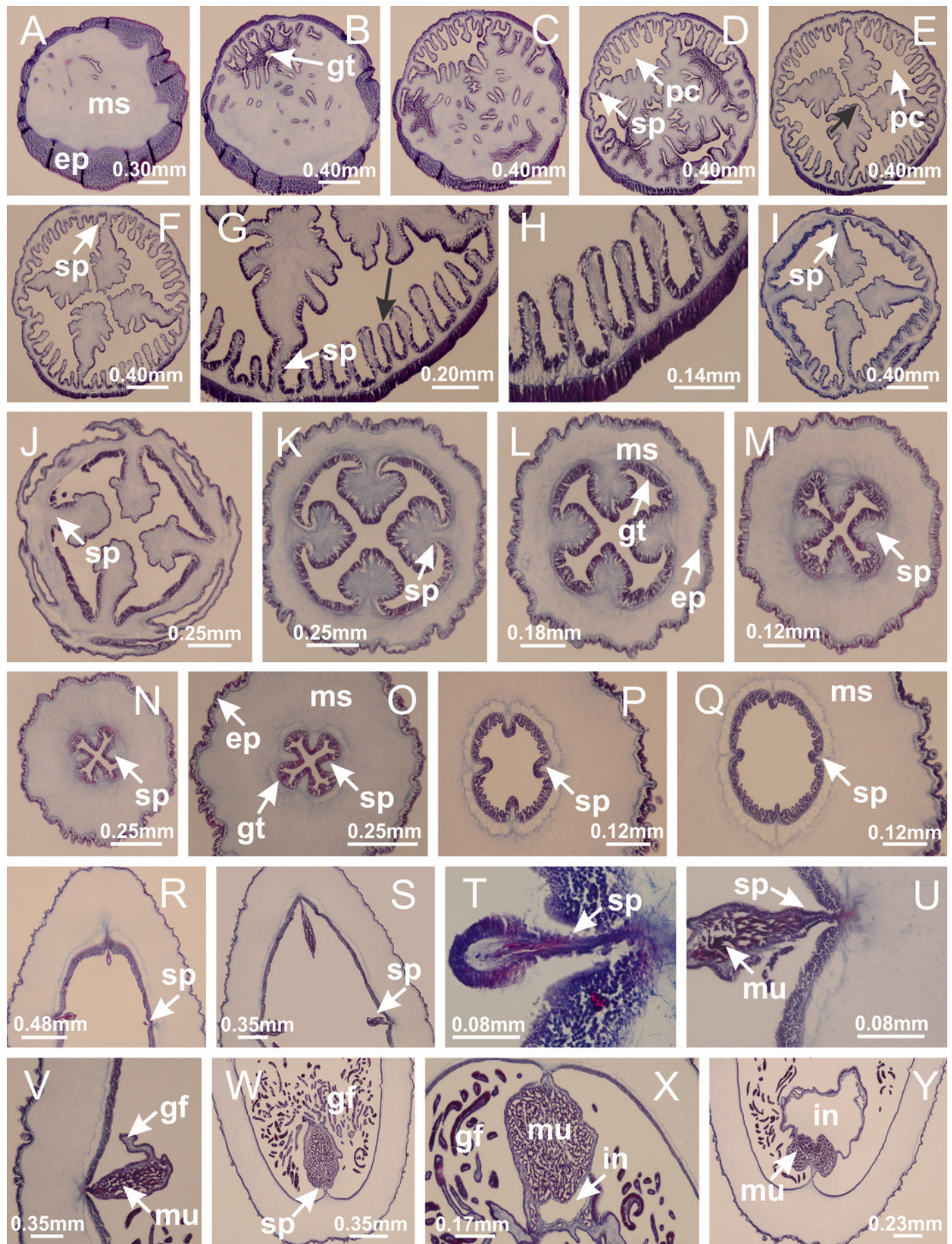
Figure 40

Gonads and gametoduct of *Calvadosia corbini.*

A-E) Internal organization of nodular gonads, composed of many vesicles, as an evagination of gastric radial pocket; F-H) internal organization of male vesicles, with spermatocytes adjacent to gastrodermis, and spermatozoa adjacent to epidermis; I) battery of nematocysts in the epidermis (subumbrella) between adjacent vesicles; J) detail of gametoduct; K) detail of internal organization of male vesicle; L-P) sequence of gametoduct connecting the spermatocytes with the gastrovascular cavity. A-P: longitudinal sections of gonad (cross sections of animals). See Table 2 for abbreviations.
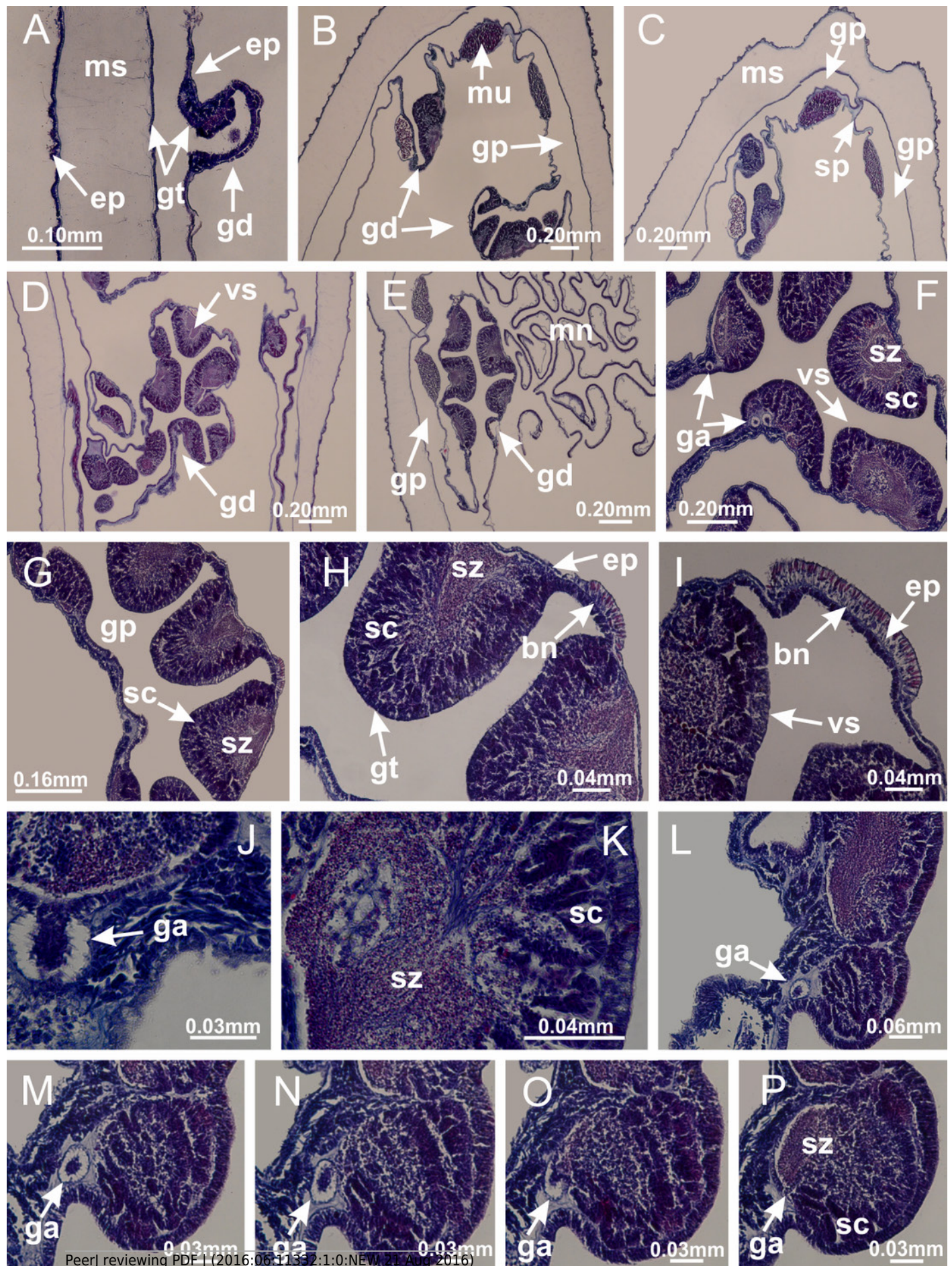
Figure 41

Intertentacular lobules of *Calvadosia corbini.*

A, B) Tip of arms; C) region between secondary tentacles and intertentacular lobules, structures composed of a double layer of gastrodermis (of adjacent tentacles) and a central layer of mesoglea; D, E) region between secondary tentacles and intertentacular lobules. A-E: longitudinal sections. See Table 2 for abbreviations.
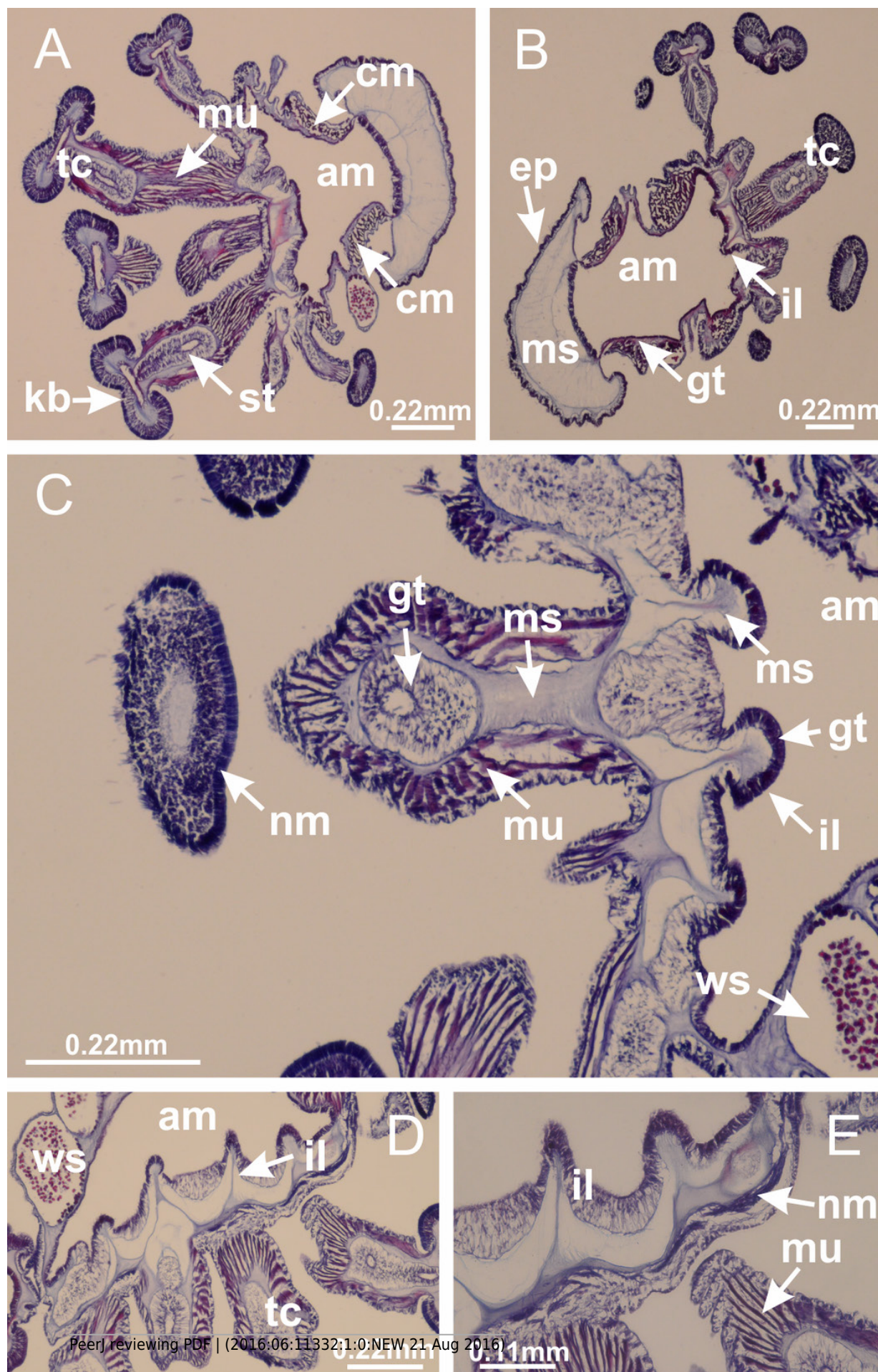
Figure 42

General view of *Calvadosia cruciformis.*

A) General view (exumbrella) of paired arms, peduncle, and primary tentacles; B, C) general view (subumbrella) of paired arms, manubrium, gonads, and white spots of nematocysts; D, E) primary tentacles, with horseshoe shaped knob; F, G) paired arms with gonads, tentacular cluster and interradial primary tentacle, H) pad-like adhesive structures in the outermost secondary tentacles; I) detail of pedal disk with axial canal. See Table 2 for abbreviations.
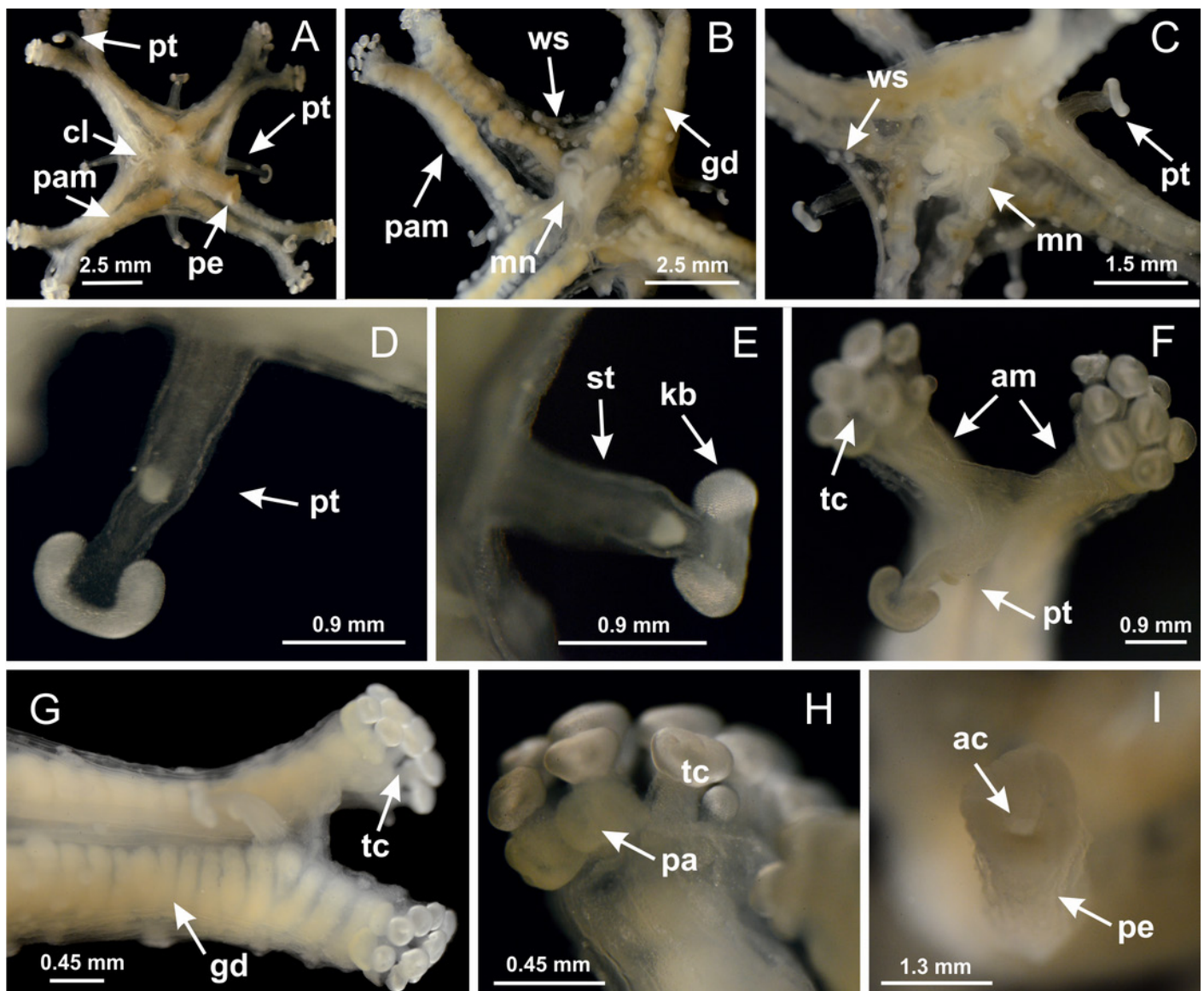
Figure 43

Peduncle and septa of *Calvadosia cruciformis* (from base moving upward in A-P).

A) Base of peduncle, with four perradial chambers (delimited by gastrodermis), and a central axial canal (delimited by exumbrellar epidermis); B) detail of axial canal; C, D) four perradial chambers (delimited by gastrodermis), and a central axial canal (delimited by exumbrellar epidermis); E-J) gradual fusion of perradial chambers (indicated by black arrows) and delimitation of four interradial septa without interradial longitudinal muscles; K-M) modification in shape and size of interradial septa and central cruciform chamber; N) septum at the peduncle/calyx connection, with infundibulum delimited by epidermis, and interradial longitudinal muscle; O, P) septa at calyx base, with gastric filaments as lateral evaginations of septal gastrodermis, and infundibula delimited by epidermis. A-P: cross sections. See Table 2 for abbreviations.
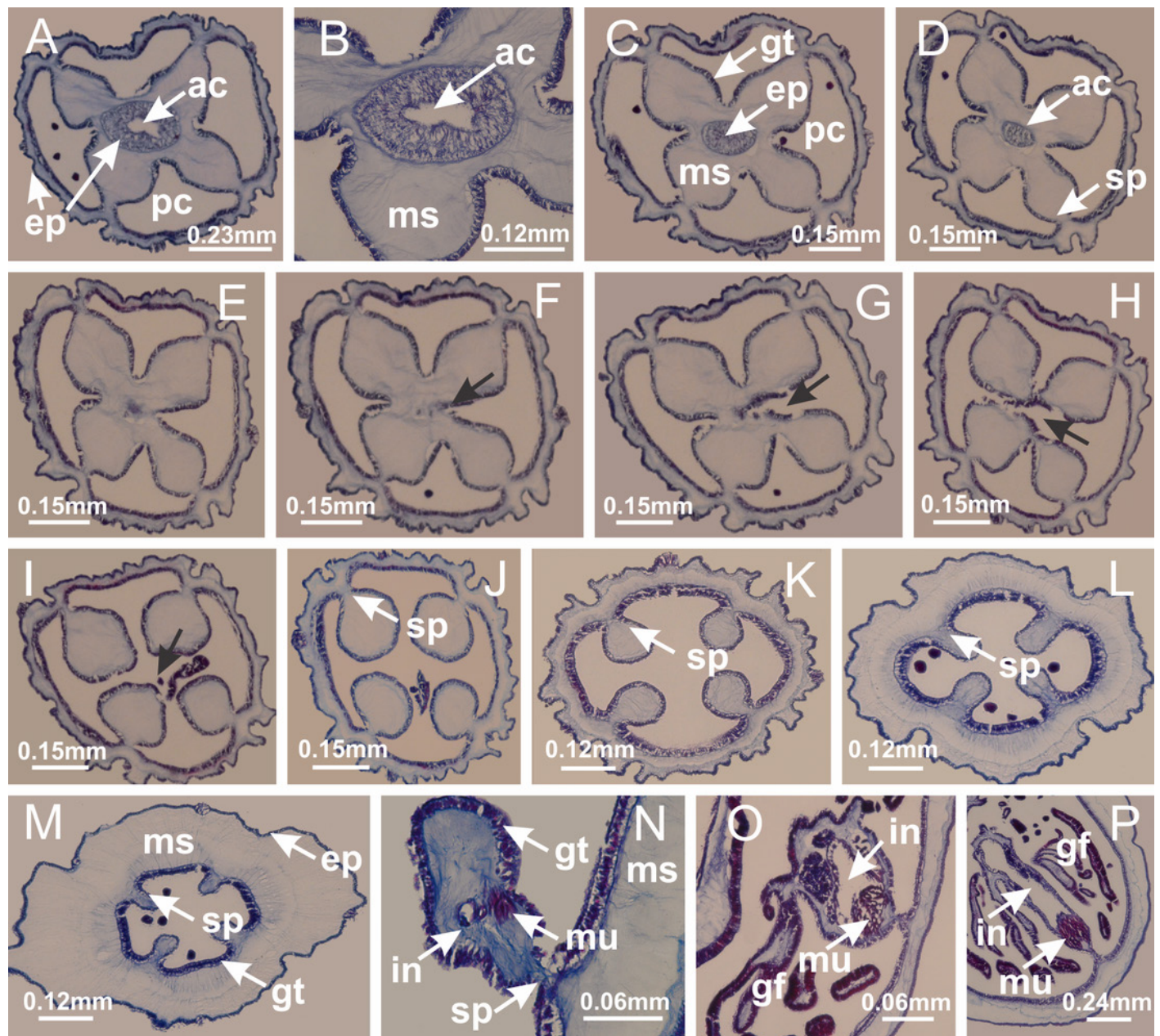
Figure 44

Gonads and gametoduct of *Calvadosia cruciformis.*

A) General view of female vesicles, inside gastric radial pockets in paired arms; B) detail of vesicle, with central mature oocytes and peripheral immature oocytes; C) organization of vesicles in a paired arm; D-L) sequence of gametoduct connecting the mature oocytes with the gastrovascular cavity (gastric radial pockets). A-L: cross sections of animal (longitudinal sections of vesicles). See Table 2 for abbreviations.
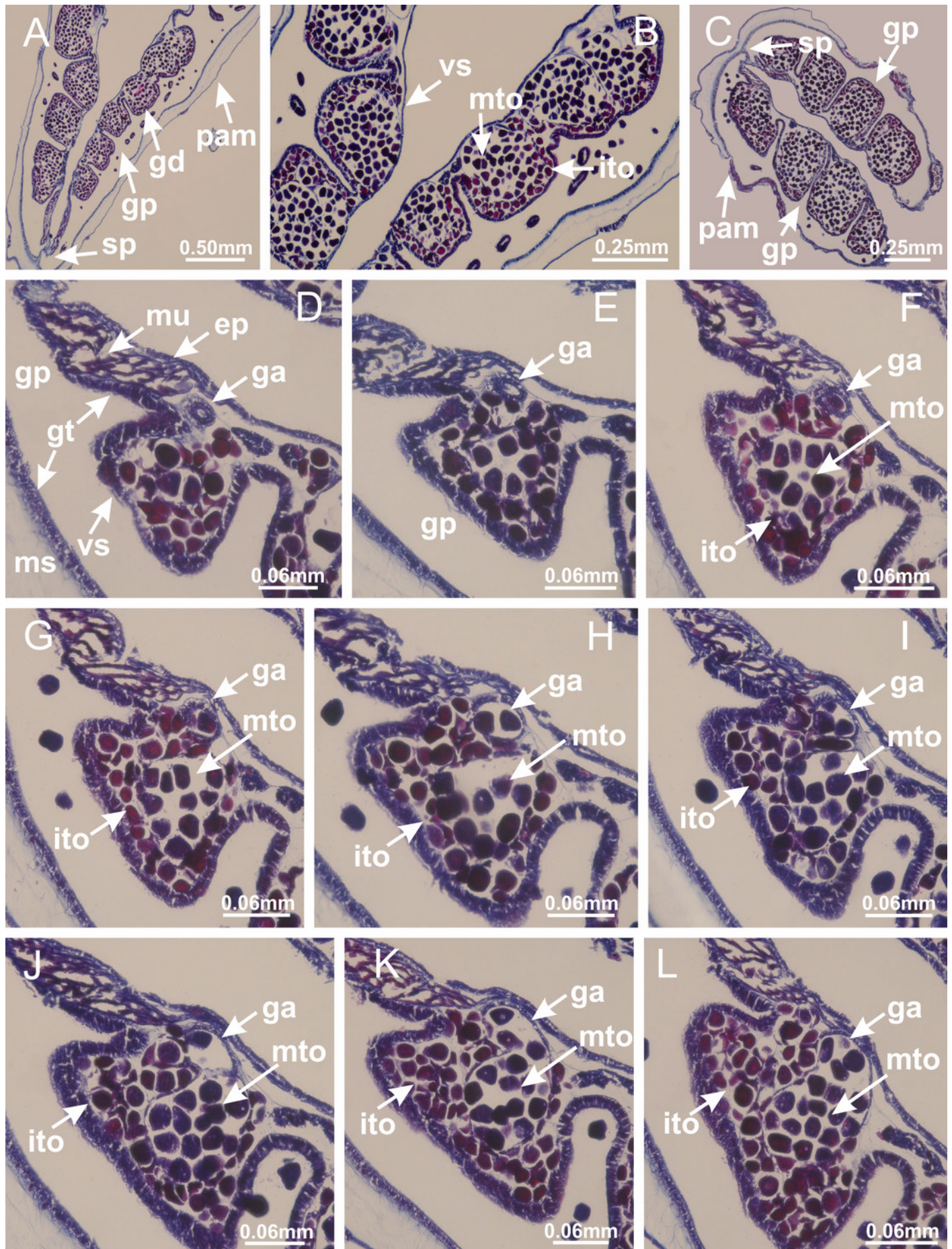
Figure 45

Intertentacular lobules of *Calvadosia cruciformis.*

A) General organization of tip of arms; B-D) secondary tentacles and intertentacular lobules, structures composed of a double layer of gastrodermis (of adjacent tentacles) and a central layer of mesoglea. A-D: longitudinal sections. See Table 2 for abbreviations.
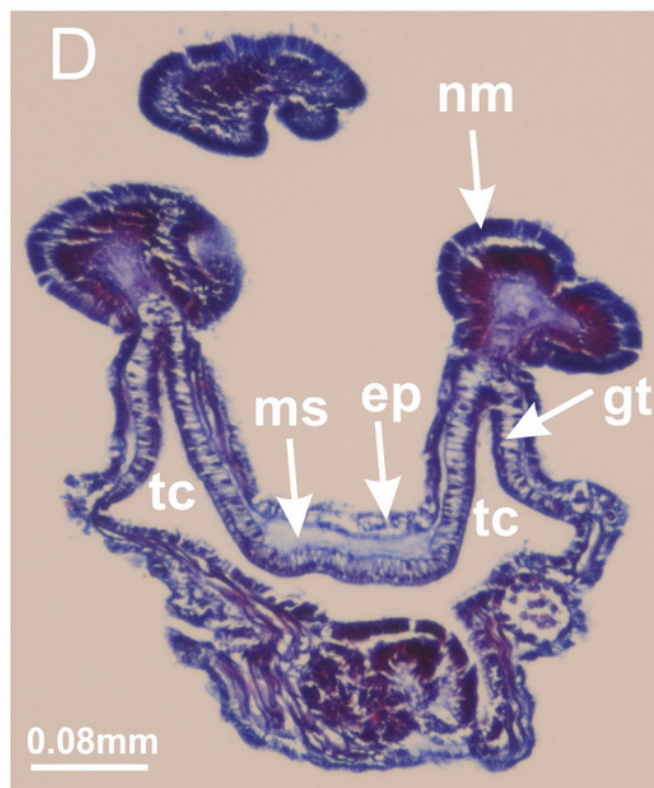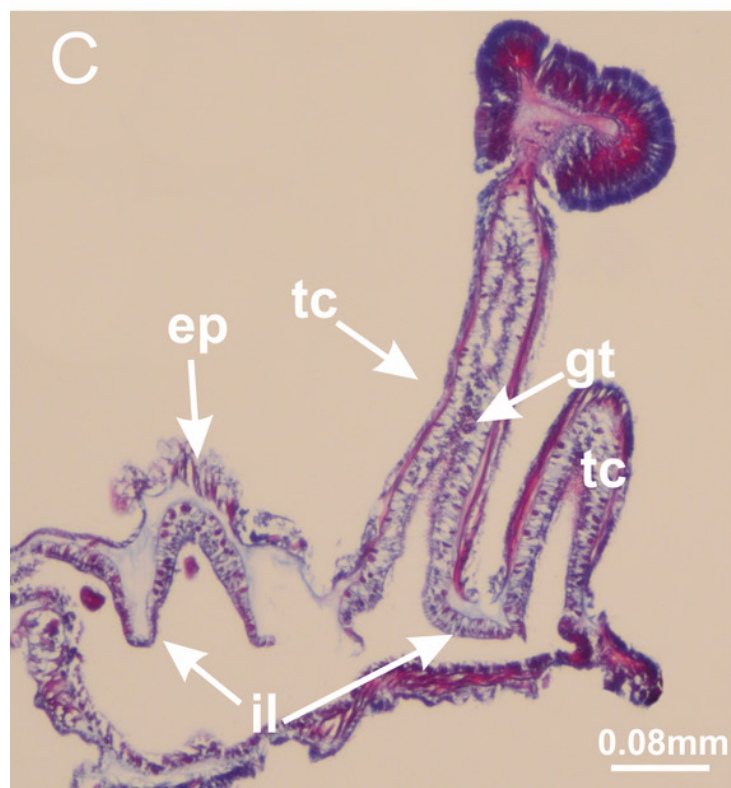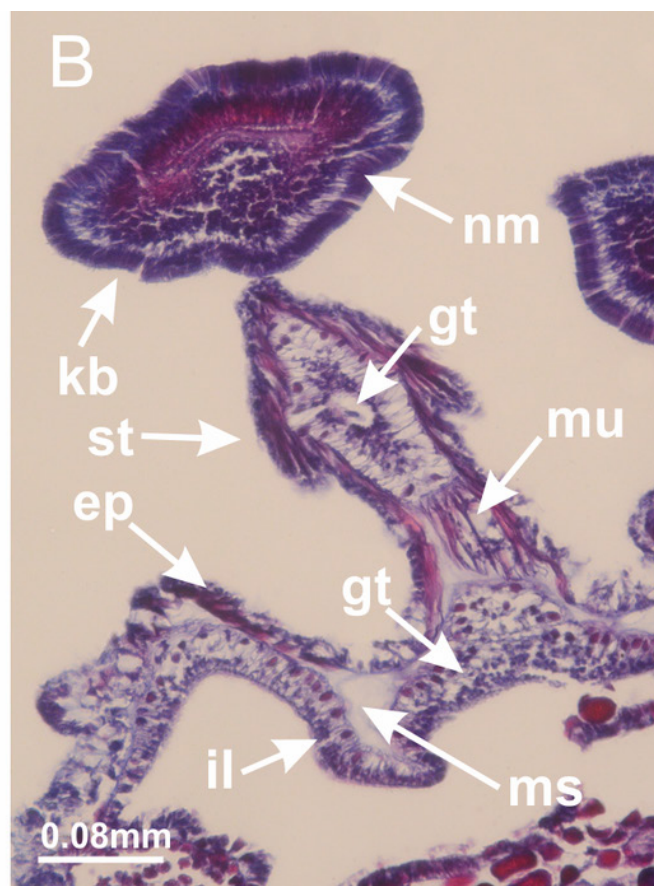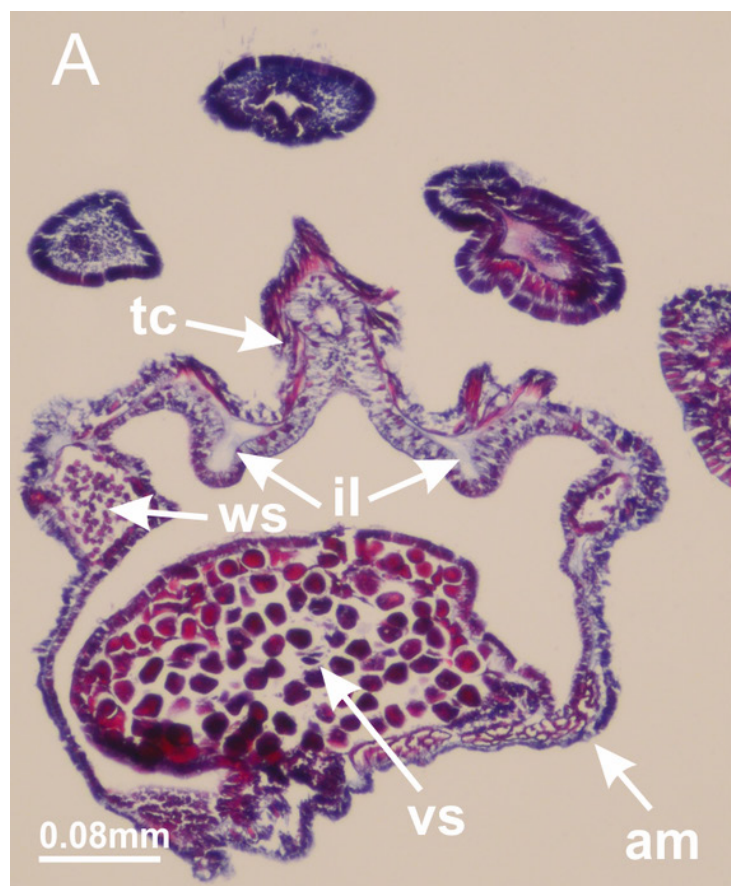
Figure 46

General view of *Calvadosia vanhoeffeni.*

A, B) General view of calyx (exumbrella), with gonads, arms, and tentacular cluster; C) batteries of nematocysts in the exumbrella; D) general view of calyx and peduncle; E) detail of peduncle; F) detail of pedal disk, with invaginations; G, H) subumbrellar view of calyx, with arms, gonads, white spots of nematocysts, and manubrium; I-L) tip of arms, with tentacular cluster and outermost secondary tentacles with pad-like adhesive structures. See Table 2 for abbreviations.
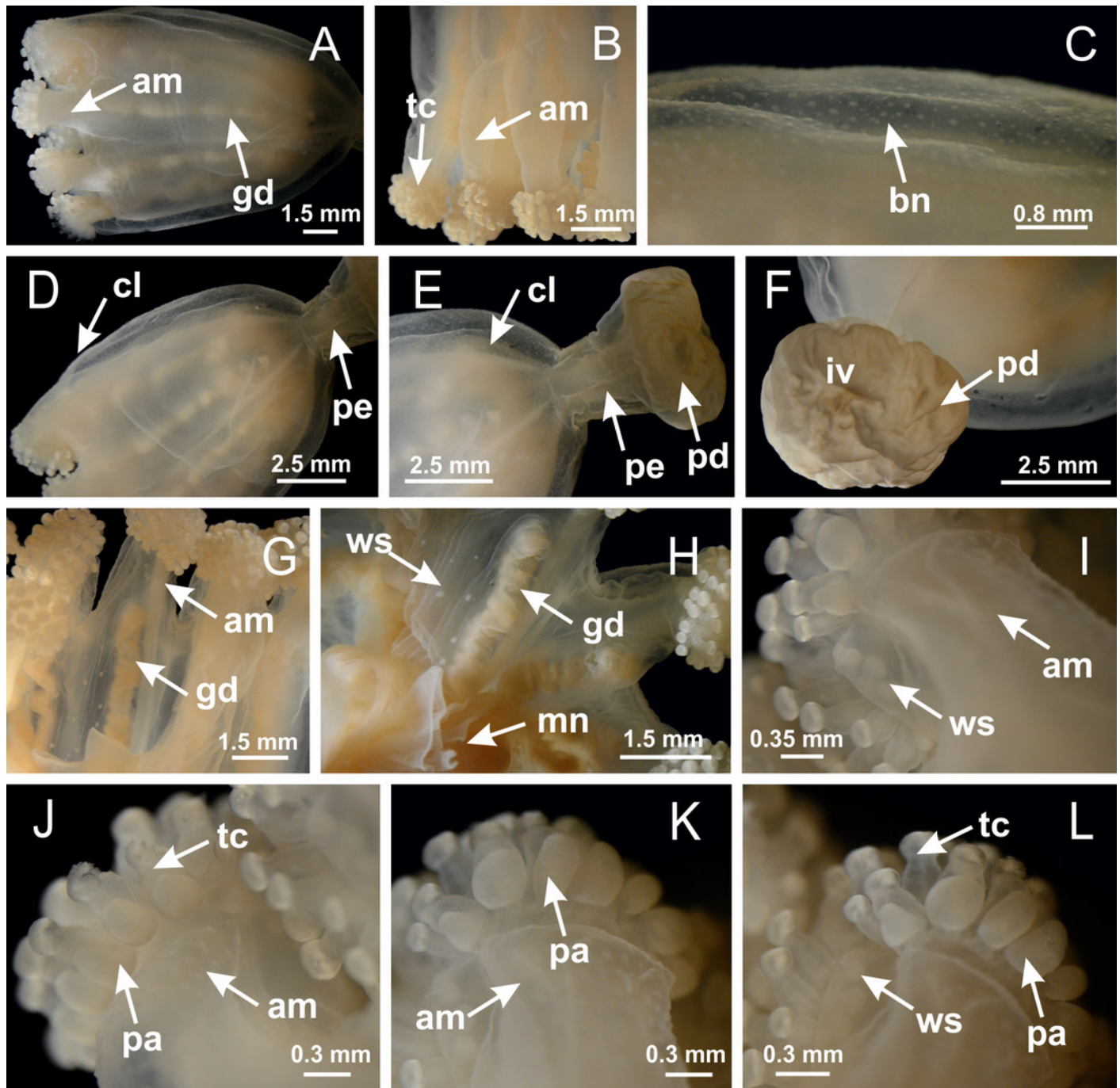
Figure 47

Peduncle and septa of *Calvadosia vanhoeffeni* (from base moving upward in A-P).

A) Base of peduncle; B, C) perradial chamber (one in evidence, but four in total), delimited by gastrodermis, and separated by interradial and central layer of mesoglea; D-H) fusion of four perradial chambers, and delimitation of the four interradial septa (indicated by black arrows); I) detail of interradial septum, without interradial longitudinal muscle; J, K) four interradial septa, with a central chamber delimited by gastrodermis; L, M) septa at the peduncle/calyx connection, with interradial longitudinal muscles; N) detail of septum with interradial longitudinal muscle; O, P) gastric filaments as lateral evaginations of septal gastrodermis, and septa with infundibula delimited by epidermis, at calyx base. A-P: cross sections. See Table 2 for abbreviations.
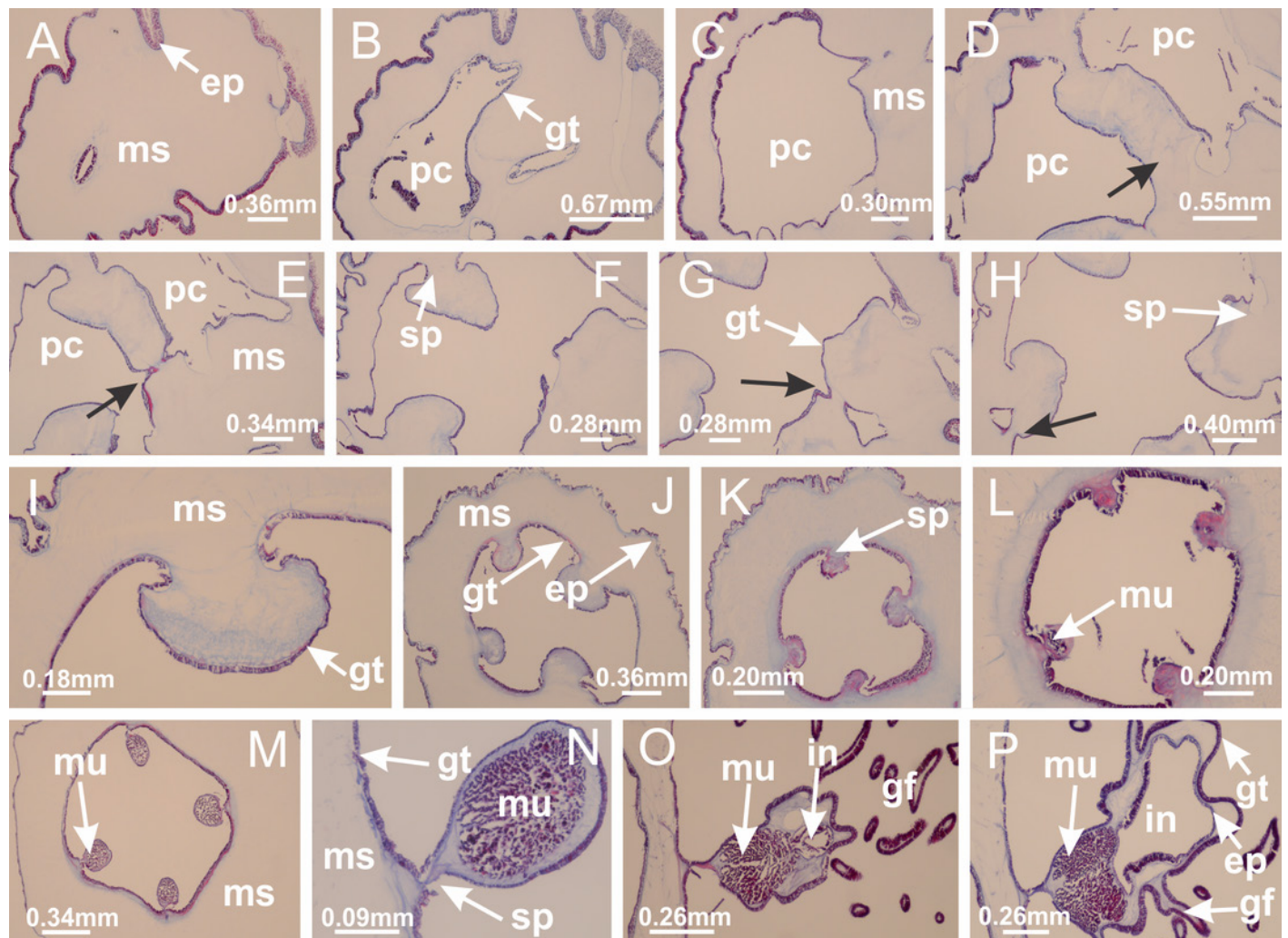
Figure 48

Gonads and gametoduct of *Calvadosia vanhoeffeni.*

A) General view of gonad, as lateral evaginations of septum; B-E) gonadal content between a layer of gastrodermis (adjacent to spermatocytes) and epidermis (adjacent to spermatozoa); F-S) sequence of gametoduct connecting the spermatozoa and spermatocytes with the gastrovascular cavity of gastric radial pocket (indicated by black arrows); T-W) sequence of gametoduct connecting the spermatozoa and spermatocytes with the gastrovascular cavity of gastric radial pocket (indicated by black arrows); X) detail of gametoduct. A-X: cross sections of body, and longitudinal sections of gonads. See Table 2 for abbreviations.
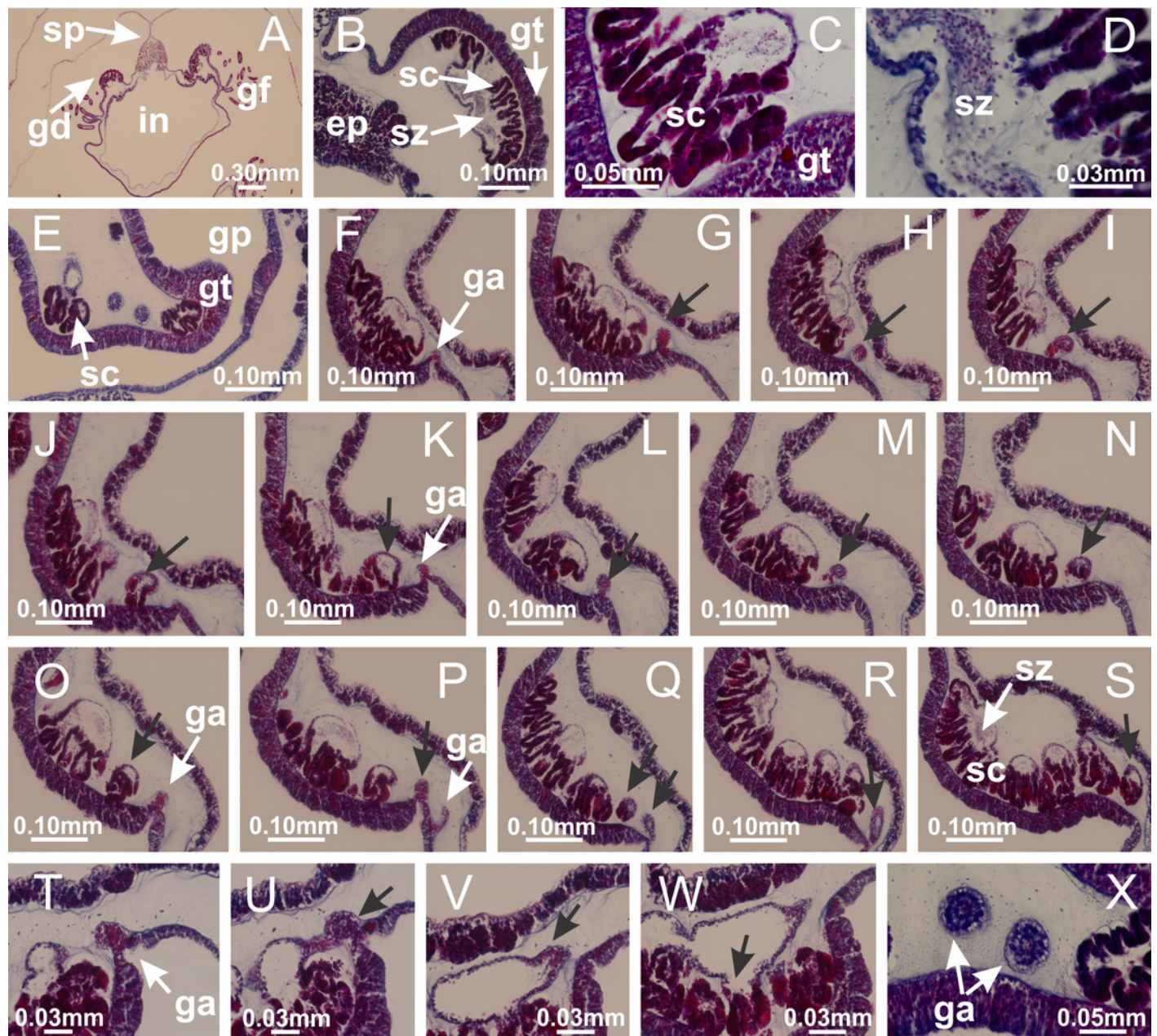
Figure 49

Gonads and gametoduct of *Calvadosia vanhoeffeni.*

A-G) Sequence of gametoduct connecting the spermatozoa and spermatocytes with the gastrovascular cavity of gastric radial pocket (indicated by black arrows); H-J) sequence of gametoduct connecting the spermatozoa and spermatocytes with the gastrovascular cavity of gastric radial pocket; K) detail of gametoduct; L) gametoduct connecting the spermatozoa and spermatocytes with the gastrovascular cavity of gastric radial pocket; M-O) detail of gametoduct. A-O: longitudinal sections of gonads. See Table 2 for abbreviations.
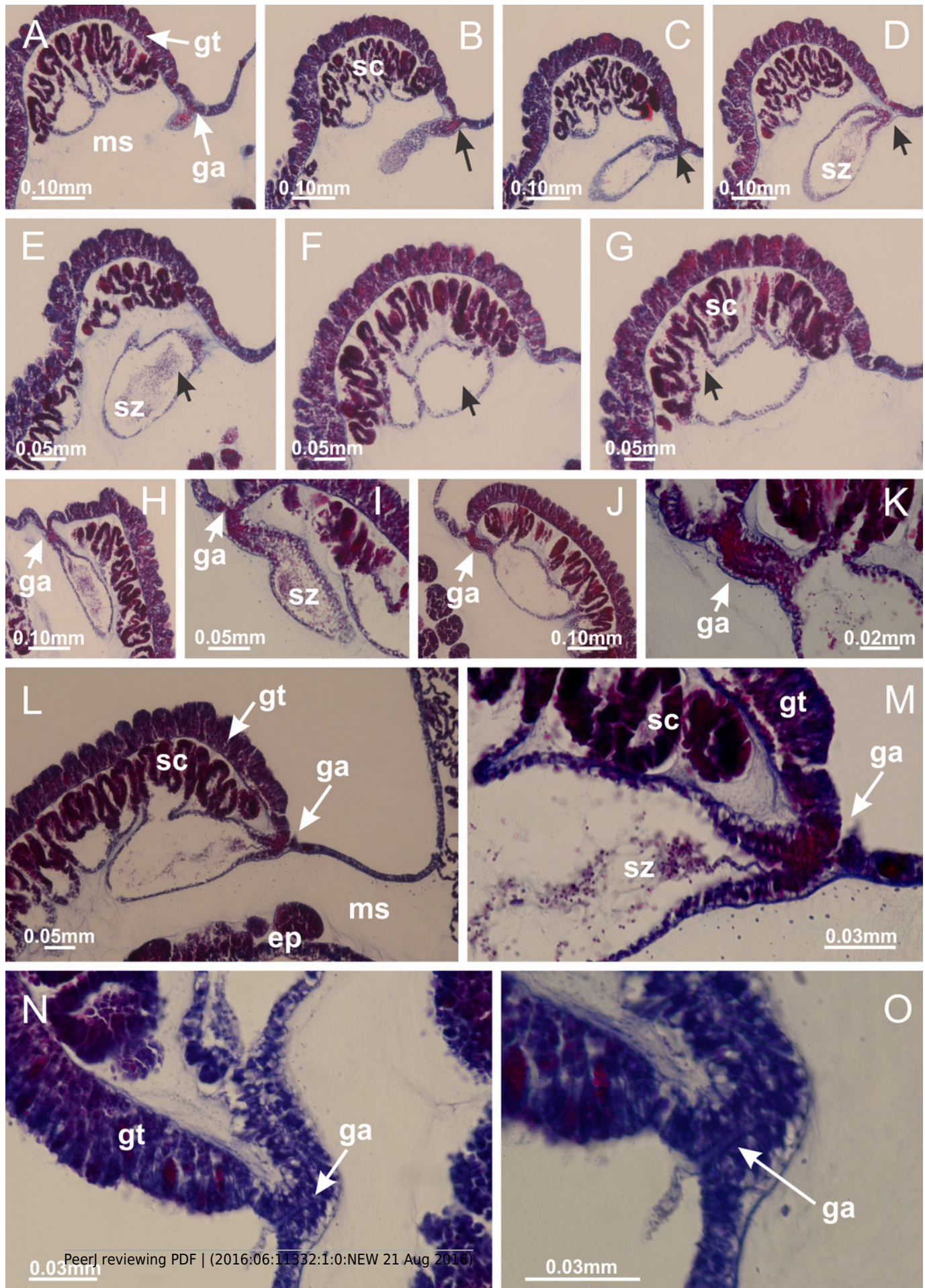
Figure 50

Intertentacular lobules of *Calvadosia vanhoeffeni.*

A) General organization of tip of arms, in the region between intertentacular lobules and secondary tentacles; B-D) detail of intertentacular lobules, structures composed of a double layer of gastrodermis (of adjacent tentacles) and a central layer of mesoglea. A-D: longitudinal sections. See Table 2 for abbreviations.
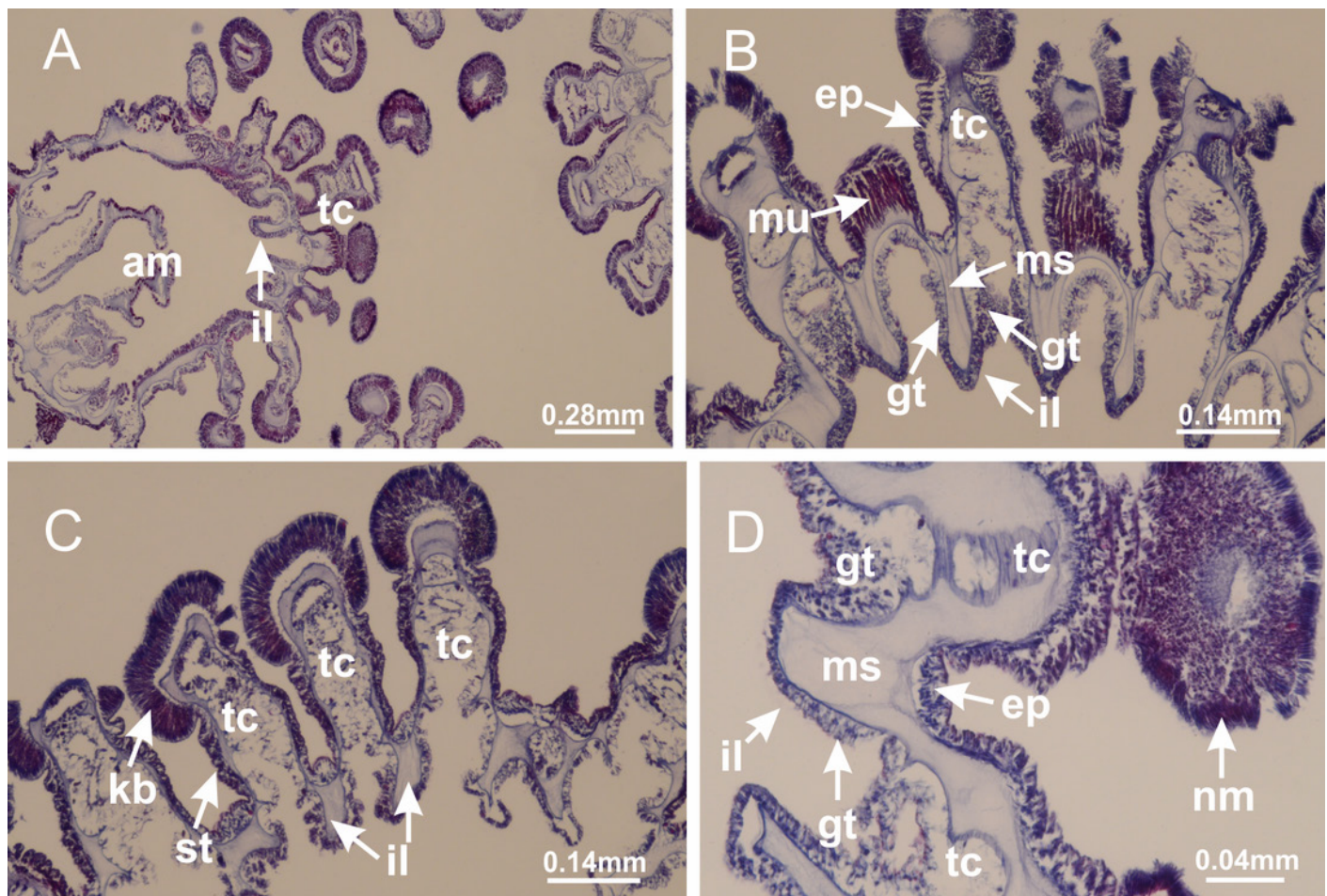
Figure 51

General view of *Craterolophus convolvulus.*

A) General view of calyx; B) peduncle; C) detail of pedal disk, with a central pit (indicated by black arrow); D) tentacular cluster; E-G) secondary tentacles and pad-like adhesive structures in the outermost secondary tentacles; H, I) subumbrellar view, with manubrium and gonads. See Table 2 for abbreviations.
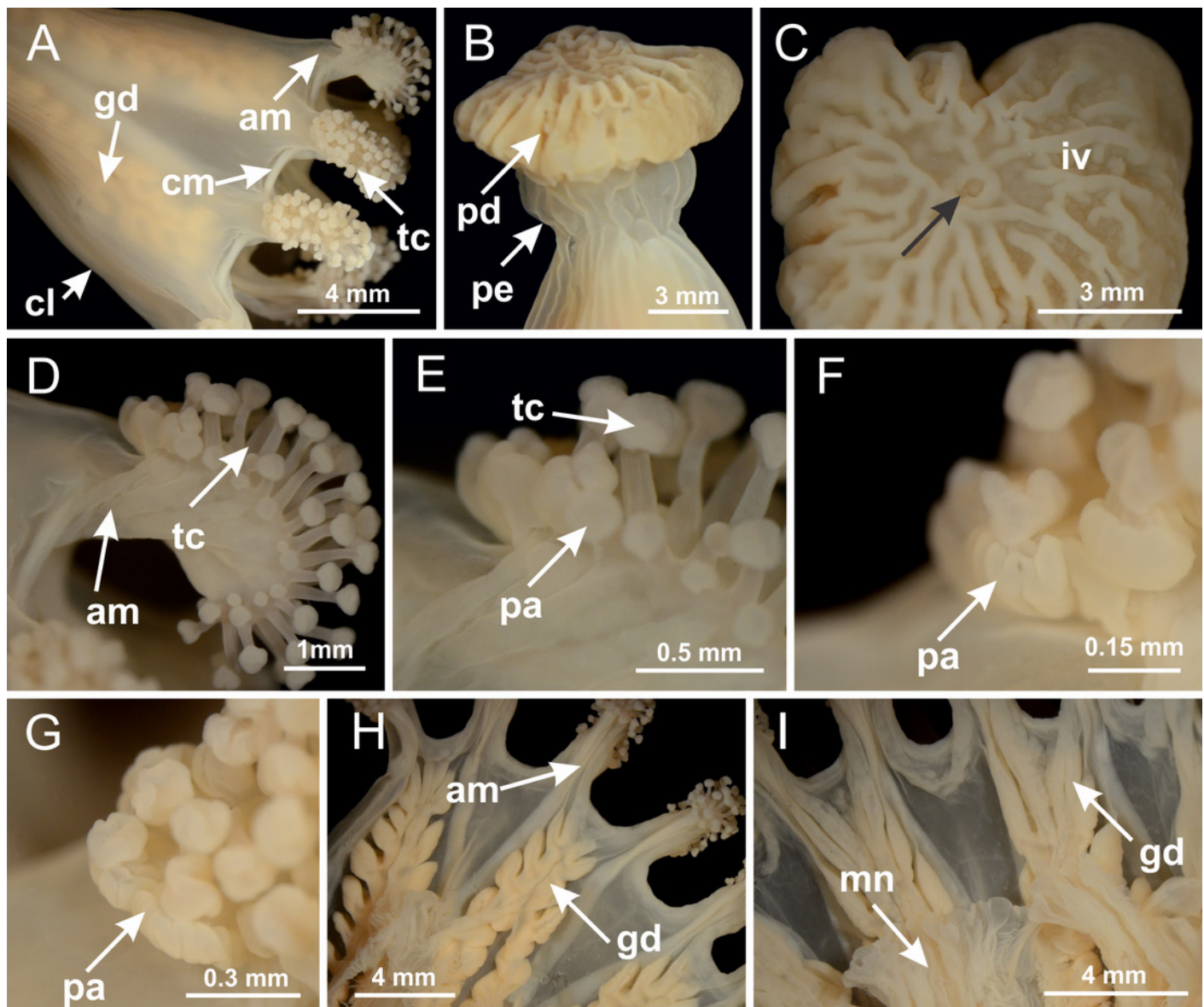
Figure 52

Peduncle and septa of *Craterolophus convolvulus* (from base moving upward in A-S).

A) Four perradial chambers in peduncle; B) detail of epidermis, mesoglea, and gastrodermis of peduncle; C-I) variation of shape and size of perradial chambers in peduncle; J, K) delimitation of four interradial septa, L) detail of delimitation of septum; M-O) delimitation of four interradial septa (connection of four perradial chambers and reduction of central mesoglea), P-S) projections of lateral tissue (double layer of gastrodermis and central layer of mesoglea; indicated by black arrows), and infundibula at central region of septa. A-S: cross sections. See Table 2 for abbreviations.
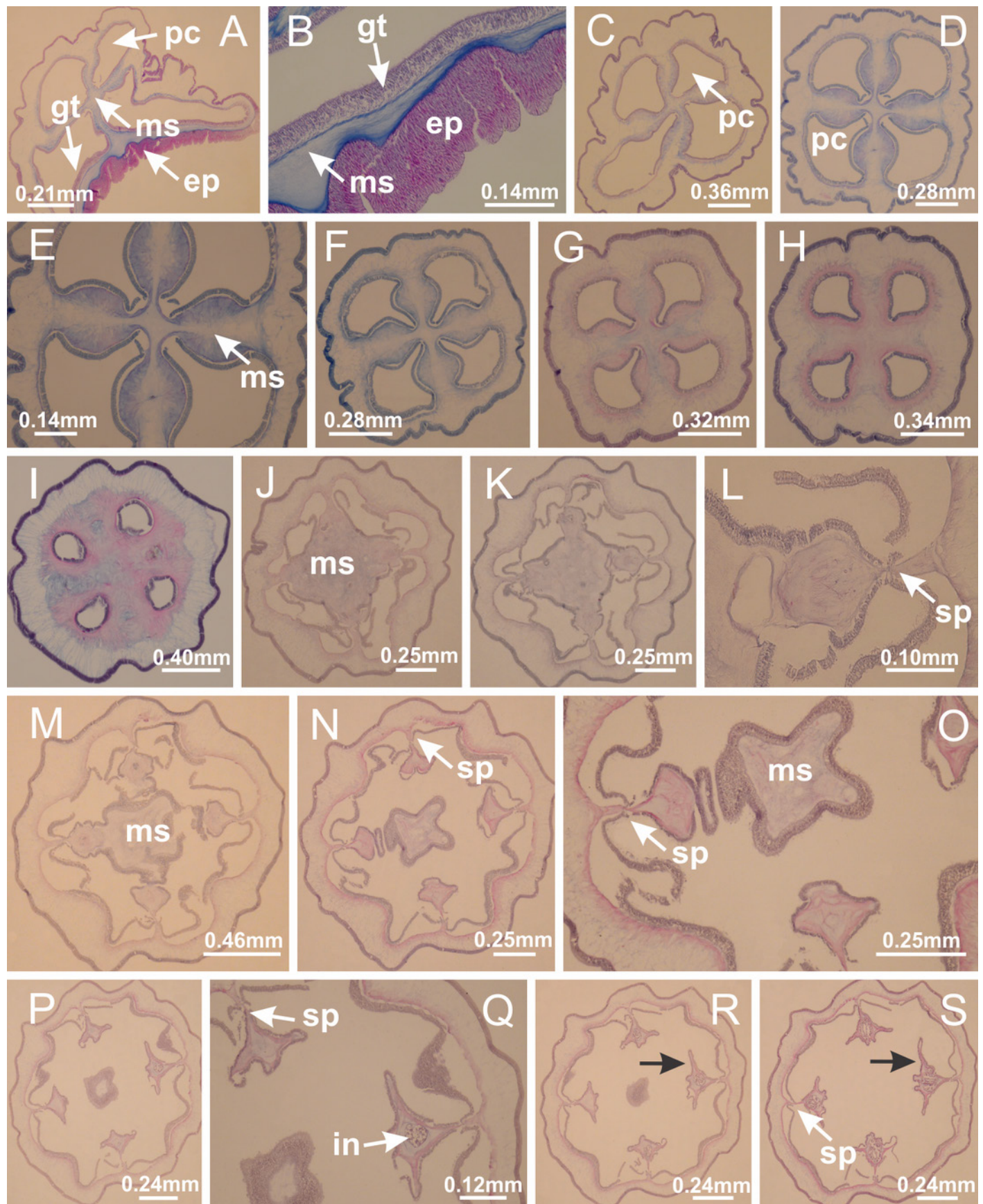
Figure 53

Claustra in *Craterolophus convolvulus.*

A-D) Claustra delimitation (lateral projections of adjacent septa, indicated by black arrows); E) detail of claustra delimitation (fusion of lateral projections of adjacent septa); F) claustra dividing the gastrovascular cavity, delimiting accessory radial pockets; G) formation of auxiliary radial pockets, due to folds in the septum containing gonadal content (indicated by black arrows); H) organization of septum with auxiliary radial pockets at the base of calyx (below manubrium delimitation); I) fusion of gastrodermis and epidermis of adjacent septa (indicated by black arrows), during delimitation of manubrium and principal radial pocket (gastric filaments associated with principal radial pocket); J) complete delimitation of principal radial pocket and auxiliary radial pocket. A-J: cross sections. See Table 2 for abbreviations.
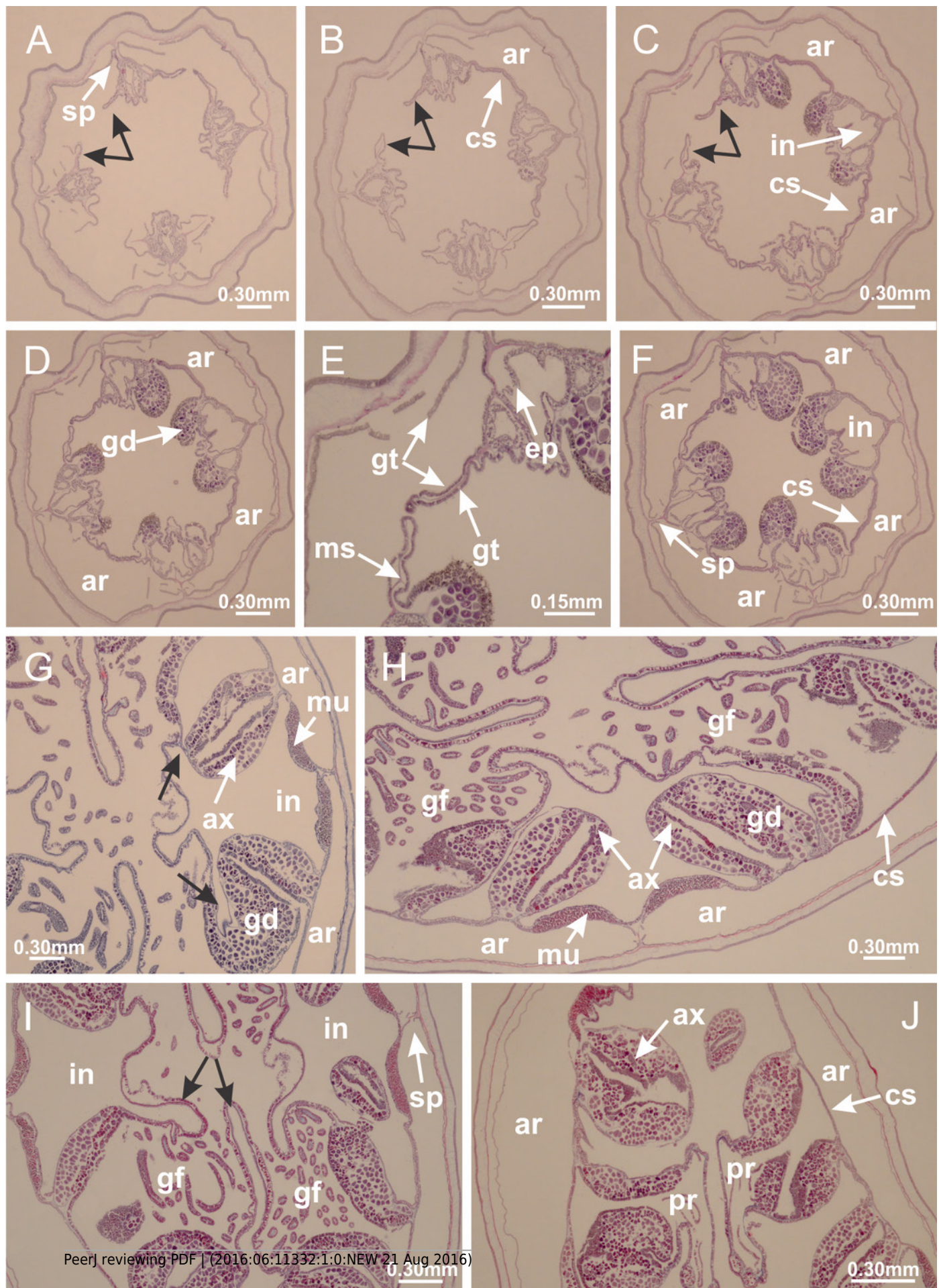
Figure 54

Organization of gonads in *Craterolophus convolvulus.*

A) Gonads associated with principal radial pockets and auxiliary radial pockets; B) organization of auxiliary radial pocket inside infundibulum or outside principal radial pocket (central gastrodermis associated with immature oocytes; and mature oocytes associated with external epidermis); C) auxiliary radial pocket inside principal radial pocket; D) organization of auxiliary radial pocket inside principal radial pocket (central epidermis associated with mature oocytes, and external gastrodermis associated with immature oocytes); E-G) delimitation of internal auxiliary radial pocket (indicated by black arrows); H-L) delimitation of external auxiliary radial pocket (indicated by black arrows). A-L: cross sections. See Table 2 for abbreviations.
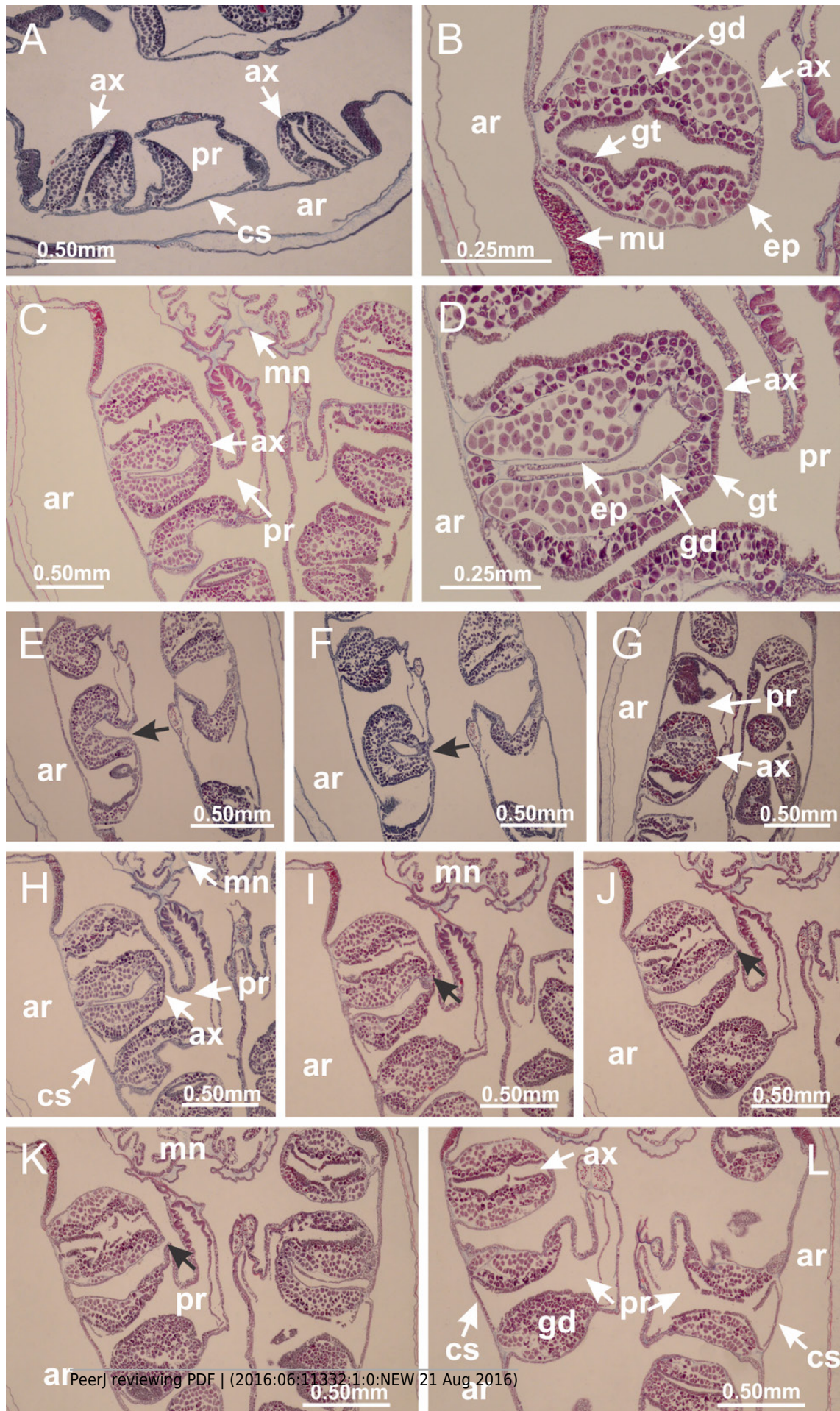
Figure 55

Gonads and gametoduct of *Craterolophus convolvulus.*

A, B) Gonadal content between a layer of gastrodermis and epidermis of septum; C) immature oocytes adjacent to gastrodermis, and mature oocytes adjacent to epidermis; D-K) gametoduct connecting the mature oocytes with the gastrovascular cavity of principal radial pocket (indicated by black arrows); L-N) gametoduct; O-Q) detail of gametoduct, showing direct connection of mature oocytes with gastrovascular cavity. A-N: cross sections; O-Q: longitudinal sections. See Table 2 for abbreviations.
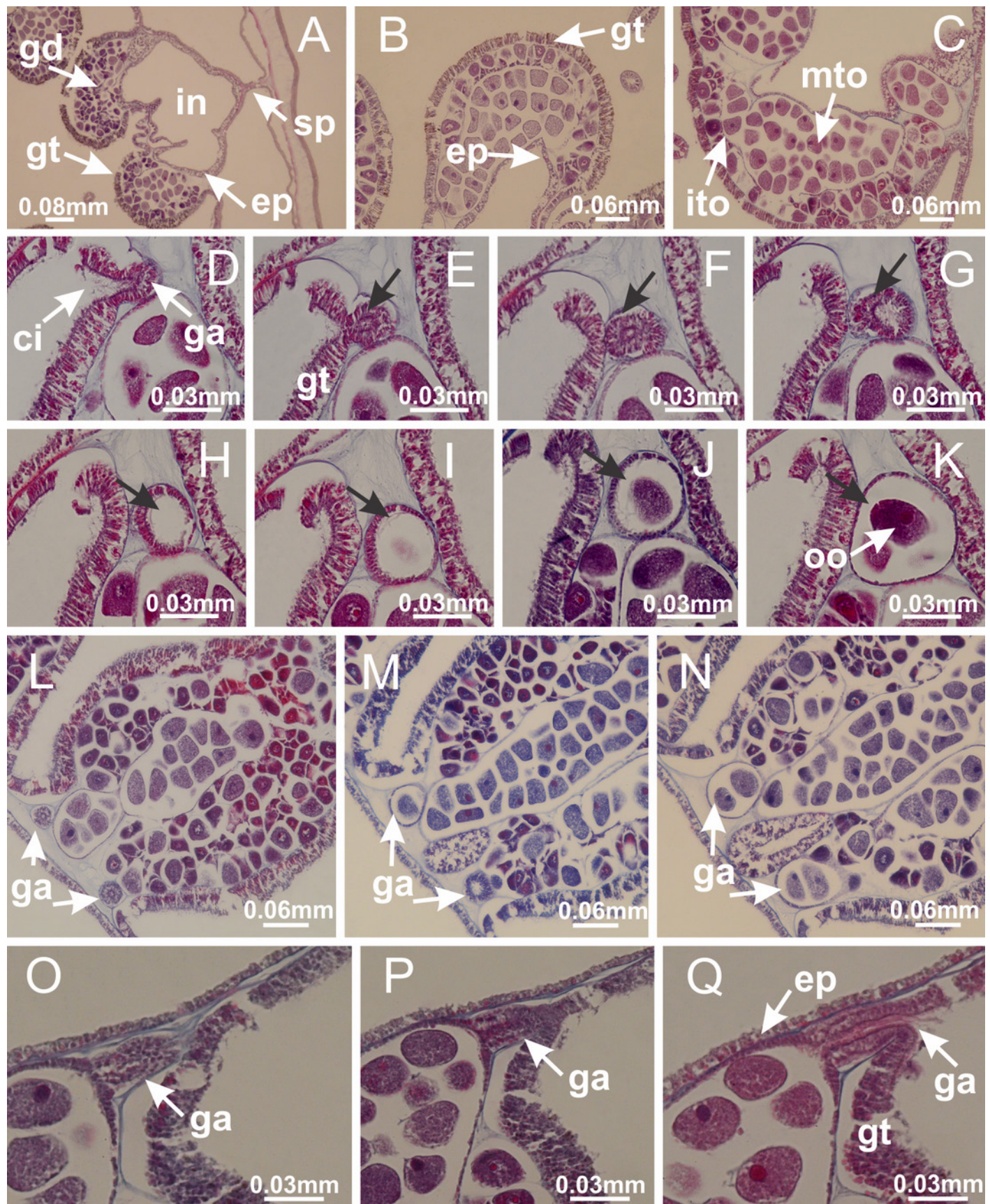
Figure 56

Intertentacular lobules of *Craterolophus convolvulus.*

A, B) Tip of the arms; C) tentacles, with longitudinal muscle; D, E) organization of tip of arms and intertentacular lobules; F) detail of intertentacular lobules, structures composed of a double layer of gastrodermis (of adjacent tentacles) and a central layer of mesoglea. A-F: longitudinal sections. See Table 2 for abbreviations.
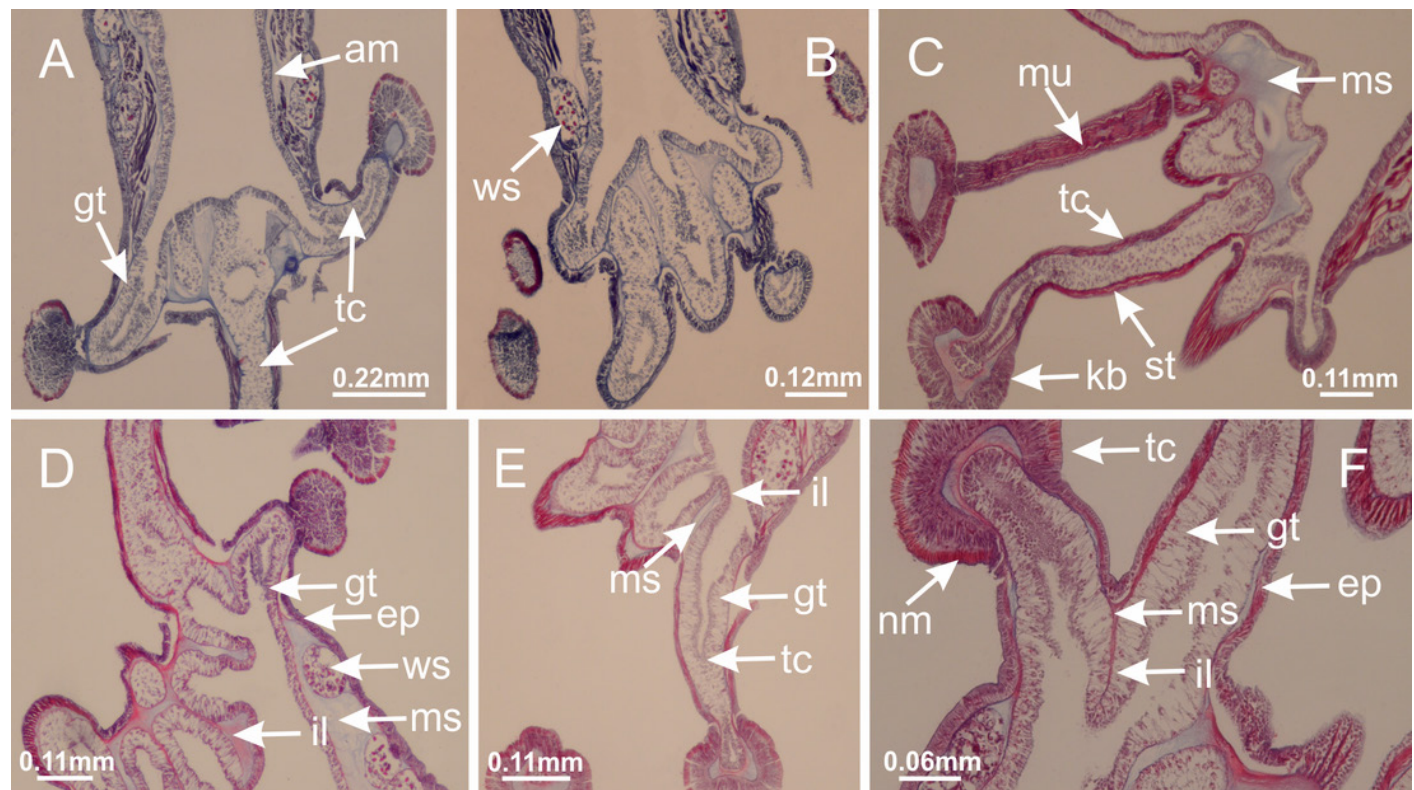
Figure 57

General body plan of different species and their phylogenetic relationship (modified from Miranda et al., 2016).

Manania uchidai: A) peduncle with one chamber and four interradial longitudinal muscles; B, C) peduncle with four chambers; D) four interradial infundibula; E) delimitation of claustra; F) claustra and four accessory radial pockets; G, H) delimitation of principal radial pockets and manubrium; I) accessory and principal radial pockets separated by claustra; J) interradial ostia, and perradial anchors connected to the gastrovascular cavity; K) interradial anchors connected to the gastrovascular cavity; L) total separation of arms; ***Haliclystus tenuis* and *H. antarcticus*** (modified from Miranda, Collins & Marques, 2013): A) four perradial chambers and four interradial longitudinal muscles; B) fusion of the four chambers into one chamber; C) delimitation of interradial septa; D) four interradial infundibula; E) formation of gonads and gastric filaments; F, G) delimitation of gastric radial pockets and manubrium; H) four gastric radial pockets and a central manubrium; I) interradial ostia, and perradial anchors connected to the gastrovascular cavity; J) interradial anchors connected to the gastrovascular cavity; K) total separation of arms; ***Lucernaria quadricornis, L. bathyphila, L. sainthilairei***: A) four gastric septa with internal interradial longitudinal muscles; B) four interradial infundibula; C) formation of gonads and gastric filaments; D, E) delimitation of gastric radial pockets and manubrium; F) four gastric radial pockets and a central manubrium; G) interradial ostia; H, I) separation of arms; ***Calvadosia cruciformis***: A) four perradial chambers and one central axial canal; B) four perradial chambers; C, D) delimitation of four interradial septa; E) four interradial septa with four interradial longitudinal muscles and infundibula; F) formation of gonads and gastric filaments; G, H) delimitation of gastric radial pockets and manubrium; I) four gastric radial pockets and a central manubrium; J) interradial ostia, and perradial primary tentacles connected to the gastrovascular cavity; K) interradial primary tentacles connected to the gastrovascular

cavity; L) total separation of arms; **_Calvadosia corbini_** and **_Calvadosia vanhoeffeni_**: A) four perradial chambers; B, C) delimitation of four interradial septa; D) four interradial septa with four interradial longitudinal muscles and infundibula; E) formation of gonads and gastric filaments; F, G) delimitation of gastric radial pockets and manubrium; H) four gastric radial pockets and a central manubrium; I) interradial ostia; J, K) separation of arms;

Craterolophus convolvulus: A) four perradial chambers; B, C) delimitation of four interradial septa (central layer of mesoglea below complete delimitation); D) four interradial septa with infundibula; E) delimitation of claustra; F) claustra and four accessory radial pockets; G, H) delimitation of principal radial pockets, auxiliary radial pockets, and manubrium; I) accessory and principal radial pockets separated by the claustra, and lateral auxiliary radial pockets (oval projections with gonads); J) interradial ostia; K, L) separation of arms. Legend: epidermis, black; gastrodermis, red; mesoglea, gray; longitudinal muscles, blue; coronal muscle, purple; gonads, green; AR, adradii; IR, interradii; PR, perradii.
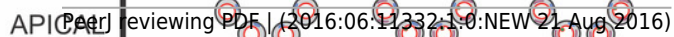
Figure 58

Gonads and claustra.

Haliclystus tenuis: A) general view of gonads associated with adradial arms in animals without claustrum; ***Manania uchidai***: B) general view of gonads at perradii in animals with claustra; ***H. tenuis***: C) cross section of calyx with gonads in the gastric radial pockets; D) cross section of adradial arms with gonads; ***M. uchidai***: E) cross section of calyx with gonads in the principal radial pockets, at perradii. See Table 2 for abbreviations.
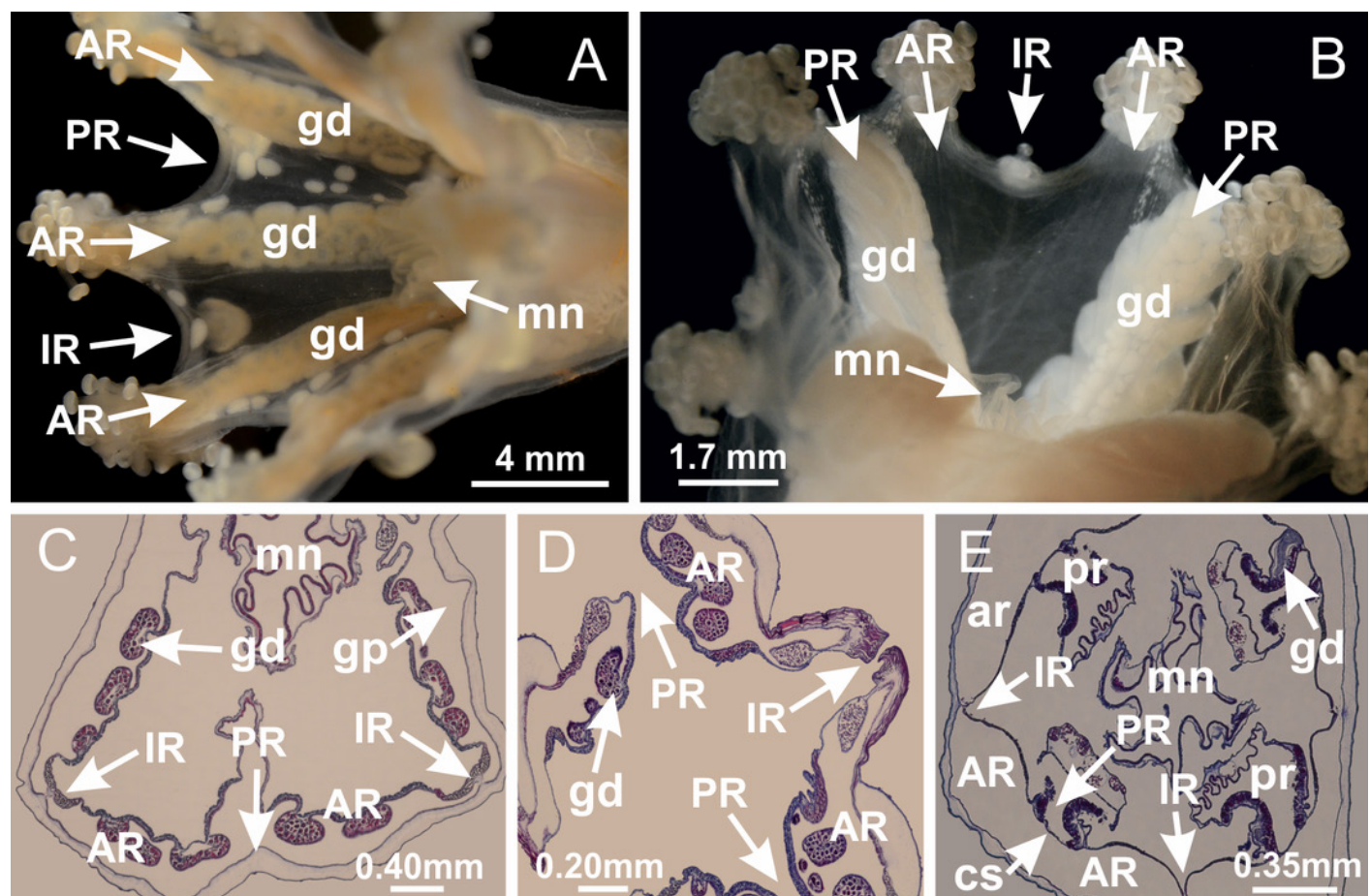
Figure 59

Hypothesis of character evolution for staurozoan genera included in the recent molecular phylogenetic hypothesis (Miranda et al., 2016).

ACCTRAN optimization of morphological and life-history features (modified from Miranda et al., 2016). Characters 1-10 examined in this study (see Table 3 for detailed information). "?" Equivocal character (see Table 3). If claustrum is considered a symplesiomorphy of Staurozoa, it was lost in *Calvadosia*, *Haliclystus*, and in the clade *Lucernaria + Lipkea* (most parsimonious reconstruction). *Presence of gametoducts in other cnidarians requires further studies.